بسم الله الرحمن الرحيم

Palestine Polytechnic University

College of Engineering and Technology

Mechanical Engineering Department

Graduation Project

Internet-Based Control of Double Inverted Pendulum on a Cart

Project Team

Aziz Arafeh

Mohammad Al-Bakri

Project Supervisor

Prof. Karim A. Tahboub

Hebron-Palestine

June, 2007

Abstract

The double inverted pendulum on a cart (DIPC) system represents a challenging problem in control. This system consists of two jointed links, the first one is attached to a small motorized cart with a revolute joint. The links are allowed to move freely relative to the cart and relative to each other. The cart is driven over a linear rail by means of an Ac servomotor, whose torque represents the input of the system. System outputs, which are the angular displacements of the links and the cart position, are measured using optical encoders. The function of control system in DIPC is to stabilize both links in their vertical position, while tracing a desired position of the cart along the rail, in addition to reject disturbances that may act on the system. The controller is designed and simulated using MATLAB® and Simulink. In order to meet the hard real time requirements of such a system, the controller is implemented on a desktop computer equipped with DAQ using xPC target technique with either local or global host-to-target connections. With the developed DIPC system and its flexible control platform, several experiments are performed, where robust tracking and disturbance rejection state feedback controllers with extended observers are designed and applied practically to the cart alone, single and double inverted pendulum systems. Furthermore, self erection controller for the single inverted pendulum is demonstrated and applied. Being an under-actuated mechanical system, inherently open loop unstable, with high nonlinear dynamics, the DIPC system is considered as an excellent test-bed for a wide range of classical and modern control techniques.

Dedication

To our parents for their support

To our brothers and sisters

To our teachers for their advices

To our friends

Table of Contents

Chapter Two Mathematical Model

Chapter Three Electrical Components and Interfacing

Chapter Four Computer and Information System

Chapter Six Experimental Results

Chapter Seven Conclusions and recommendations

Appendices

References

List of Figures

List of Tables

List of Symbols

Symbol	Definition	SI Units
x	Cart position along the track	m
θ_1	Angle between the cart and link1	rad
θ_2	Angle between link1 and link 2	rad
M	Mass of the cart	kg
m_1	Mass of rod1	kg
m_2	Mass of the link2	kg
r_p	Radius of the pulley	m
l_1	Length of C.O.G of rod1	m
l_2	Length of C.O.G of the link2.	m
L_1	Total length of link1	m
L_2	Total length of link2	m
J_p	Moment of inertia of the two pulleys	$kg.m^2$
J_1	Mass moment of inertia of the link about its C.O.G	$kg.m^2$
J_2	Mass moment of inertia of the link2.	$kg.m^2$
F_{fric}	Friction force	N
F_{d1}	Disturbance force acting at the cart	N
F_{d2}	Disturbance force acting on link1	N
F_{d3}	Disturbance force acting on link2	N
T_m	Input torque from the motor	N
g	Gravitational constant	m/s^2

Chapter One

The Double Inverted Pendulum: An Overview

1.1 Introduction

The double inverted pendulum on a cart (DIPC) represents a challenging problem in control. This system consists of two jointed links; the first one is attached to a small cart with a revolute joint. The links are allowed to move freely relative to the cart and relative to each other. The cart is driven over a linear rail by means of an electrical motor, whose torque represents the only input to the system. The main objective of the DIPC system is to stabilize both links vertically upward, while tracking a desired position of the cart along the rail. Furthermore robustness and disturbance rejection are to be achieved. Being an under-actuated mechanical system, inherently open-loop unstable, with high nonlinear dynamics, and with some states that are not directly measurable, double inverted pendulum system is considered as an excellent test-bed for a wide range of classical and modern control techniques.

The applications of the double inverted pendulum ranges widely from robotics to human beings motion and space rocket guidance systems. Originally inverted pendulum systems were used to illustrate the ideas of linear control theories, but the inherent nonlinear nature of such systems helped them to maintain their usefulness along the years, and they are now used to illustrate several ideas emerging in the field of modern nonlinear control.

1.2 Recognition of the need

As an educational tool, inverted pendulum systems are used for testing various controllers and control techniques including:

- State feed back control.
- Root locus and frequency domain techniques.
- Optimal control methods.
- Digital control methods.
- Intelligent control techniques.
- Nonlinear control methods.

Such control methods can be tested and compared via a set of performance specifications including:

- Stabilization control.
- Position tracking.
- Disturbance rejection.
- Robustness.

Sampling frequency and computational and transport time delays effects on stability and response are relevant issues that can be demonstrated and tested.

Furthermore, the DIPC system will be an interactive area for testing and practical application of many other technological disciplines including:

- Sensors and actuators.
- Signal processing.
- Systems interfacing.
- Embedded systems.
- Network communications.

All of that makes the double inverted pendulum system a valuable addition to the control laboratory in this university.

1.3 Literature review

Double inverted pendulum was always an interesting and challenging field of study, thus there are many researches and papers that take the DIPC as the core of their studies using a wide variety of designs, software packages and control techniques.

This project is based on a graduation project titled "Design of a Computer Controlled Double Inverted Pendulum Apparatus" conducted at the Palestine Polytechnic University in 2006. Students then managed to build the mechanical structure of the DIPC, interface the angle encoders used in the system to a data acquisition card and get their readings by an xPC target application [2].

1.4 Double inverted pendulum design process

As a mechatronic system, the most convenient way to be followed during the design and implementation of the DIPC is the concurrent design approach. This approach consists of a sequence of stages, which are:

1.4.1 Conceptual design and functional specifications

The DIPC system consists of two jointed links (rods) attached to a small motorized cart with a revolute joint. These links are allowed to move freely relative to the cart and relative to each other. The cart moves linearly over a linear track by means of a robe and pulley arrangement, as shown in Fig. 1.1.

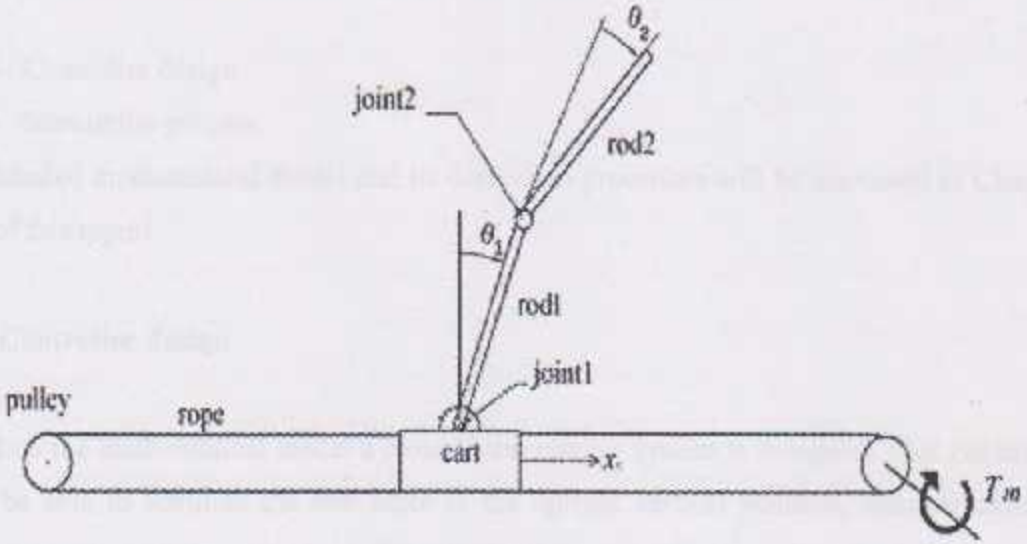

Figure 1.1 The double inverted pendulum on cart system.

System outputs, which are the angular displacement between the two links (θ_2), the angle between first link and the cart (θ_1), and the cart position along the track (x), are measured using three optical angular encoders placed at system's joints (two encoders are placed at joints 1 and 2 in Fig. 1.1, while the third one reads the angular displacement of motor's shaft). The input of the system is the torque generated by an AC servomotor coupled directly to the pulley's shaft. The role of the control part is to determine the value of the

driving torque required for balancing the pendulum vertically while tracking a desired position of the cart along the rail, and to compensate for disturbances that may act on the system. This controller is implemented using a standard PC hardware equipped with data acquisition cards and a real-time operating system. In order to get accurate and reliable data, signal conditioning, filtering and isolation circuits between the DAQ, sensors and the actuator are used.

1.4.2 Mathematical model

The next step in the design process is mathematical modeling, which includes a set of differential equations that describe system's behavior. This model will not only give a better understanding of the system, but also it will be used for two major purposes, which are:

1- Controller design.
2- Simulation process.

The detailed mathematical model and its derivation procedure will be discussed in Chapter Two of this report.

1.4.3 Controller design

Based on the mathematical model a closed loop control system is designed. That controller must be able to stabilize the two links in the upright vertical position, while tracking a desired position of the cart along the rail. Furthermore, the controller should be able to reject, or to compensate for, the disturbances that may act either on the cart or on each of the two links. The performance of the entire system is then simulated and tested virtually, thus any malfunction in the system performance is handled before applying the controller to the real system.

More details about control theories and techniques that are applicable to the DIPC system will be introduced later in this chapter, while a detailed controller design for single and

double inverted pendulum systems with simulation and experimental results are demonstrated in Chapters Five and Six of this report.

1.4.4 Sensors and actuators

Based on the basic understanding of the system, its performance, control system design and its requirements, sensors and actuators needed for the system are precisely selected. For the sensors they are selected to meet resolution, accuracy and noise immunity requirements. While the selection criteria of the actuator, which is the driving motor, are based on its inertia, power, speed and torque limits, in addition to the control accuracy.

1.4.5 Hardware-in-the-loop simulation

Hardware-in-the-loop simulation involves interfacing the physical plant together with its sensors and actuators to the simulation environment where the controller runs. In other words, the control loop that runs on a PC does not employ a mathematical model of the plant and its sensors and actuators but the plant itself. In this step of the design process, all of the signals of the sensors, the actuator and the interfacing circuits are tested, in addition to the controller performance. This helps in predicting any malfunction in the previously mentioned components or in the interconnection between them.

1.4.6 System implementation

Since the main objective for developing the DIPC system is to use it as a control test-bed, the flexibility with which changes in controller design are implemented is of significant importance. Thus it is not desired to have a hardwired controller for the system, on the contrary, it is intended to construct a flexible system, in terms of its control, where various controllers can be implemented and tested as easy as possible. Furthermore, high real-time control abilities are necessary for dealing with such rapid dynamic system. To meet these requirements, a flexible solution for real-time control implementation is used, as discussed in Chapter Four of this report.

1.5 DIPC elementary components

The DIPC system represents the integration of four basic subsystems, which are, the mechanical, electrical, computer and control, which are the four basic disciplines that make up mechatronics, as shown in Fig. 1.2.

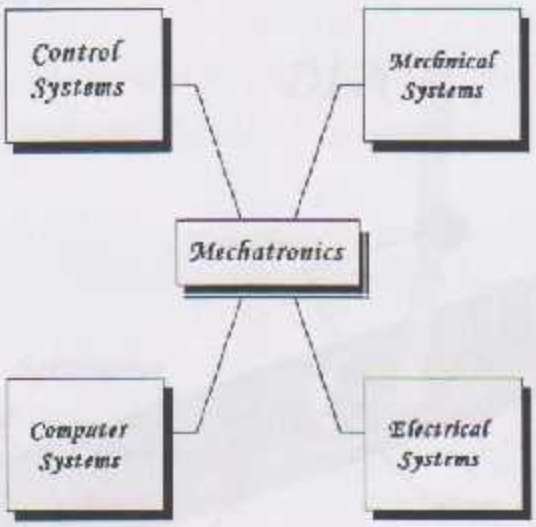

Figure 1.2 Mechatronics basic disciplines.

1.5.1 Mechanical part

The mechanical part of the DIPC involves the design of several mechanical components that make up the physical structure of the system. Each component is studied, designed and analyzed in terms of strength, geometry, durability and material properties. Thus, these components will operate in the system without failure or defect. Furthermore, issues related to control system design are taken into consideration.

Figure 1.3 shows the basic mechanical components of the DIPC system, which are:

1) The base plate: which is the base on which the system is assembled, this part must be heavy enough and made of a high damping capacity material (such as gray cast iron); in order to be able to absorb and eliminate the vibrations generated by the driving motor and the motion of the system.

2) The linear rail (track): along which the cart moves during system operation, this part should be rigid enough to handle the system motion without any failure or distortion.
3) Cart and carriage: which are the parts that slide along the rail and carry the two links (the two compound pendulums). An important point to be taken into account, during the design of these components is to have a minimal friction with the rail, as will be explained later.

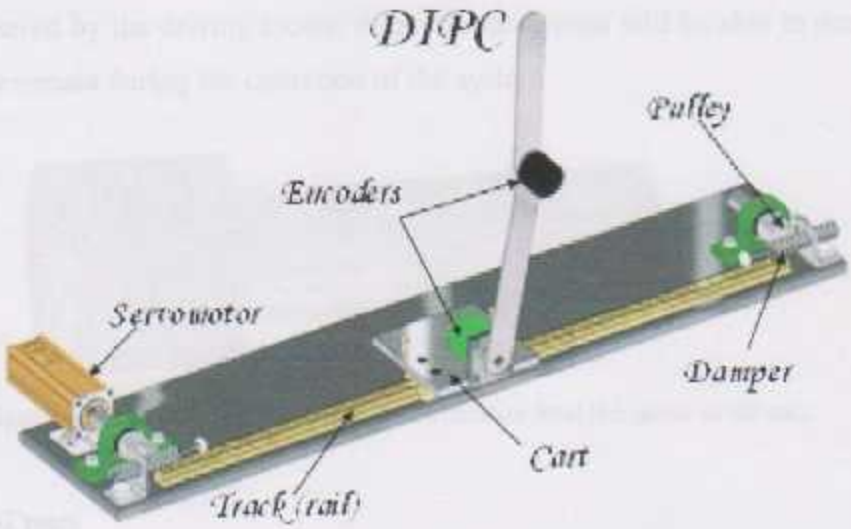

Figure 1.3 Double inverted pendulum on cart.

4) The two inverted pendulums (the two links): these links rotate freely relative to the cart and relative to each other by means of revolute joints.
5) Pulley and rope arrangement: The cart is driven on a rail (track) through a novel cable transmission connected to a pulley. Such arrangement has two major advantages:
    - There is no backlash in the system, since no gears are used.
    - The cart weight is low as the motor is not mounted on it.

    On the other hand, the system needs a cable such that no elongation occurs under loading. Another point to be taken in consideration is the fact that no slippage between the robe and the pulleys is permitted during operation; therefore specially-designed helical pulleys are used, as shown in Fig. 1.4.

For all of the previously mentioned components, two essential requirements should be satisfied:

- Friction coefficient between the moving parts should be at the minimum possible value.
- Very high friction between the rope and the pulleys; so as to prevent any slippage.

Meeting these specifications is important to ensure that minimal inertia and friction forces will be encountered by the driving motor; therefore this motor will be able to deal with the quick motion reversals during the operation of the system.

Figure 1.4 Helical pulley used for power transition from the motor to the cart.

1.5.2 Electrical part

The electrical part in the DIPC includes sensors, actuators, and the interfacing circuits that connect those sensors and actuators with the controller. In more details the electrical part includes:

1) The driving motor:

Since the operation of the system requires quick changes in the direction of the cart velocity and acceleration, which is necessary to stabilize the pendulums vertically and generate the required inertial forces during self erecting process. It is important for the driving motor used in such a system to have:

- The ability to generate enough torque independently of the speed value
- Low rotor inertia.
- Simple and precise control.

Therefore a low inertia AC servo motor with a driver is chosen to be used in this system.

2) Displacement sensors:

Designing a real time closed-loop feedback control system is essential to stabilize the DIPC system. Such a control system requires measuring some variables that specify the state of the system. These measurements are:

- The linear displacement of the cart.
- The angular displacement of the first link relative to the cart.
- The angular displacement of the second link relative to the first one.

To have an accurate and real-time control system, the sensors need to be relatively noiseless with a fast response, so that the information received from the sensors accurately reflects the state of the system. Thus optical encoders are chosen since they satisfy all the above requirements, in addition to the following advantages:

- High accuracy.
- High resolution.
- Digital output.

3) Interfacing circuits:

The environment in which the DIPC system works is noisy due to the power lines, and the magnetic fields generated by the motor. Therefore signal conditioning and filtering circuits are of essential importance to make the sensor's output reliable and accessible by the computer.

Another function for the interfacing circuits is protecting DAQ cards from high voltages and high current demand (over loading), when being connected to the sensor and the motor driver. To achieve this protection, two types of isolation circuits are used:

- Digital isolation between the DAQ and encoders' outputs, using opt-couplers.
- Analog isolation between the DAQ and the motor driver, using a special capacitive isolation amplifier.

Further discussion and details about the electrical components, interfacing circuits and technical issues are demonstrated in Chapter Three.

1.5.3 Computer and information system

As a mechatronic application, computer and information system are essential parts of the DIPC system. These parts include, in addition to the PC hardware used for controller implementation, a set of software packages that is used to design, simulate, and control the entire system.

1.5.3.1 Computer part

With DIPC system, computers are used for two major purposes:

1. Design, analyze, and simulate the mechanical and control parts of the system.
2. Running the real-time controller.

To achieve the first requirement, a set of software packages is used. MATLAB and Simulink provide a wide variety of functions, numerical algorithms, and toolboxes that help significantly not only to design and simulate the control system, but also to build executable real-time applications. For the purposes of mechanical design and analysis, software packages such as CATIA and ANSYS are very helpful to create a three dimensional mechanical models, specify the constraints for each part, define the relations between different parts, in addition to apply loads to the system and study their effects.

The second requirement of the computer part, which is controlling the DIPC system at real-time, is achieved using xPC target technique, which is introduced in the following subsection.

1.5.3.2 xPC target

The xPC target technique is a solution for prototyping, testing and deploying real-time systems, using standard PC hardware and its peripherals such as DAQ cards. This technique comes as a part of MATLAB software provided by MathWorks Company. In particulate xPC target is a toolbox within MATLAB's Simulink.

In xPC target technique two PCs are used; host and target. With the host PC, one can design the controller, simulate it, and download it to the target PC. The target PC, which is connected to the controlled plant, is just used to run control functions in real time and monitor the controlled application.

xPC target technique is considered as an excellent solution for educational and rapid prototyping purposes due to the following facts:

- Changes and modifications in controller design are easily introduced to the host PC, and the modified controller is downloaded to the target PC almost with no effort. Online tuning of some parameters is also possible.
- Hard real-time requirements can be satisfied since the target PC processor is fully dedicated for running the controller.
- Host and target PCs can be connected serially, through network or even through the internet. Furthermore the target PC can operate alone without any connection with the host.
- xPC target technique supports a wide range of DAQ cards and IO boards, which gives the designer a high level of flexibility to choose the suitable hardware.

All of that make xPC target technique an attractive solution for implementing control functions for the DIPC system, and other rapid prototyping and hardware-in-the-loop simulation purposes.

1.5.4 Control system

Inverted pendulum systems, in general, are used in control laboratories as test-beds for various control theories, including the classical linear control theories, and can be extended to intelligent and nonlinear control fields.

As stated earlier, inverted pendulum systems present a number of complications and challenges in terms of their control, due to the fact that they are under-actuated mechanical systems, inherently open-loop unstable, with highly-nonlinear dynamics. These underlying complications make for a control problem which is both interesting and challenging.

Any controller applied to an inverted pendulum system must guarantee first the closed-loop stability at the unstable inverted position. Second, the cart position should track a desired input while keeping both rods vertically stable. Third, disturbance rejection and robustness are also to be achieved. The possibility for a controller to satisfy these requirements varies according to the control strategy behind it. Here is a brief description of the main control techniques that may be used in the case of inverted pendulum systems:

1) State feedback control

In control engineering, a state space representation is a mathematical model of a physical system as a set of input, output and state variables related by first-order differential equations. The state space representation (also known as the "time-domain approach") provides a convenient and compact way to model and analyze systems with multiple inputs and outputs. Unlike the frequency domain approach, the use of the state space representation is not limited to time-invariant systems with linear components and zero initial conditions.

For MIMO (multi-input multi-output) systems, pole placement can be performed mathematically using a state-space representation of the open-loop system and calculating a feedback matrix assigning poles in the desired positions in order to

achieve the desired system response, as shown in Fig. 1.5. In complex systems this may require computer-aided calculation-capabilities, and can not always ensure robustness.

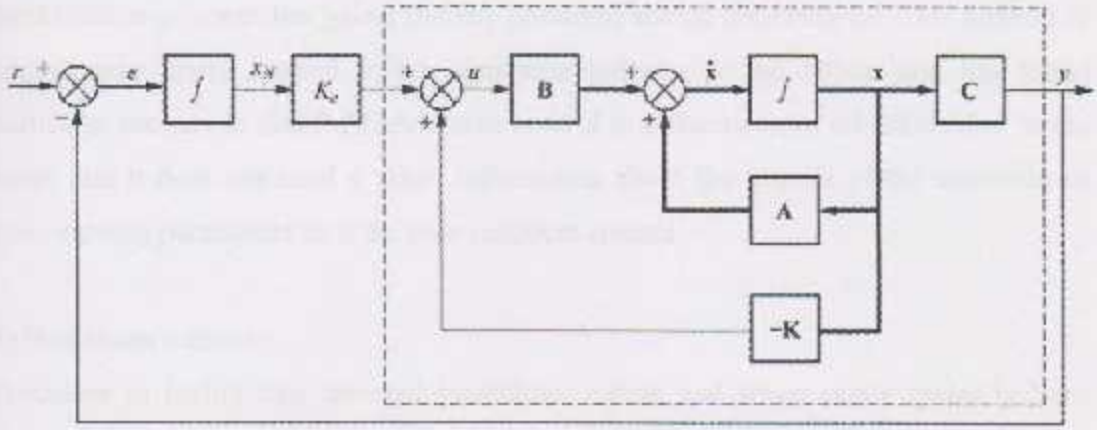

Figure 1.5 State feed back control.

2) PID controllers

The so-called PID controller is probably the most-used feedback control design, since it is the simplest one. "PID" is an abbreviation for Proportional-Integral-Derivative, referring to the three terms operating on the error signal to produce a control signal.

The desired closed loop dynamics is obtained by adjusting the three parameters K_P, K_I and K_D, as in Fig. 1.6, based on the linear system transfer function, its root locus and other frequency domain techniques [6]. Stability can often be ensured using only the proportional term. The integral term used to meet the steady state requirements, while the derivative term is used to improve the transient response.

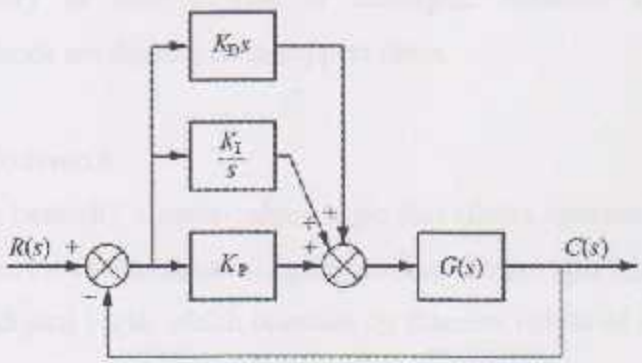

Figure 1.6 PID controller.

3) Adaptive control

Adaptive control uses an on-line identification of the process parameters and modification of controller gains; thereby obtaining robust performance. This method of control was firstly applied in the aerospace industry in the 1950s, and has found particular success in that field. Adaptive control is different from robust control in the sense that it does not need a priori information about the bounds of the uncertain or time-varying parameters as it the case in robust control

4) Non-linear control

Processes in reality like inverted pendulum, robots and space crafts typically have strong non-linear dynamics. In control theory it is sometimes possible to linearize such classes of systems and apply linear techniques, but in many cases is desirable to expand the sight beyond linear theories, permitting the control of nonlinear systems. These normally take advantage of results based on Lyapunov's theory [4]. Differential geometry has been widely used as a tool for generalizing well-known linear control concepts to the non-linear case, as well as showing the subtleties that make it a more challenging problem [16].

5) Intelligent control

All control techniques that use various AI (artificial intelligence) computing approaches like neural networks, Bayesian probability, fuzzy logic, machine learning, and genetic algorithms can be put into the class of intelligent control. New control techniques are created continuously as new models of intelligent behavior are created, and computational methods are developed to support them.

5.1) Fuzzy logic control

Fuzzy Logic is basically a multi-valued logic that allows intermediate values to be defined between the conventional crisp values like yes/no, true/false, etc, in contrast to classical or digital logic, which operates on discrete values of either 0 or 1 (true or false).

With fuzzy logic intuitive linguistic notions can be formulated mathematically, and processed by computers. In this way problem solutions can be cast in terms that human operators can understand, so that their experience can be used in the design of the controller. This makes it easier to mechanize tasks that are already successfully performed by humans.

Since fuzzy logic control is based on the designer's experience rather than a mathematical model, this control method is very useful when dealing with highly nonlinear processes and the very complex ones, where no simple mathematical model can be obtained. Furthermore, the resulting controller will be less sensitive to parameter fluctuations, and it will not be dedicated to a specific operating regions.

6) Optimal control

Optimal control is a particular control technique in which the control signal is selected in such a way to optimize a certain constraints as cost, performance etc. Two optimal control design methods have been widely used in industrial applications, as they proved their ability to guarantee closed-loop stability [16]. These are Model Predictive Control (MPC) and Linear-Quadratic-Gaussian control (LQG). The first can more explicitly take into account constraints on the signals in the system, which is an important feature in many industrial processes. Together with PID controllers, MPC systems are the most widely used control technique in process control.

1.6 Conclusions

Based on the previous discussion, it is clear that the DIPC can be considered as a typical mechatronic system, since it represents the interaction between the basic disciplines from which mechatronics is constructed, which are mechanical, electrical, computer and control disciplines, as shown in Fig. 1.7.

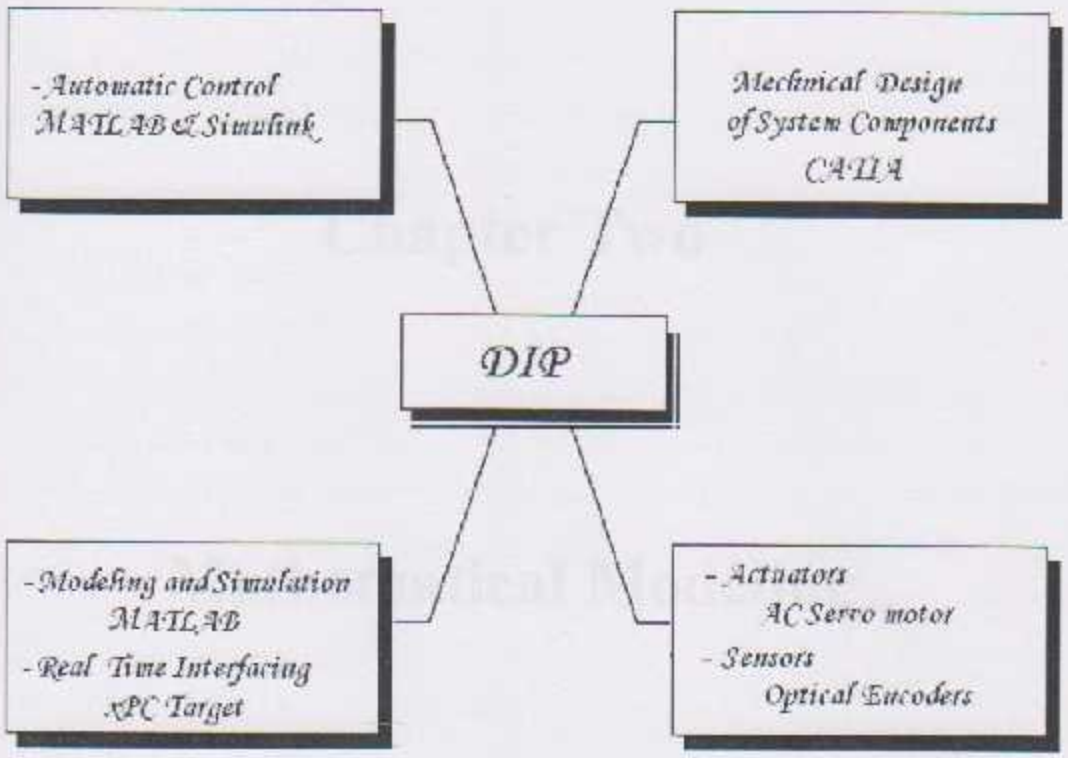

Figure 1.7 DIPC system as a mechatronic system.

Chapter Two

Mathematical Modeling

2.1 Introduction

Mathematical modeling of the DIPC system tends to represent all important features of the system and describe its behavior in terms of differential equations. The needed model accuracy (closeness to the actual system) depends on the purpose. Generally a simplified model is needed to study the main characteristics of the system, while a detailed model is needed for precise simulation and prediction studies.

In general, there are two main purposes for modeling a physical system:

- Develop a mathematical model in order to predict the dynamic behavior of the system as accurately as possible. Using numerical solution methods, such a model serves as a tool for extensive evaluation of system behavior without actually using or building the real system.
- Develop models to gain insight into the behavior of the dynamic system qualitatively instead of exact response prediction, i.e. knowledge of stability margins, controllability, observability, and the sensitivity of response to parameter changes, such a model needs not to contain all of the details of the actual system, but only the most essential features so as to provide the needed insight from an engineering stand point.

Therefore two models will be derived for the inverted pendulum system, a simple and linear one for controller design and analysis purposes, and a nonlinear model for testing and simulating the dynamic system response as accurately as possible.

In the case of inverted pendulum systems (both single and double), the following assumptions are used in deriving their mathematical models:

1. The friction at the two revolute joints is neglected.
2. The center of gravity of each link is located at the link's axis of symmetry.
3. The angle between the rope (which drives the cart along the slider) and the x-axis is very small and considered to be negligible.

In order to obtain the mathematical model of the system, Lagrange's approach is used to derive the basic differential equations that govern system's dynamics. The main formula and a brief description of this method are presented in the following subsection.

2.1.1 Lagrange's approach

Lagrange's approach is used to derive the nonlinear equations that describe the motion of the system at each of its principal coordinates. The basic formula of Lagrange's equation is:

$$\frac{d}{dt}\left(\frac{\partial T}{\partial \dot{q}_n}\right)-\frac{\partial T}{\partial q_n}+\frac{\partial U}{\partial q_n}=Q_n \qquad (2\text{-}1)$$

Where:

- T: the total kinetic energy of the system.
- U: the total potential energy of the system.
- Q_n: Forces and torques that act in each coordinate including the non-conservative forces due to Coulomb friction and viscous damping.
- $q_1 \ldots q_n$: the generalized coordinates that describe system's motion.
  Where a set of (n) generalized coordinates are needed to describe the motion of an n-degree-of-freedom system.

In the upcoming sections this equation will be used to derive the mathematical models for the single and double inverted pendulum systems respectively. These models will be used later in Chapter Five of this report for controller design and simulation purposes.

2.2 Mathematical model for the single inverted pendulum

In this section a nonlinear model for the single inverted pendulum is derived. This model includes the effect of friction force between the cart and the rail. The effect of disturbances acting on the system is also included.

2.2.1 Nonlinear model

The mathematical model of the system consists of two second-order nonlinear differential equations, these equations are derived using Lagrange's approach explained earlier. Based on Fig. 2.1, the total kinetic and potential energies of the system can be found as follows:

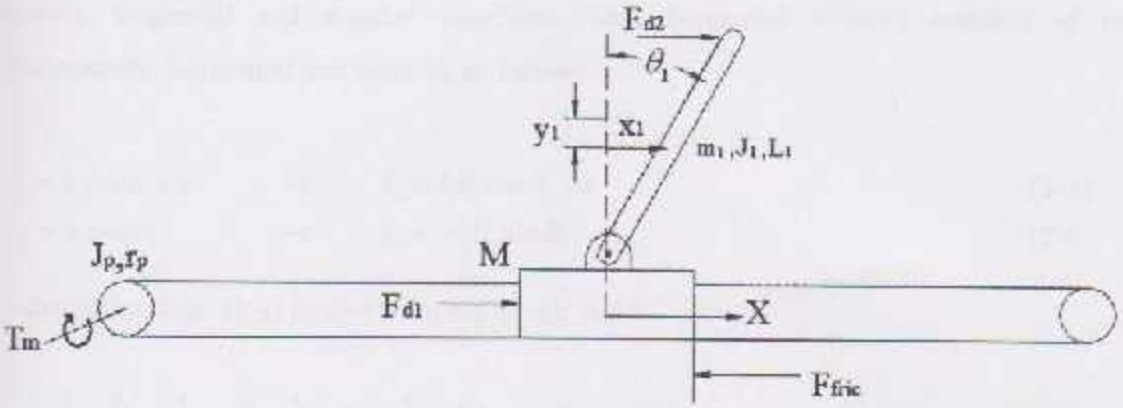

Figure 2.1 Single inverted pendulum on a cart system.

Where: M: Mass of the Cart.
m_1: Mass of the link.
J_1: Mass moment of inertia of the link.
l_1: Distance to center of mass of the link.
J_p: Mass moment of inertia of the pulleys.
d: the motor viscous damping coefficient.
r_p: Radius of the pulley.
T_m: Input torque from the motor.
F_{fric}: Friction force.
F_{d1}: Disturbance force acting at the cart.
F_{d2}: Disturbance force acting at the link.

The total kinetic energy of the system is the sum of those energies for each of the system components, i.e. kinetic energy for the motor and pulleys, in addition to that for the cart and the link.

$$T = T_{motor} + T_{pulleys} + T_{cart} + T_{link1} \tag{2-2}$$

In more details:

$$T = \frac{1}{2} J \dot{\theta}_m^2 + \frac{1}{2} M \dot{x}^2 + \frac{1}{2} J_1 \dot{\theta}_1^2 + \frac{1}{2} m_1 v_{Tmg,1}^2 \tag{2-3}$$

Where:

J: is the equivalent mass moment of inertia for the motor and pulleys.

θ_m : is the angular displacement of the motor.

The angular displacement of the motor (θ_m) can be related to the displacement of the cart by the radius of the pulley, as follows:

$$\theta_m = \frac{x}{r_p} \quad \rightarrow \quad \dot{\theta}_m = \frac{\dot{x}}{r_p} \tag{2-4}$$

The kinetic energy of the link (the inverted compound pendulum) is due to its center of gravity tangential and angular velocities. That tangential velocity consists of two components, horizontal and vertical, as follows:

$$x_1 = l_1 \sin\theta_1 + x \quad \rightarrow \quad \dot{x}_1 = l_1\dot{\theta}_1 \cos\theta_1 + \dot{x} \tag{2-5}$$

$$y_1 = l_1 \cos\theta_1 \quad \rightarrow \quad \dot{y}_1 = -l_1\dot{\theta}_1 \sin\theta_1 \tag{2-6}$$

Substituting Eqs. (2-4) to (2-6) into Eq. (2-3), yields:

$$T = \frac{1}{2}J\frac{\dot{x}^2}{r_p^2} + \frac{1}{2}M\dot{x}^2 + \frac{1}{2}J_1\dot{\theta}_1^2 + \frac{1}{2}m_1\left[\left(l_1\dot{\theta}_1\cos\theta_1 + \dot{x}\right)^2 + \left(l_1\dot{\theta}_1\sin\theta_1\right)^2\right] \tag{2-7}$$

The total potential energy (U) of the system is only due to the link center of mass elevation change, thus (U) is given by:

$$U = m_1 g y_1 = m_1 g l_1 \cos\theta_1 \tag{2-8}$$

Applying Lagrange's equation for each generalized coordinate, x and θ_1, yields:

1) In x direction:

The Lagrange's equation in x-direction is given as follows:

$$\frac{d}{dt}\left(\frac{\partial T}{\partial \dot{x}}\right) - \frac{\partial T}{\partial x} + \frac{\partial U}{\partial x} = Q_x \tag{2-9}$$

Where:

$$\frac{\partial T}{\partial \dot{x}} = \frac{J}{r_p^2}\dot{x} + M\dot{x} + m_1\left(\dot{x} + l_1\dot{\theta}_1\cos\theta_1\right)$$

$$\frac{\partial T}{\partial x} = 0$$

$$\frac{\partial U}{\partial x} = 0$$

$$Q_x = \frac{T_m}{r_p} - \frac{d}{r_p^2}\dot{x} - F_{fric} + f_{d1} + f_{d2}$$

Applying Eq. (2-9) and simplifying it yields:

$$\left(M + m_1 + {}^{J}\!/_{r_p^2}\right)\ddot{x} + \left(m_1 l_1 \cos\theta_1\right)\ddot{\theta}_1 - \dot{\theta}_1^2 m_1 l_1 \sin\theta_1 = \frac{T_m}{r_p} - \frac{d}{r_p^2}\dot{x} - F_{fric} + f_{d1} + f_{d2} \qquad (2\text{-}10)$$

2) In θ_1 direction:

The Lagrange's equation in θ_1 direction is given as follows:

$$\frac{d}{dt}\left(\frac{\partial T}{\partial \dot{\theta}_1}\right) - \frac{\partial T}{\partial \theta_1} + \frac{\partial U}{\partial \theta_1} = Q_{\theta_1} \qquad (2\text{-}11)$$

Where:

$$\frac{\partial T}{\partial \dot{\theta}_1} = J_1\dot{\theta}_1 + m_1\left(\dot{x}l_1\cos\theta_1 + l_1^2\dot{\theta}_1\right)$$

$$\frac{\partial T}{\partial \theta_1} = -m_1 l_1 \dot{x}\,\dot{\theta}_1 \sin\theta_1$$

$$\frac{\partial U}{\partial \theta_1} = -m_1 l_1 g \sin\theta_1$$

$$Q_{\theta_1} = f_{d2} L_1 \cos\theta_1$$

Applying Eq. (2-11) and simplifying it yields:

$$\left(m_1 l_1 \cos\theta_1\right)\ddot{x} + \left(m_1 l_1^2 + J_1\right)\ddot{\theta}_1 - m_1 g l_1 \sin\theta_1 = f_{d2} L_1 \cos\theta_1 \qquad (2\text{-}12)$$

Equations (2-10) and (2-12) that describe the single inverted pendulum can be written in a more compact matrix form:

$$\begin{bmatrix} M + m_1 + {}^{J}\!/_{r_p^2} & m_1 l_1 \cos\theta_1 \\ m_1 l_1 \cos\theta_1 & m_1 l_1^2 + J_1 \end{bmatrix}\begin{bmatrix} \ddot{x} \\ \ddot{\theta}_1 \end{bmatrix} + \begin{bmatrix} \frac{d}{r_p^2} \\ 0 \end{bmatrix}\dot{x} + \begin{bmatrix} 0 \\ -m_1 g l_1 \end{bmatrix}\sin\theta_1 + \begin{bmatrix} m_1 l_1 \dot{\theta}_1^2 \sin\theta_1 \\ 0 \end{bmatrix} =$$

$$\begin{bmatrix} {}^{1}\!/_{r_p} \\ 0 \end{bmatrix} T_m + \begin{bmatrix} -1 \\ 0 \end{bmatrix} F_{fric} + \begin{bmatrix} 1 & 1 \\ 0 & L_1\cos\theta_1 \end{bmatrix}\begin{bmatrix} f_{d1} \\ f_{d2} \end{bmatrix} \qquad (2\text{-}13)$$

The friction force can be evaluated based on Fig. 2.2. Firstly the normal force acting on the rail due to the system operation is found as follows:

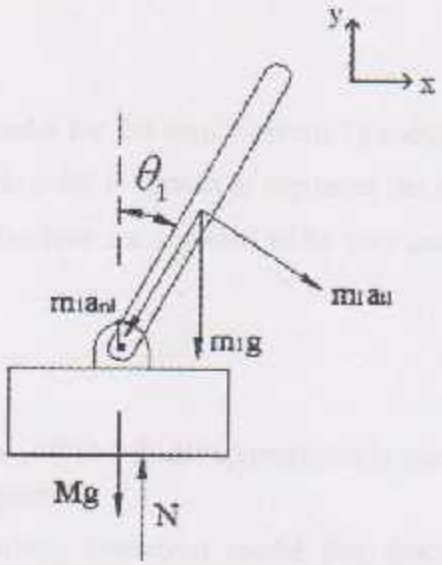

Figure 2.2 Single inverted pendulum friction force.

$$N-(M+m_1)g+a_t m_1\sin\theta_1+a_n m_1\cos\theta_1=0 \tag{2-14}$$

Where: N is the normal force.

a_t is the tangential acceleration of the link's center of mass.

a_n is the normal acceleration of the link's center of mass.

Substituting the values of a_t and a_n yields:

$$N=(M+m_1)g-m_1l_1\sin\theta_1\ddot{\theta}_1-m_1l_1\dot{\theta}_1^2\cos\theta_1 \tag{2-15}$$

The friction force consists of two components, static and dynamic:

$$F_{fric}=\mu_{static}N*\delta(\dot{x})+\mu_{dynamic}N*Sgn(\dot{x}) \tag{2-16}$$

Where:

The unit impulse function $\delta(\dot{x})=\begin{cases}1 & \dot{x}=0\\ 0 & \dot{x}\neq 0\end{cases}$ (2-17)

The sign function $Sgn(\dot{x})=\begin{cases}1 & \dot{x}>0\\ -1 & \dot{x}<0\end{cases}$ (2-18)

2.2.2 Linearized model

In order to obtain the linear model for the single inverted pendulum system, an operating point is to be selected first. This point is chosen to represent the upper vertical position, in other words x, θ_1 and their derivatives are assumed to be very small (approximately zero). Thus it could be assumed that:

- $\cos\theta_1 \approx 1$.
- $\sin\theta_1 \approx \theta_1$
- All the higher orders of θ_1 and $\dot{\theta}_1$ are approximately zero.
- The dry friction is ignored.

Based on Eq. (2-13) the resulting linearized model that describes the system in the operating region is:

$$\begin{bmatrix} M+m_1+\dfrac{J}{r_p^2} & m_1 l_1 \\ m_1 l_1 & m_1 l_1^2 + J_1 \end{bmatrix} \begin{bmatrix} \ddot{x} \\ \ddot{\theta}_1 \end{bmatrix} + \begin{bmatrix} \dfrac{d}{r_p^2} & 0 \\ 0 & 0 \end{bmatrix} \begin{bmatrix} \dot{x} \\ \dot{\theta}_1 \end{bmatrix} + \begin{bmatrix} 0 & 0 \\ 0 & -m_1 g l_1 \end{bmatrix} \begin{bmatrix} x \\ \theta_1 \end{bmatrix} = \begin{bmatrix} \dfrac{1}{r_p} \\ 0 \end{bmatrix} T + \begin{bmatrix} 1 & 1 \\ 0 & L_1 \end{bmatrix} \begin{bmatrix} f_{d1} \\ f_{d2} \end{bmatrix} \tag{2-19}$$

Defining the matrices:

- Mass matrix:

$$M = \begin{bmatrix} M+m_1+J/r_p^2 & m_1 l_1 \\ m_1 l_1 & m_1 l_1^2 + J_1 \end{bmatrix} \tag{2-20}$$

- Damping matrix:

$$D_m = \begin{bmatrix} \dfrac{d}{r_p^2} & 0 \\ 0 & 0 \end{bmatrix} \tag{2-21}$$

- Quasi stiffness matrix:

$$K = \begin{bmatrix} 0 & 0 \\ 0 & -m_1 g l_1 \end{bmatrix} \tag{2-22}$$

- Input matrix:

$$B = \begin{bmatrix} 1/r_p \\ 0 \end{bmatrix} \tag{2-23}$$

- Disturbance matrix:

$$B_d = \begin{bmatrix} 1 & 1 \\ 0 & L_1 \end{bmatrix} \tag{2-24}$$

Regarding these matrices, it could be noted that:

- The mass matrix is symmetric, regular and positive definite matrix.
- The system has a dynamic coupling in the mass matrix only, while there is no static coupling in the quasi stiffness matrix.
- The quasi stiffness matrix (K) is a destabilizing matrix, since it tends to take the system away from its operating point.

Using the previous matrices, Eq. (2-19) could be expressed as:

$$M\ddot{x} + D_m\dot{x} + Kx = BT + B_d f_d \tag{2-25}$$

Where: $x = [x \quad \theta_1]^T$

To yield the state-space representation for the linear system, four states are needed to describe the system. These are chosen to be x, $\dot{x}$, θ_1, and $\dot{\theta}_1$. The input to the system is the motor torque (T_m). As the system is equipped with the necessary sensors, the four states ($x, \theta_1, \dot{x}$, and $\dot{\theta}_1$) are the measurable outputs of the system[1]. Based on the previous discussion, the state-space model of the system is expressed as follows:

$$\begin{bmatrix} \dot{x} \\ \ddot{x} \end{bmatrix} = \begin{bmatrix} 0 & I_2 \\ -M^{-1}K & -M^{-1}D_m \end{bmatrix} \begin{bmatrix} x \\ \dot{x} \end{bmatrix} + \begin{bmatrix} 0 \\ M^{-1}B \end{bmatrix} T + \begin{bmatrix} 0 \\ M^{-1}B_d \end{bmatrix} f_d$$
$$y = I_4 \begin{bmatrix} x \\ \dot{x} \end{bmatrix} \tag{2-26}$$

[1]- Both x and θ_1 are directly measured, while the other two states (velocities) are estimated using backward numerical differentiation, as shown in Chapter Six.

System parameters are defined in Table 2.1[1].

Table (2-1): Single inverted pendulum parameters

Symbol	Description	Value	Units
M	Mass of the cart	1.45	Kg
m_1	Mass of rod1	0.145	Kg
r_p	Radius of the pulley	0.02	m
l_1	Distance to center of mass of rod1	0.162	m
J_p	Moment of inertia of the 2 pulleys	1.55×10^{-4}	$Kg.m^2$
J_1	Mass moment of inertia of the link about its C.O.G	0.0013	$Kg.m^2$
d	Damping coefficient of the motor and bearings	5.8×10^{-3}	N.m.s/rad

Substituting the values given in Table 2.1 into matrices (2-20) to (2-24), then in Eq. (2-26) yields:

$$\begin{bmatrix} \dot{x} \\ \dot{\theta}_1 \\ \ddot{x} \\ \ddot{\theta}_1 \end{bmatrix} = \underbrace{\begin{bmatrix} 0 & 0 & 1 & 0 \\ 0 & 0 & 0 & 1 \\ 0 & -0.64 & -0.85 & 0 \\ 0 & 48.1 & 3.93 & 0 \end{bmatrix}}_{A} \begin{bmatrix} x \\ \theta_1 \\ \dot{x} \\ \dot{\theta}_1 \end{bmatrix} + \underbrace{\begin{bmatrix} 0 \\ 0 \\ 29.7 \\ -137.8 \end{bmatrix}}_{B} T_m + \underbrace{\begin{bmatrix} 0 & 0 \\ 0 & 0 \\ 0.6 & 0.32 \\ -2.75 & 67.11 \end{bmatrix}}_{B_d} \begin{bmatrix} f_{d1} \\ f_{d2} \end{bmatrix} \qquad (2\text{-}27)$$

$$y = \underbrace{I_4}_{C} \begin{bmatrix} x & \theta_1 & \dot{x} & \dot{\theta}_1 \end{bmatrix}^T$$

[1] - Parameters values shown in Table 2.1 are based on calculations and tests performed in [2].

2.3 Mathematical model for the double inverted pendulum

In this section a nonlinear model for the double inverted pendulum on a cart is derived. This model includes the effect of friction force between the cart and rail, in addition to the effect of disturbances acting at the cart and each of the two links.

2.3.1 Nonlinear model

The mathematical model for the double inverted pendulum consists of a set of three second-order nonlinear ordinary differential equations, these equations are derived using Lagrange's approach discussed earlier in this chapter. The DIPC system is represented graphically in Fig. 2.3, where the friction force and the disturbances acting on the system are included, so as to be modeled and counted for during controller design and simulation. Based on Fig. 2.3, the total kinetic energy (T) of the DIPC system, as it is the case for the single inverted pendulum, is the sum of those energies for each of the system components, i.e. kinetic energy of the motor, pulleys, in addition to that for the cart and the two links:

$$T = T_{motor} + T_{pulleys} + T_{cart} + T_{link\,1} + T_{link\,2} \tag{2-28}$$

In more details:

$$T = \frac{1}{2}J\dot{\theta}_m^2 + \frac{1}{2}M\dot{x}^2 + \frac{1}{2}J_1\dot{\theta}_1^2 + \frac{1}{2}m_1 v_{1mg,1}^2 + \frac{1}{2}J_2\dot{\theta}_2^2 + \frac{1}{2}m_2 v_{1mg,2}^2 \tag{2-29}$$

Where:

J : is the equivalent mass moment of inertia for the motor, and pulleys.

θ_m : is the angular displacement of the motor.

The angular displacement of the motor (θ_m) is related to the displacement of the cart by the radius of the pulley, as shown in Eq. (2-4) and repeated again here:

$$\theta_m = \frac{x}{r_p} \quad \rightarrow \quad \dot{\theta}_m = \frac{\dot{x}}{r_p} \tag{2-30}$$

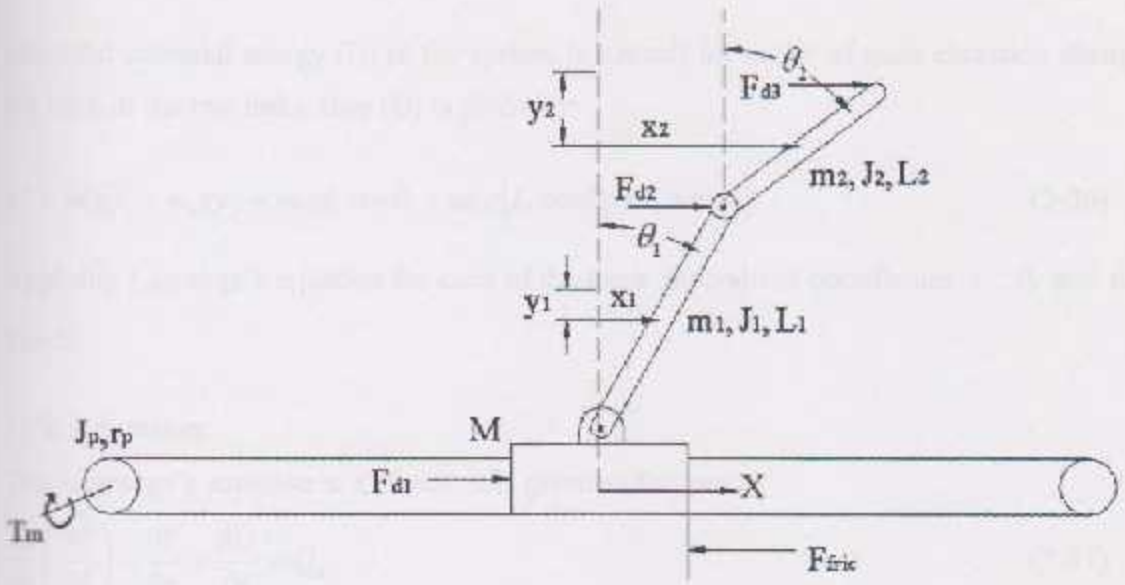

Figure 2.3 Double inverted pendulum system.

Where: M: Mass of the Cart. m_1: Mass of the link1.
m_2: Mass of the link2. J_1: Mass moment of inertia of the link1.
J_2: Mass moment of inertia of the link2. l_1: Distance to center of mass of the link1.
l_2: Distance to center of mass of the link2. J_p: Mass moment of inertia of the pulleys.
r_p: Radius of the pulley. T_m: Input torque from the motor.
F_{fric}: Friction force. d: the motor viscous damping coefficient.
F_{d1}: Disturbance force acting at the cart. F_{d2}: Disturbance force acting at the first link.
F_{d3}: Disturbance force acting at the second link.

The kinetic energy of each link is a result of the tangential and angular velocities of its center of mass. That tangential velocity consists of two components, horizontal and vertical, as follows

- For the first link:

$$x_1 = l_1 \sin\theta_1 + x \quad \rightarrow \quad \dot{x}_1 = l_1\dot{\theta}_1 \cos\theta_1 + \dot{x} \tag{2-31}$$

$$y_1 = l_1 \cos\theta_1 \quad \rightarrow \quad \dot{y}_1 = -l_1\dot{\theta}_1 \sin\theta_1 \tag{2-32}$$

- For the second link:

$$x_2 = x + L_1 \sin\theta_1 + l_2 \sin\theta_2 \quad \rightarrow \quad \dot{x}_2 = \dot{x} + L_1\dot{\theta}_1 \cos\theta_1 + l_2\dot{\theta}_2 \cos\theta_2 \tag{2-33}$$

$$y_2 = L_1 \cos\theta_1 + l_2 \cos\theta_2 \quad \rightarrow \quad \dot{y}_2 = -\left(L_1\dot{\theta}_1 \sin\theta_1 + l_2\dot{\theta}_2 \sin\theta_2\right) \tag{2-34}$$

Substituting Eqs. (2-30) to (2-34) in Eq. (2-29) yields:

$$T = \frac{1}{2}\left(M + \frac{J}{r_p^2}\right)\dot{x}^2 + \frac{1}{2}J_1\dot{\theta}_1^2 + \frac{1}{2}J_2\dot{\theta}_2^2 + \frac{1}{2}m_1\left[\left(\dot{x} + l_1\dot{\theta}_1\cos\theta_1\right)^2 + \left(l_1\dot{\theta}_1\sin\theta_1\right)^2\right]$$

$$+\frac{1}{2}m_2\left[\left(\dot{x} + L_1\dot{\theta}_1\cos\theta_1 + l_2\dot{\theta}_2\cos\theta_2\right)^2 + \left(L_1\dot{\theta}_1\sin\theta_1 + l_2\dot{\theta}_2\sin\theta_2\right)^2\right] \tag{2-35}$$

The total potential energy (U) in the system is a result for center of mass elevation change for each of the two links, thus (U) is given by:

$$U = m_1 g y_1 + m_2 g y_2 = m_1 g l_1 \cos\theta_1 + m_2 g\left[L_1 \cos\theta_1 + l_2 \cos\theta_2\right] \tag{2-36}$$

Applying Lagrange's equation for each of the three generalized coordinates x , θ_1 and θ_2, yields:

1) In x direction:

The Lagrange's equation in x direction is given as follows:

$$\frac{d}{dt}\left(\frac{\partial T}{\partial \dot{x}}\right) - \frac{\partial T}{\partial x} + \frac{\partial U}{\partial x} = Q_x \tag{2-37}$$

Where:

$$\frac{\partial T}{\partial \dot{x}} = M\dot{x} + m_1\left(\dot{x} + l_1\dot{\theta}_1\cos\theta_1\right) + m_2\left(\dot{x} + L_1\dot{\theta}_1\cos\theta_1 + l_2\dot{\theta}_2\cos\theta_2\right)$$

$$\frac{\partial T}{\partial x} = 0$$

$$\frac{\partial U}{\partial x} = 0$$

$$Q_x = \frac{T_m}{r_p} - \frac{d}{r_p^2}\dot{x} - F_{fric} + f_{d1} + f_{d2} + f_{d3}$$

Applying Eq. (2-37) and simplifying it yields:

$$\left(M + m_1 + m_2 + {}^{J}\!/_{r_p^2}\right)\ddot{x} + \left(m_1 l_1 + m_2 L_1\right)\cos\theta_1\ddot{\theta}_1 + \left(m_2 l_2 \cos\theta_2\right)\ddot{\theta}_2 - \dot{\theta}_1^2\left(m_1 l_1 + m_2 L_1\right)\sin\theta_1$$

$$-\dot{\theta}_2^2 m_2 l_2 \sin\theta_2 = {}^{T}\!/_{r_p} - \frac{d}{r_p^2}\dot{x} - F_{fric} + f_{d1} + f_{d2} + f_{d3} \tag{2-38}$$

2) In θ_1 direction:

The Lagrange's equation in θ_1 direction is given as follows:

$$\frac{d}{dt}\left(\frac{\partial T}{\partial \dot{\theta}_1}\right) - \frac{\partial T}{\partial \theta_1} + \frac{\partial U}{\partial \theta_1} = Q_{\theta_1} \tag{2-39}$$

Where:

$$\frac{\partial T}{\partial \dot{\theta}_1} = J_1\dot{\theta}_1 + m_1\left[\left(\dot{x} + l_1\dot{\theta}_1\cos\theta_1\right)l_1\cos\theta_1 + \left(l_1\dot{\theta}_1\sin\theta_1\right)l_1\sin\theta_1\right]$$
$$+ m_2\left[\left(\dot{x} + L_1\dot{\theta}_1\cos\theta_1 + l_2\dot{\theta}_2\cos\theta_2\right)L_1\cos\theta_1 + \left(L_1\dot{\theta}_1\sin\theta_1 + l_2\dot{\theta}_2\sin\theta_2\right)L_1\sin\theta_1\right]$$

$$\frac{\partial T}{\partial \theta_1} = m_1\left[-\left(\dot{x} + l_1\dot{\theta}_1\cos\theta_1\right)l_1\dot{\theta}_1\sin\theta_1 + l_1^2\dot{\theta}_1^2\sin\theta_1\cos\theta_1\right]$$
$$+ m_2\left[-\left(\dot{x} + L_1\dot{\theta}_1\cos\theta_1 + l_2\dot{\theta}_2\cos\theta_2\right)L_1\dot{\theta}_1\sin\theta_1 + \left(L_1\dot{\theta}_1\sin\theta_1 + l_2\dot{\theta}_2\sin\theta_2\right)L_1\dot{\theta}_1\cos\theta_1\right]$$

$$\frac{\partial U}{\partial \theta_1} = -\left(m_1 l_1 g\sin\theta_1 + m_2 L_1 g\sin\theta_1\right)$$

$$Q_{\theta_1} = f_{d2}L_1\cos\theta_1 + f_{d3}L_1\cos\theta_1$$

Applying Eq. (2-39) and simplifying it yields:

$$\left(m_1 l_1 + m_2 L_1\right)\cos\theta_1\ddot{x} + \left(m_1 l_1^2 + m_2 L_1^2 + J_1\right)\ddot{\theta}_1 + \left(m_2 L_1 l_2\cos(\theta_1 - \theta_2)\right)\ddot{\theta}_2$$
$$+\left(m_2 L_1 l_2\sin(\theta_1 - \theta_2)\right)\dot{\theta}_2^2 - \left(m_1 l_1 + m_2 L_1\right)g\sin\theta_1 = f_{d2}L_1\cos\theta_1 + f_{d3}L_1\cos\theta_1 \qquad (2\text{-}40)$$

3) In θ_2 direction:

The Lagrange's equation in θ_2 direction is given as follows:

$$\frac{d}{dt}\left(\frac{\partial T}{\partial \dot{\theta}_2}\right) - \frac{\partial T}{\partial \theta_2} + \frac{\partial U}{\partial \theta_2} = Q_{\theta_2} \qquad (2\text{-}41)$$

Where:

$$\frac{\partial T}{\partial \dot{\theta}_2} = J_2\dot{\theta}_2 + m_2\left[\left(\dot{x} + L_1\dot{\theta}_1\cos\theta_1 + l_2\dot{\theta}_2\cos\theta_2\right)l_2\cos\theta_2 + \left(L_1\dot{\theta}_1\sin\theta_1 + l_2\dot{\theta}_2\sin\theta_2\right)l_2\sin\theta_2\right]$$

$$\frac{\partial T}{\partial \theta_2} = m_2\left[-\left(\dot{x} + L_1\dot{\theta}_1\cos\theta_1 + l_2\dot{\theta}_2\cos\theta_2\right)l_2\dot{\theta}_2\sin\theta_2 + \left(L_1\dot{\theta}_1\sin\theta_1 + l_2\dot{\theta}_2\sin\theta_2\right)l_2\dot{\theta}_2\cos\theta_2\right]$$

$$\frac{\partial U}{\partial \theta_2} = -m_2 l_2 g\sin\theta_2$$

$$Q_{\theta_2} = f_{d3}L_2\cos\theta_2$$

Applying Eq. (2-41) and simplifying it yields:

$$\left(m_2 l_2\cos\theta_2\right)\ddot{x} + \left(m_2 L_1 l_2\cos(\theta_1 - \theta_2)\right)\ddot{\theta}_1 + \left(m_2 l_2^2 + J_2\right)\ddot{\theta}_2 - \left(m_2 L_1 l_2\sin(\theta_1 - \theta_2)\right)\dot{\theta}_1^2$$
$$-m_2 l_2 g\sin\theta_2 = f_{d3}L_2\cos\theta_2 \qquad (2\text{-}42)$$

Equations (2-38), (2-40) and (2-42) that describe the double inverted pendulum on a cart dynamics can be written in a more compact form as follows:

$$\begin{bmatrix} M+m_1+m_2+J/r_p^2 & (m_1l_1+m_2L_1)\cos\theta_1 & m_2l_2\cos\theta_2 \\ (m_1l_1+m_2L_1)\cos\theta_1 & m_1l_1^2+m_2L_1^2+J_1 & m_2L_1l_2\cos(\theta_1-\theta_2) \\ m_2l_2\cos\theta_2 & m_2L_1l_2\cos(\theta_1-\theta_2) & m_2l_2^2+J_2 \end{bmatrix} \begin{bmatrix} \ddot{x} \\ \ddot{\theta}_1 \\ \ddot{\theta}_2 \end{bmatrix} + \begin{bmatrix} d/r_p^2 \\ 0 \\ 0 \end{bmatrix} \dot{x}$$

$$\begin{bmatrix} 0 & -\dot{\theta}_1^2(m_1l_1+m_2L_1)\sin\theta_1 & -\dot{\theta}_2^2m_2l_2\sin\theta_2 \\ 0 & 0 & \dot{\theta}_2^2m_2L_1l_2\sin(\theta_1-\theta_2) \\ 0 & -\dot{\theta}_1^2m_2L_1l_2\sin(\theta_1-\theta_2) & 0 \end{bmatrix} + \begin{bmatrix} 0 \\ -(m_1l_1+m_2L_1)g\sin\theta_1 \\ -m_2l_2g\sin\theta_2 \end{bmatrix} +$$

$$\begin{bmatrix} 1 \\ 0 \\ 0 \end{bmatrix} F_{fric} = \begin{bmatrix} 1/r_p \\ 0 \\ 0 \end{bmatrix} T_m + \begin{bmatrix} 1 & 1 & 1 \\ 0 & L_1\cos\theta_1 & L_1\cos\theta_1 \\ 0 & 0 & L_2\cos\theta_2 \end{bmatrix} \begin{bmatrix} f_{d1} \\ f_{d2} \\ f_{d3} \end{bmatrix}$$

(2-43)

In order to evaluate the friction force, the normal force is to be firstly found. Based on Fig. 2.4:

$$N = (M+m_1+m_2)g - (m_1l_1+m_2L_1)\sin\theta_1\ddot{\theta}_1 - m_2l_2\sin\theta_2\ddot{\theta}_2 - (m_1l_1+m_2L_1)\dot{\theta}_1^2\cos\theta_1 - m_2l_2\cos\theta_2\dot{\theta}_2^2 \quad (2\text{-}44)$$

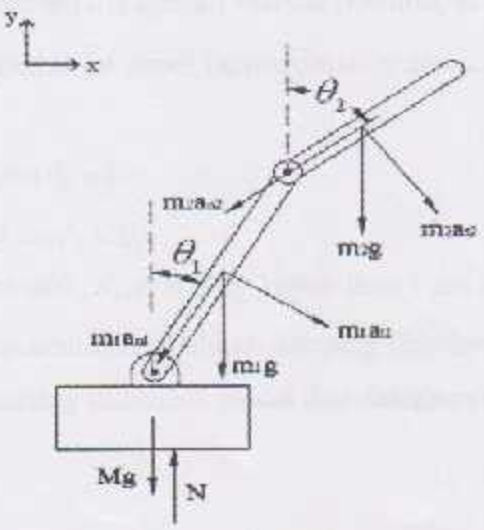

Figure 2.4 Double inverted pendulum friction force.

Where: N: normal force, a_t: the tangential acceleration, a_n: the normal acceleration

The friction force consists of two components, static friction and dynamic friction as shown in Fig. 2.5. These components can be expressed as follows:

$$F_{fric} = \mu_{static} N * \delta(\dot{x}) + \mu_{dynamic} N * Sgn(\dot{x}) \qquad (2\text{-}45)$$

Where $\delta(\dot{x})$ and $Sgn(\dot{x})$ are given in Eqs. (2 -17) and (2 -18) respectively.

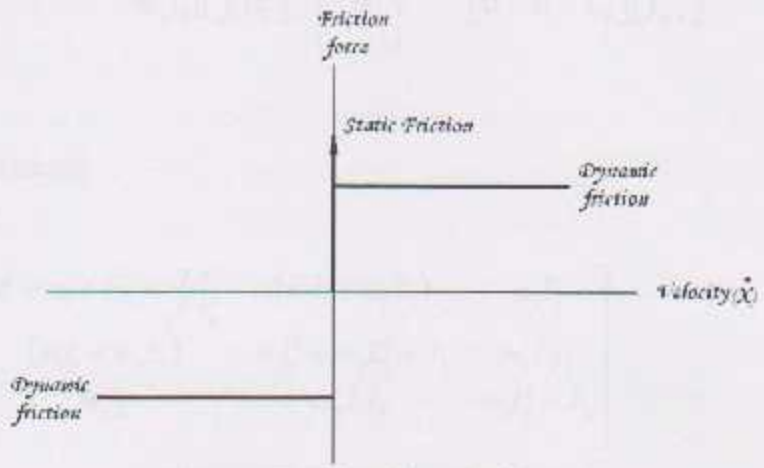

Figure 2.5 Static and dynamic friction.

2.3.2 Linear model

In order to obtain the linear model for the DIPC, an operating point is to be selected first. This point is chosen to represent the upright vertical position, in other words x, θ_1 , θ_2 and their derivatives are assumed to be small (approximately zero). Thus it could be assumed that:

- $\cos\theta_1 = 1$ and $\cos\theta_2 = 1$.
- $\sin\theta_1 = \theta_1$ and $\sin\theta_2 = \theta_2$.
- All of the orders of $\theta_1, \theta_2, \dot{\theta}_1$ and $\dot{\theta}_2$ higher than 1 are equal to 0.
- The effect of the nonlinear coulomb damping (friction) is ignored.

Based on Eq.(2.43) the resulting linearized model that describes the system in the operating region is:

$$\begin{bmatrix} M+m_1+m_2+J/r_p^2 & (m_1l_1+m_2L_1) & m_2l_2 \\ (m_1l_1+m_2L_1) & m_1l_1^2+m_2L_1^2+J_1 & m_2L_1l_2 \\ m_2l_2 & m_2L_1l_2 & m_2l_2^2+J_2 \end{bmatrix} \begin{bmatrix} \ddot{x} \\ \ddot{\theta}_1 \\ \ddot{\theta}_2 \end{bmatrix} + \begin{bmatrix} d/r_p^2 & 0 & 0 \\ 0 & 0 & 0 \\ 0 & 0 & 0 \end{bmatrix} \begin{bmatrix} \dot{x} \\ \dot{\theta}_1 \\ \dot{\theta}_2 \end{bmatrix}$$

$$\begin{bmatrix} 0 & 0 & 0 \\ 0 & -(m_1l_1+m_2L_1)g & 0 \\ 0 & 0 & -m_2l_2g \end{bmatrix} \begin{bmatrix} x \\ \theta_1 \\ \theta_2 \end{bmatrix} = \begin{bmatrix} 1/r_p \\ 0 \\ 0 \end{bmatrix} T_m + \begin{bmatrix} 1 & 1 & 1 \\ 0 & L_1 & L_1 \\ 0 & 0 & L_2 \end{bmatrix} \begin{bmatrix} f_{d1} \\ f_{d2} \\ f_{d3} \end{bmatrix} \qquad (2\text{-}46)$$

Defining the matrices:

- Mass matrix:

$$M = \begin{bmatrix} M+m_1+m_2+J/r_p^2 & (m_1l_1+m_2L_1) & m_2l_2 \\ (m_1l_1+m_2L_1) & m_1l_1^2+m_2L_1^2+J_1 & m_2L_1l_2 \\ m_2l_2 & m_2L_1l_2 & m_2l_2^2+J_2 \end{bmatrix} \qquad (2\text{-}47)$$

- Damping matrix:

$$D_m = \begin{bmatrix} d/r_p^2 & 0 & 0 \\ 0 & 0 & 0 \\ 0 & 0 & 0 \end{bmatrix} \qquad (2\text{-}48)$$

- Quasi stiffness matrix:

$$K = \begin{bmatrix} 0 & 0 & 0 \\ 0 & -(m_1l_1+m_2L_1)g & 0 \\ 0 & 0 & -m_2l_2g \end{bmatrix} \qquad (2\text{-}49)$$

- Input matrix:

$$B = \begin{bmatrix} 1/r_p \\ 0 \\ 0 \end{bmatrix} \qquad (2\text{-}50)$$

- Disturbance matrix:

$$B_d = \begin{bmatrix} 1 & 1 & 1 \\ 0 & L_1 & L_1 \\ 0 & 0 & L_2 \end{bmatrix} \tag{2-51}$$

From the previous matrices, one could note:

- The mass matrix is symmetrical, regular and positive definite matrix.
- The system has dynamic coupling only in the mass matrix while there is no static coupling in the stiffness matrix.
- The stiffness matrix (K) is a destabilizing matrix, since it tends to take the system away from its operating region.

Using the matrices defined by Eqs. (2-47) to (2-51), Eq. (2-46) can be expressed as:

$$M\ddot{x} + D_m\dot{x} + Kx = BT + B_d f_d \tag{2 -52}$$

Where:

$$x = [x \quad \theta_1 \quad \theta_2]^T$$

To yield the state-space representation for the linear system, six states are needed. These are chosen to be $x, \theta_1, \theta_2, \dot{x}$, $\dot{\theta}_1$, and $\dot{\theta}_2$. The input to the system is the motor torque (T_m). As the system is equipped with the necessary sensors, the six states are the measurable outputs of the system[1]. Based on the previous discussion, the state-space model of the DIPC system is expressed as follows:

$$\begin{bmatrix} \dot{x} \\ \ddot{x} \end{bmatrix} = \begin{bmatrix} 0 & I_2 \\ -M^{-1}k & -M^{-1}D_m \end{bmatrix} \begin{bmatrix} x \\ \dot{x} \end{bmatrix} + \begin{bmatrix} 0 \\ M^{-1}B \end{bmatrix} T + \begin{bmatrix} 0 \\ M^{-1}B_d \end{bmatrix} f_d$$
$$y = I_6 \begin{bmatrix} x \\ \dot{x} \end{bmatrix} \tag{2.53}$$

System parameters are defined in Table 2.2.

---

[1] As in the case of SIPC, Both x , θ_1 and θ_2 are directly measured, while the other three states (the velocities) are estimated using backward numerical differentiation, as shown in Chapter Six.

Table (2-2): DIPC parameters

Symbol	Description	Value	Units
M	Mass of the cart	1.45	Kg
m_1	Mass of rod1	0.33	Kg
m_2	Mass of rod2	0.132	Kg
L_1	Length of rod1	0.335	m
r_p	Radius of the pulley	0.02	m
l_1	Length of center of mass of rod1	0.2276	m
l_2	Length of center of mass of rod2	0.125	m
J_p	Moment of inertia of the 2 pulleys	1.55×10^{-4}	$Kg.m^2$
J_1	Moment of inertia of link1 about its C.O.G	0.0436	$Kg.m^2$
J_2	Moment of inertia of link2 about its C.O.G	6.98×10^{-4}	$Kg.m^2$
g	Gravitational constant	9.81	m/s^2

Substituting the values given in Table 2.2 in matrices (2 -47) to (2 -51), then in Eq. (2 -53), yields:

$$\begin{bmatrix} \dot{x} \\ \dot{\theta}_1 \\ \dot{\theta}_2 \\ \ddot{x} \\ \ddot{\theta}_1 \\ \ddot{\theta}_2 \end{bmatrix} = \underbrace{\begin{bmatrix} 0 & 0 & 0 & 1 & 0 & 0 \\ 0 & 0 & 0 & 0 & 1 & 0 \\ 0 & 0 & 0 & 0 & 0 & 1 \\ 0 & -0.67 & -0.25 & -0.65 & 0 & 0 \\ 0 & 18.3 & -4.5 & 8.32 & 0 & 0 \\ 0 & -32.6 & 69.1 & 2.2 & 0 & 0 \end{bmatrix}}_{A} \begin{bmatrix} x \\ \theta_1 \\ \theta_2 \\ \dot{x} \\ \dot{\theta}_1 \\ \dot{\theta}_2 \end{bmatrix} + \underbrace{\begin{bmatrix} 0 \\ 0 \\ 0 \\ 22.3 \\ -28.7 \\ -75.9 \end{bmatrix}}_{B} T_m +$$

$$\underbrace{\begin{bmatrix} 0 & 0 & 0 \\ 0 & 0 & 0 \\ 0 & 0 & 0 \\ 0.45 & 0.25 & -0.18 \\ -0.57 & 4.67 & -3.27 \\ -1.52 & -10.84 & 110.78 \end{bmatrix}}_{B_d} \begin{bmatrix} f_{d1} \\ f_{d2} \\ f_{d3} \end{bmatrix} \tag{2.54}$$

$$y = \underbrace{I_6}_{C} \begin{bmatrix} x & \theta_1 & \theta_2 & \dot{x} & \dot{\theta}_1 & \dot{\theta}_2 \end{bmatrix}^T \tag{2 -55}$$

Chapter Three

Electrical Components and Interfacing

3.1 Introduction

As a mechatronic system, electrical part is an essential component of the DIPC. This part includes the sensors and the actuator used in the system, in addition to the interfacing circuits necessary to connect those sensors and actuators with the controller, which is implemented using a desktop PC.

In DIPC system, and as stated in earlier chapters, it is desired to establish a closed-loop control system that is able to stabilize the two links in the upright vertical position while tracking a desired position of the cart along the track. To achieve that, sensors are used to measure the outputs of the system (i.e. cart position, the angle between the first link and the cart, and the angle between the two links), and feed them back to the controller which is a desktop computer working under xPC target environment, as will be discussed later. The controller role is to generate the suitable actuating signal, and send it to the servomotor driver, which in turn commands the motor to generate the desired torque value. To connect these sensors and the actuator to the controller, two data acquisition cards are used with external conditioning and filtering circuits. Figure 3-1 shows the basic connections between the electrical components. Each of these components will be discussed in the upcoming sections.

3.2 AC servomotor and driver

Servomotors are used in closed-loop control systems in three modes of control, position velocity, and torque control modes. In DIPC system a high-performance AC servomotor is used to meet the requirements of smooth rotation down to stall with full control of torque, and fast accelerations and decelerations, and accurate torque control ability. The servo driver is connected to a PC based controller that generates a voltage signal related to the amount of torque to be generated by the motor. An incremental optical encoder is incorporated within the servomotor. This provides the servomotor's position and velocity feedback signals, which are used by the controller.

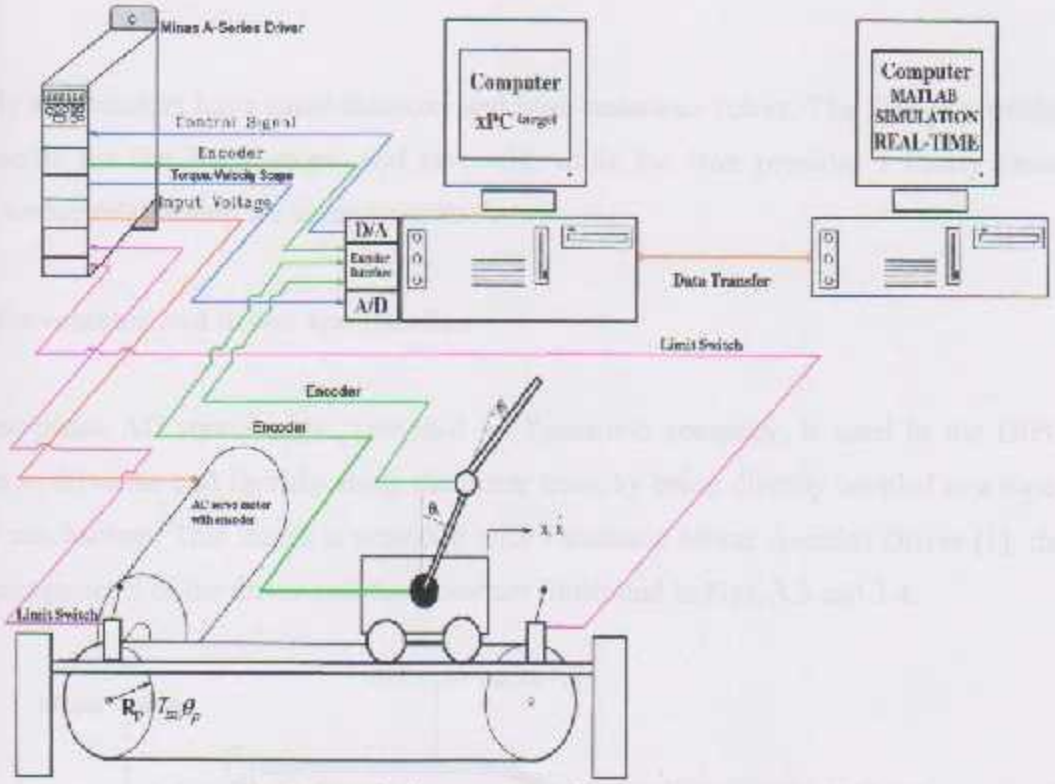

Figure 3.1 Schematic diagram shows the electrical part of the DIPC.

In fact, the concept of the loop within a loop is applied in DIPC system, where the servomotor driver is considered as the inner loop of the control system, which is responsible to generate the required torque value according to the voltage command generated by the outer loop. The inner loop is selected to be much faster than the outer loop, so as to get the required torque instantaneously. Figure 3.3 shows the inner/outer loop relationship.

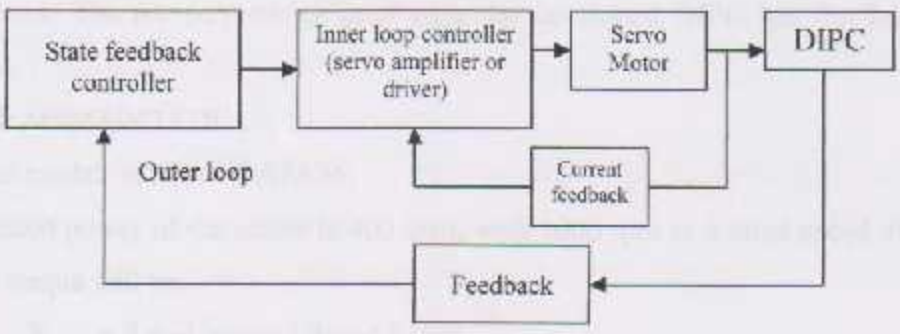

Figure 3.2 The loop-within-a-loop controller.

Usually servomotors have small-diameter and high-resistance rotors. The former provides low inertia for fast starts, stops, and reversals, while the later provides a nearly linear speed-torque relationship for accurate control.

3.2.1 Servomotor and driver specification

A three phase AC servo motor, provided by Panasonic company, is used in the DIPC system to drive the cart linearly along the linear track by being directly coupled to a rope-pulley mechanism. This motor is provided with Panasonic Minas A-series Driver [1], the main components of the driver and the motor are illustrated in Figs. 3.3 and 3.4.

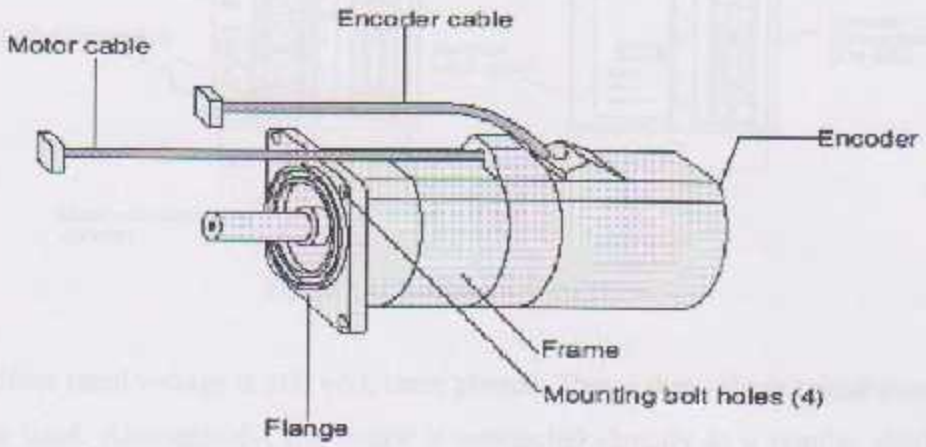

Figure 3.3 AC Servo Motor Components.

This AC servomotor meets the requirements of low inertia, high torque at low speed, and accurate control. The Ac servomotor used with the developed DIPC has the following specifications.

Motor model: MSMA042A1E.

- Driver model: MSDA043A2A26.
- The rated power of the motor is 400 watt, with 3000 rpm as a rated speed, thus the rated torque will be:

$$T_{rated} = \text{Rated Power} / \text{Rated Speed}$$
$$= 400 / 314.6 = 1.273 \text{ N.m.}$$

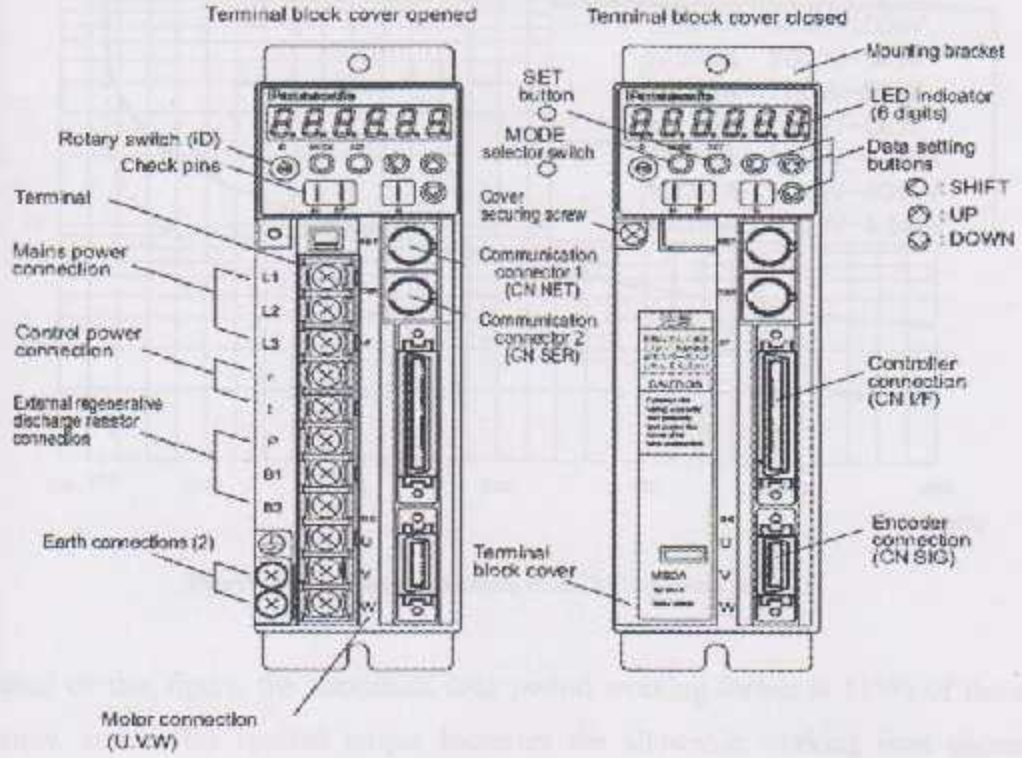

Figure 3.4 Components of the driver.

- Motor rated voltage is 200 volt, three phases. Thus a three phase transformer should be used. Alternatively, the motor is connected directly to a regular single phase instead of three.
- The encoder provided with this model is an incremental encoder that generates 2500 pulse per revolution as a maximum value.
- Allowable radial and thrust loads on the shaft of the motor during operation is:

  Radial load = 245 N.

  Thrust load = 98 N.
- Over load protection over time: The motor provides a protection against over load, thus it can run while over loaded for a specified interval of time depending on the overloading value, as shown in the Fig. 3.5.

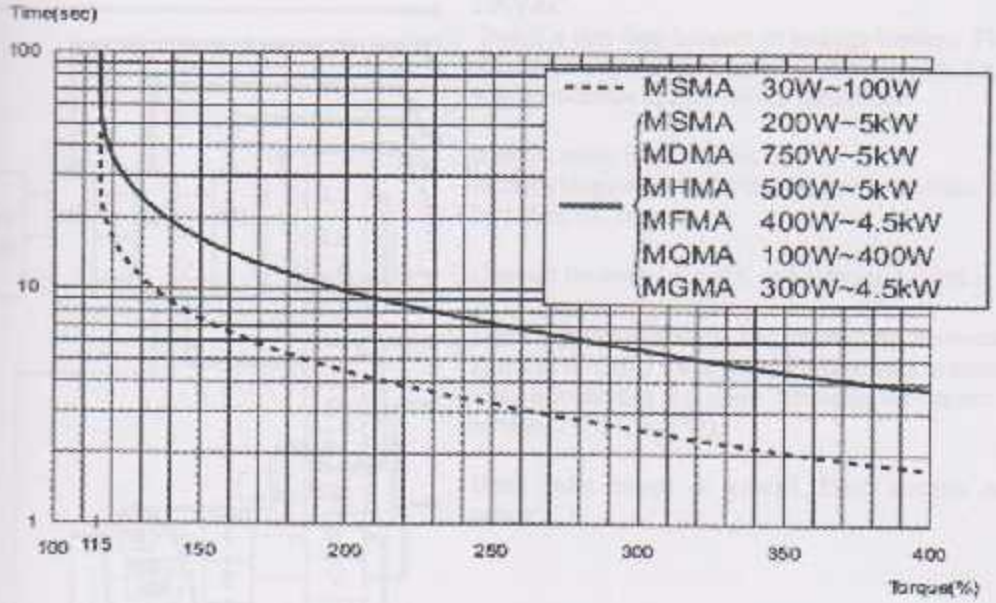

Figure 3.5 Overload protection, time limiting characteristics.

Based on this figure, the maximum long period working torque is 115% of the rated torque, and as the applied torque increases the allowable working time decreases. Mina's driver provides a limiting of the instantaneous torque generated by the motor, this limit is set by the parameter (Pr5E) as will be shown later.

3.2.2 AC servo motor connection

Figure 3.6 shows the connections between the main power supply, the driver and the servomotor. Other components are connected as follows:

- Encoder cable is connected to the CN SIG connector "shown in Fig.3-4", and it should be at least 30 cm from the main power lines.
- CN SER connector is connected to the RS232C of the PC, so that the PANATERM software could be used.
- CN I/F connector is used for controller connections, as will be shown later.

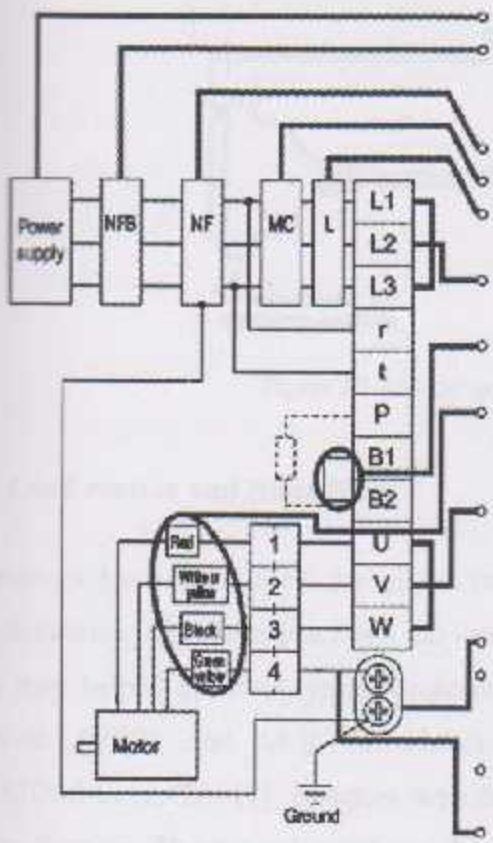

200VAC
Install a non-fuse breaker or leakage breaker. The latter should be a special one intended for inverters, i.e. with a countermeasure against higher harmonics.

Install a noise filter without fail.
Install a surge absorber to the magnetic contactor coil.
Install an AC reactor.

Connect between L1 and r, and between L3 and t.

Don't remove the short bar connecting between B1 and B2. Remove this only when an external resistor is connected.
Ensure matching in color between the motor wires and terminals (U, V and W).

Don't short circuit or ground. Don't connect to the main power.

Connect to the grounding system of the facility.
Never fail to connect between the driver's protective earth terminal and control board's protective earth terminal (PE) in order to avoid electric shocks.
No multiple connections to a single earth terminal permissible. There are two earth terminals.

Figure 3.6 Schematic diagram shows the connections of the main circuit of Minas- A series AC servomotor driver

3.2.3 Additional Components

Additional components could be used with the motor and its driver; such components improve motor performance, provide protection, and increase the flexibility. These components include:

1. Communication cable

Special cable (RS232C) can be used to connect the motor driver with PC. Such a connection enables the user to set motor parameters and monitor the response of motor using graphical interface.

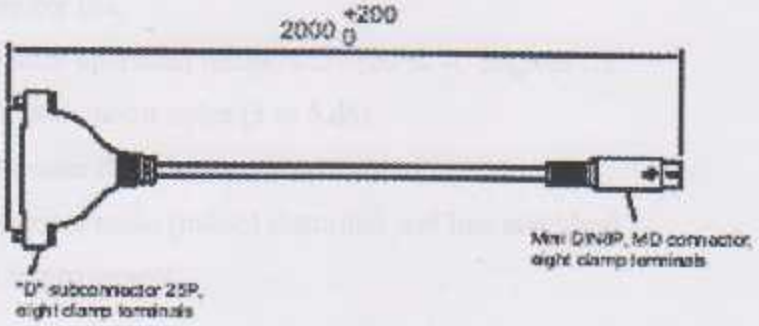

Figure 3.7 RS232C used to connect the driver with PC.

2. Load reactor and Noise filter

Reactors have been used for many years to solve problems in variable speed drive installations. About ten years ago the use of line reactors started to become more common as they helped to solve typical problems on the input (line side) of variable frequency drives (VFD) and SCR (Thyristor) controllers which include the driver type (MSDA043A2A26) [1]. Reactors are often used as low cost substitutes for 1:1 isolation transformers. The typical problems that line reactors solve are drive nuisance tripping, voltage notch reduction (for SCR controllers) and harmonic attenuation. Load reactors are usually called "line reactors" because they were always used on the "line side" or input of a variable speed drive. Attempts to use "line reactors" on the output side of a drive tended to fail, because line reactors typically overheated due to the harmonic content of the output waveform [5].

In DIPC system, the need to line reactor and noise filter appear due to the noise effects on the rectifier that supplies the encoder of motor, the input voltage of encoder was very noisy, which significantly affects encoder's readings. With the Noise filter, the readings were improved, but still need a special interfacing circuit, which are discussed later in this chapter.

The benefits of using line reactors and noise filters can be summarized as follows:

- Attenuation of line harmonics.
- Extended switching component life (transistors, SCRS).

- Extended motor life.
- Reduced motor operating temperature (20 to 40 degrees C).
- Reduced audible motor noise (3 to 5 db).
- Minimized power disturbances.
- Filtered electrical noise (pulsed distortion and line notching).
- Waveform improvement.

3.2.4 Operation at torque control mode

One of the advantages of Minas A-series driver is that its ability to provide three modes of control; position control, velocity control, and torque control modes, in addition to hybrid modes of control, velocity and torque for example. In the case of DIPC, torque control mode is used during system operation, where the torque value generated by the motor is determined according to a voltage command applied to the motor. This control mode is achieved using external circuit connected to the CN I/F connector. Table 3.1 shows the main connections in the torque control mode. The basic parameters used in this mode of control are demonstrated in Table 3.2. While Fig. 3.8 shows the basic connection for torque control mode.

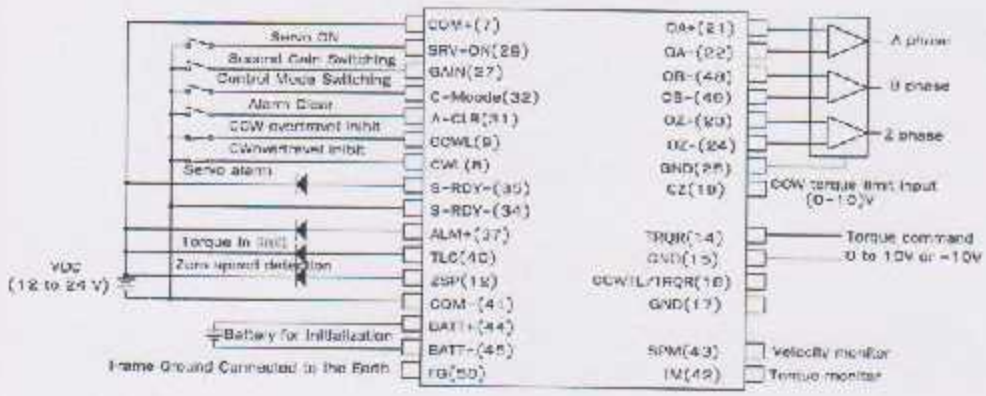

Figure 3.8 CN I/F connection of the Minas-A diver in torque control mode.

Table 3.1 CN I/F main connections in torque control mode.

Terminal Name	CN I/F Pin Number	Description and Connection
COM+	7	Connected to the positive terminal of the external power supply (12-24 volt)
COM-	41	Connected to the negative terminal of the external power supply (12-24 volt)
Servo on	29	After setting all parameters, close its connection to COM- enables the motor.
Alarm clear	31	Closing the connection with COM- clears the alarms.
Torque input	14	Analog torque command input.
GND	15	Ground terminal for Analog torque command.
Torque monitor output	42	Outputs an analog voltage related to the actual torque.
Speed moniter output	43	Outputs an analog voltage related to the motor speed. The relation between the speed and output voltage is sat by the parameter (Pr07).
GND	17	Ground terminal for both output pins 42 and 43.
CWL	8	CW over travel inhibitor.
CCWL	9	CCW over travel inhibitor.

Table 3.2 Parameters used in torque control mode.

<table>
<tr><th>Parameter Number</th><th>Description</th></tr>
<tr><td>Pr02</td><td>Set this parameter to (2), to select the torque control mode.</td></tr>
<tr><td>Pr04</td><td>Set this parameters to (0), in order to enable the CW and CCW over travel inhibit.</td></tr>
<tr><td>Pr07</td><td>One can select/set-up the relationship between the voltage to be fed-out to the speed monitor signal output (SPM: CN I/F Pin 43) and the actual velocity or commanded velocity of the motor.
<table>
<tr><th>Value</th><th>SPM signal</th><th>Relationship between output voltage level and velocity</th></tr>
<tr><td>0</td><td rowspan="5">Actual motor velocity</td><td>6V / 47 r/min</td></tr>
<tr><td>1</td><td>6V / 187 r/min</td></tr>
<tr><td>2</td><td>6V / 750 r/min</td></tr>
<tr><td>3</td><td>6V / 3000 r/min</td></tr>
<tr><td>4</td><td>1.5V / 3000 r/min</td></tr>
<tr><td>5</td><td rowspan="5">Commanded velocity</td><td>6V / 47 r/min</td></tr>
<tr><td>6</td><td>6V / 187 r/min</td></tr>
<tr><td>7</td><td>6V / 750 r/min</td></tr>
<tr><td>8</td><td>6V / 3000 r/min</td></tr>
<tr><td>9</td><td>1.5 V / 3000 r/min.</td></tr>
</table></td></tr>
<tr><td>Pr08</td><td>Set this parameter to (0), so that the torque monitor signal terminal (IM: CN I/F Pin 42) outputs 3 volt per rated torque.</td></tr>
<tr><td>Pr44</td><td>Specifies the number of the Encoder's output pulses per turn (1-2500).</td></tr>
<tr><td>Pr56</td><td>Defines the velocity limit (in rpm) at torque control mode.</td></tr>
<tr><td>Pr58</td><td>Specifies the acceleration time (in 2 ms/1000 rpm).</td></tr>
<tr><td>Pr59</td><td>Specifies the deceleration time (in 2 ms/1000 rpm).</td></tr>
<tr><td>Pr5A</td><td>Specifies the S-shaped acceleration\deceleration time (in 2 ms).</td></tr>
<tr><td>Pr5C</td><td>Set-up the relationship between the motor torque and the voltage applied to the torque command input (TRQR: CN I/F pin 14).
• The unit of this parameter is [0.1V/100%].
• The default value of 30 corresponds to 3V/rated torque</td></tr>
<tr><td>Pr5D</td><td>Used to invert the polarity of the torque command input signal, the default is [0].
<table>
<tr><th>Value</th><th>Direction of motor torque</th></tr>
<tr><td>0</td><td>CCW torque with (+) commands</td></tr>
<tr><td>1</td><td>CW torque with (+) commands</td></tr>
</table></td></tr>
<tr><td>Pr5E</td><td>Sets the maximum instantaneous torque as a percentage of the rated torque.</td></tr>
</table>

The Minas A-series driver provides some operation inhibitors, to equip the user with more control ability and enhanced safety features. In torque control mode, which is the mode of

interest in DIPC system, over travel inhibit is of significant importance to secure the system from over travel dangers, the basic properties of this feature and how to use it is explained in the following subsection.

Over travel inhibit

For linear motion and other similar motions, over traveling of the work may cause mechanical damages. To avoid this, it is necessary to provide a limit switches at each end so that traveling over the limit switch position can be inhibited, as indicated in the Fig. 3.9.

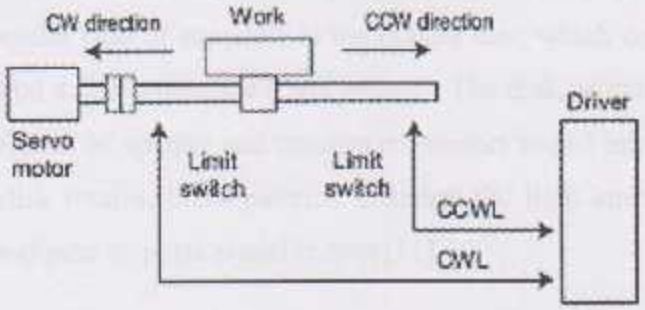

Fig 3.9 CW and CCW over travel inhibit.

The limit switch that is used to limit the motion in the CCW direction must be connected between the COM- and CCWL (CN I/F pins 9 and 41) in normally closed situation, and the one used for CW direction must be connected between the COM- and CCWL (CN I/F pins 8 and 41) in normally closed situation too.

It should be noted that the parameter Pr04 "over travel inhibit" must be set to "0" in order to enable this feature, otherwise the over travel inhibit is disabled and the system will not stop even if it passes over the limit switch.

3.3 Sensors

In order to build a closed loop control system for the DIPC, sensors are used to read the outputs of the system and feed them back to the controller. The sensors used in this project are incremental optical encoders.

3.3.1 Optical encoders

An encoder is a device that converts linear or rotary displacement into digital or pulse signals. The most popular type of encoders is the optical one, which consists of a rotating disk, a light source, and a photo detector (light sensor). The disk, which is mounted on the rotating shaft, has patterns of opaque and transparent sectors coded into the disk as shown in Fig.3.10. As the disk rotates, these patterns interrupt the light emitted onto the photo detector, generating a digital or pulse signal output [11].

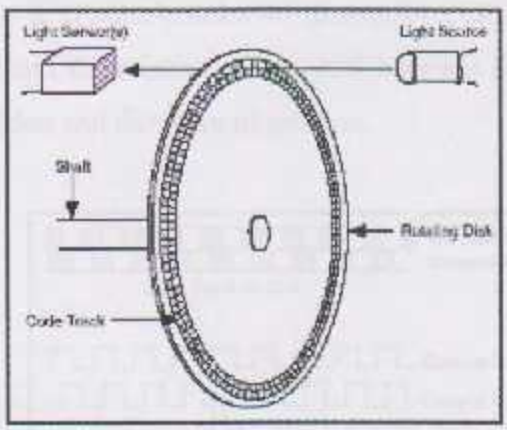

Figure 3.10 basic operation of encoder

There are two general types of encoders, absolute and incremental encoders.

- **Absolute Encoders**: An absolute encoder generates a unique word pattern for every position of the shaft. The tracks of the absolute encoder disk, generally four to six, are usually coded to generate binary code, binary-coded decimal (BCD), or gray code outputs. Absolute encoders are most commonly used in applications where the device will be inactive for long periods of time, there is risk of power down, or the starting position is unknown.

- **Incremental Encoders**: An incremental encoder generates a pulse, as opposed to an entire digital word, for each incremental step. Although the incremental encoder does not output absolute position, it does provide more resolution at a lower price. An incremental encoder with a single code track, referred to as a tachometer encoder, generates a pulse signal whose frequency indicates the velocity of displacement. However, the output of the single-channel encoder does not indicate direction. To determine direction, a two-channel, or quadrature, encoder with two detectors and two code tracks should be used.

  Quadrature encoders are the most common type of incremental encoders. This type generates two output channels (A and B) to sense position and direction, using two code tracks with sectors positioned 90° out of phase as shown in Fig. 3.11, the two output channels of the quadrature encoder indicate both position and direction of rotation. If A leads B, the disk is rotating in a clockwise direction, otherwise, the disk is rotating in a counter-clockwise direction. Therefore, by monitoring the number of pulses and the relative phase shift between signals A and B, one can track both the position and direction of rotation.

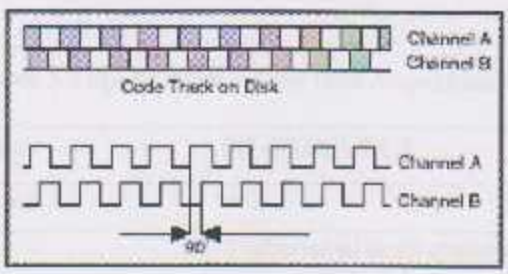

Figure 3.11 Rotary encoder output phases.

  The third output of quadrature encoder is phase Z, this output gives an indication that one complete cycle (360°) is passed, therefore it could be used to determine the home position of the encoder.

As stated earlier, three optical encoders are used in the DIPC system, these encoders are located at the joint between the two links, at the cart-link1 joint, and the third is provided with the servomotor as shown in Fig.3.1.

3.4 Data Acquisition Cards (DAQ)

Two data acquisition cards are used, one is supplied by National Instruments, while the other by Measurements Computer.

3.4.1 NI 6024E

This product is classified as general purpose data acquisition card. The function of this DAQ in DIPC is to send analog signal from the computer to the servomotor driver to generate the required torque signal, in addition to receive other analog and digital commands discussed later. Table 3.3 shows the specifications of the NI6024E card [9].

Figure 3.12 National Instruments Data Acquisition Card series.

Table 3.3 Specifications of the Data Acquisition Card.

DAQ family	**NI 6024E PCI**
Analogue Input	
Channels	8 differential or 16 single ended
Input Resolution	12 bits
Input Range	±0.05 to ±10 V
Analogue Output	
Channels	2 outputs
Output Resolution	12 bits
Output Range	±10 V
Current Drive	5mA max.

3.4.1.1 DAQ Connections

Table 3.4 summarizes the pins that are used with the NI6024E DAQ. These terminals are used for sending the control signal, i.e. torque command, receiving feedback signals representing the motor's actual velocity and the generated torque, in addition to receive the digital switching commands as explained in Chapter Six of this report.

Table 3.4 DAQ pins that are used within DIPC system.

DAQ Pins	Description
Pin 22	Analogue output
Pin 55	GND
Pin 68	Analog input
Pin 67	GND
Pin 52	Digital input
Pin 18	Digital GND

To protect the DAQ card from high voltage input and high current loads, an analog isolation circuit is used to isolate the servomotor driver form the DAQ card ports as shown in Fig. 3.19. The function of this circuit is discussed in details in section 3.6.1.

3.4.2 PCI-QUAD04

DIPC system is sensitive to noise interference, and error may occur while reading the position from sensors. So, in electrical design, special and robust equipment must be selected. PCI-QUAD04 provides accurate readings from the encoders since it has special counters, and filtering circuits.

The PCI-QUAD04 is a PCI plug-in board that provides inputs and decoding for up to four quadrature incremental encoders. It can be also used as a high speed pulse counter for general counting applications.

Figure 3.13 PCI-QUAD04

The PCI-QUAD04 provides inputs for three basic signals, phase A, phase B, and Index. Using these signals, the controller can determine system position (counts), velocity (counts per second), and the direction of rotation. Table 3.5 summarizes the basic input specifications of the PCI-QUAD04 DAQ [10].

Table 3.5 PCI-QUAD04 specifications.

Receiver type	SN75ALS175 quad differential receiver
Connection configuration	Each channel consists of Phase A input, Phase B input and Index input; each input has a switch (jumper) used to select among as single-ended or differential input modes. Differential ▪ Phase A, Phase B and Index (+) inputs at user connector routed to (+) inputs of differential receiver. ▪ Phase A, Phase B and Index (-) inputs at user connector routed to the (-) inputs of differential receiver. Single - ended ▪ Phase A, Phase B and Index (+) inputs at user connector routed to (+) inputs of differential receiver. ▪ Phase A, Phase B and Index (-) inputs at user connector routed to ground. (-) inputs of differential receiver routed to +3 V reference.
Number of channels	4
Common mode input voltage range	+12 V max.
Differential input voltage range	±12 V max.

The main differences between the NI6024E counters and those of the PCI-QUAD04 are summarized in Table 3.6.

Table 3.6 Differences between PCI-QUAD04 and NI6024E counters.

	PCI-QUAD04	**NI6024E**
Number of counters	Support four encoders	Support only two encoders
input	Have two modes, single-ended and differential.	Single-ended mode only
Input range	±12 volt maximum at single-ended and differential modes.	±5.5 volt maximum
Direction	Specify the direction automatically	Uses the digital inputs to specify the direction
Noise filter	Have noise filter	Don't have noise filter
Phase Z	Support phase Z	Not supported
Isolation	Not required (but used for more protection)	Needed (output the encoders is 12 Volt)
Resolution	Can multiply the resolution by four	The same resolution

3.5 Computer system

There are two computers used to control the DIPC system, one of them has the two DAQ cards, as discussed in the previous section, in addition to a special network card to connect between the two PCs. More information about the computer system are demonstrated in the following chapter.

3.6 Signal conditioning and technical issues

Interfacing circuits are used to connect the data acquisition cards I/O ports with the three optical encoders and the servomotor driver. Some of these circuits tend to provide protection for these devices by isolating the high power sides from the low ones. Other interfacing circuits are used for signal conditioning and filtering in order to eliminate noise effects, thus more reliable and more accurate data necessary for precise control system are obtained.

3.6.1 Isolation methods

Signal isolation is used to separate sensor signals which can be exposed to high voltages from data acquisition card inputs that operate at low voltage levels. The need and importance of isolation circuits are summarized with the following points:

- Protecting equipment from transient voltages.
- Improving noise immunity.
- Eliminating earth looping.
- Increasing common-mode voltage rejection.
- Providing protection against bad connection.

Two main methods for isolation implemented are used in this project, which are:

- Optical isolation: which is used for isolating digital signals similar to those generated by optical encoders. With this method the original signal is applied to the LED side, while the output is obtained from the phototransistor side, where the light emitted by the LED represents the only connection between the two sides. The main advantage of using of using optical isolation is its immunity to electrical and magnetic interferences, but on the other hand, transmission speed, high-power dissipation, and LED wear are the main drawbacks that should be taken into account when using optical isolation.

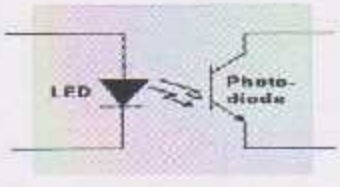

Figure 3.14 Optical isolator.

To overcome the transition speed problem, special optical isolation chips, 6N137, shown in Fig. 3.15, are used. This chip has a transition rate up to 10Mbd which is suitable to isolate the high frequency incremental encoders output from the DAQ input ports.

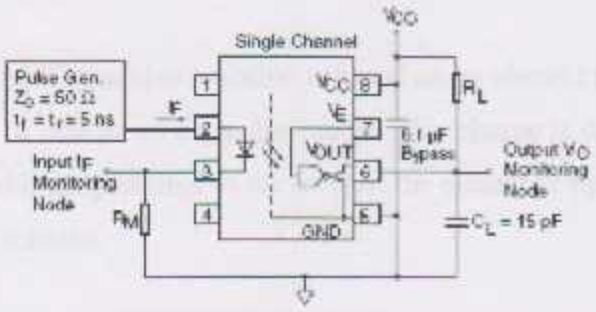

Figure 3.15 6N137 Opt-coupler connections.

Figure 3.16 shows a schematic for the entire digital isolation circuit used to isolate the PCI-Quad04 inputs from encoder outputs, using the 6N137 opt-couplers.

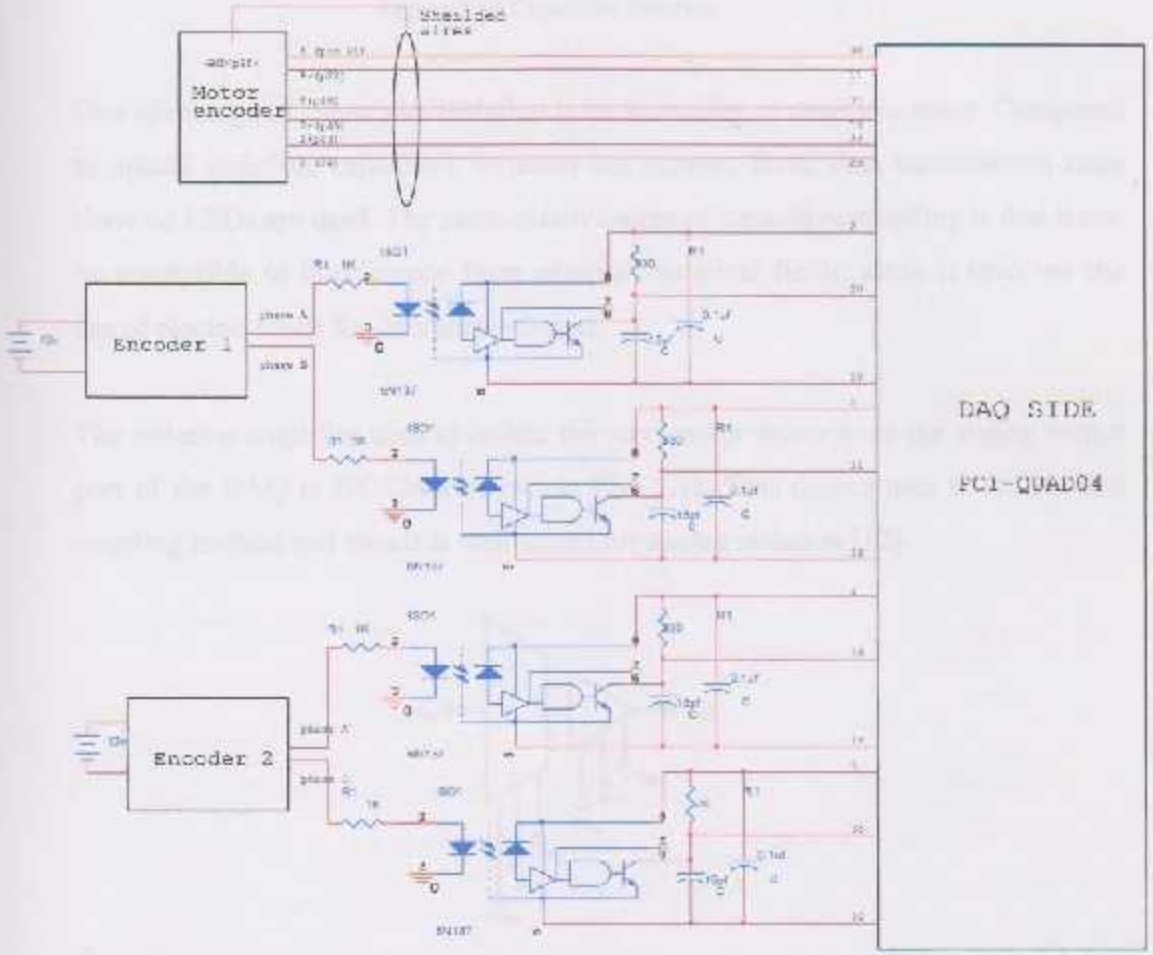

Figure 3.16 The interfacing circuit used to connect encoders with the PCI_Quad04 counters.

- Capacitive coupling: Capacitive isolation is based on an electric field that changes based on the level of charge on capacitor plates. This charge is detected across an isolation barrier and is proportional to the level of the measured signal. This method is used for analog isolation.

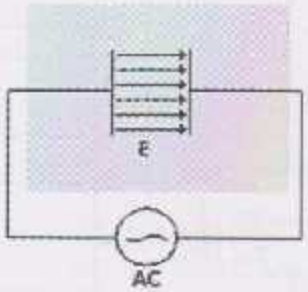

Figure 3.17 Capacitive isolation.

One advantage of capacitive isolation is its immunity to magnetic noise. Compared to optical isolation, capacitive isolation can support faster data transmission rates since no LEDs are used. The main disadvantage of capacitive coupling is that it can be susceptible to interference from external electrical fields; since it involves the use of electric fields for data transmission.

The isolation amplifier used to isolate the servomotor driver from the analog output port of the DAQ is ISO124P, shown in Fig. 3.18. This device uses the capacitive coupling method and thus it is well suited for analog isolation [12].

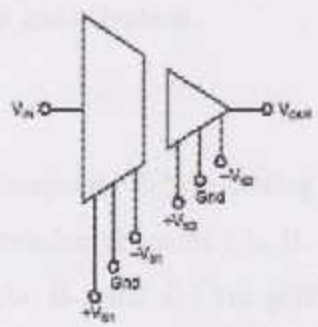

Figure 3.18 ISO124P.

The detailed interfacing circuit used for analog isolation is demonstrated in Fig. 3.19. This circuit provides a full isolation between the NI6024E analog output port at the computer side, and the torque command input port at the driver side. Thus protecting the DAQ from overloading and misconnections.

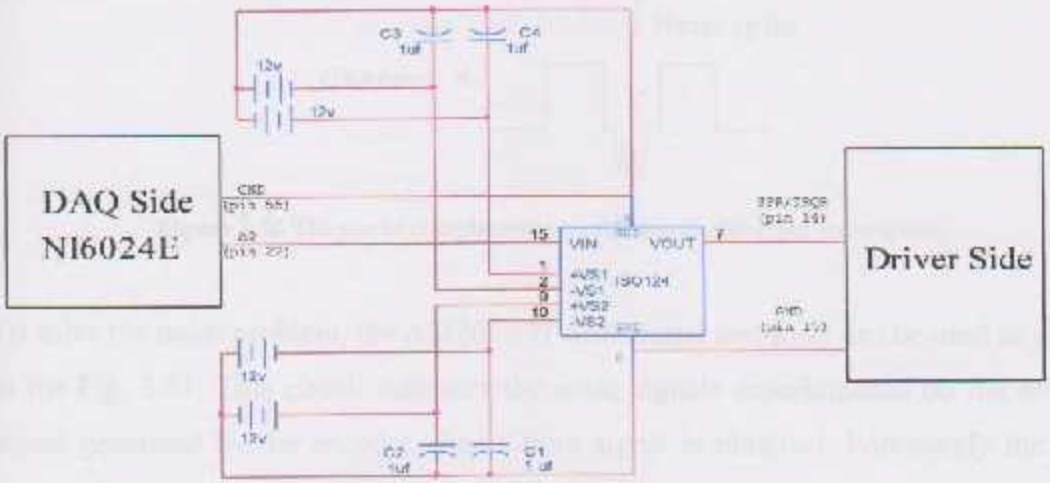

Figure 3.19 Connection between controller and driver used in torque control.

3.6.2 Digital noise filter

The purpose of the digital noise filter is to remove any kind of noise that may affect the measurement signals. A part of this noise comes from the environment due to electromagnetic fields generated by the servomotor or by communications. Other sources of noise are due to the motion or vibration of the motor. Quadrature encoders face two basic types of noise; noise spike and vibration.

- **Noise Spike**

  Noise due to electrical and magnetic fields existing in the operating environment affect the output signals of the encoder channels (A, B, and Z). To eliminate such effects, complementary channels (A-, B-, and Z-) are generated by the encoder and used for protection against noise, as shown in Fig. 3.20. In this case, the same level of noise is

present on each channel. By using differential amplifier, the noise will be subtracted and a pure signal will be obtained.

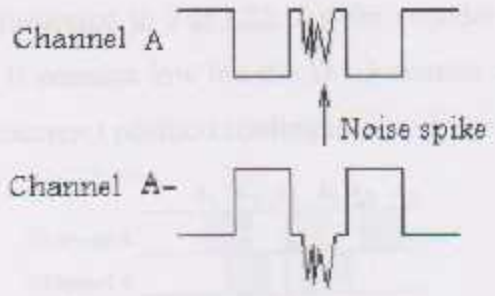

Figure 3.20 The use of complementary channels to eliminate noise spikes.

To solve the noise problem, the AM26LS32 differential amplifier can be used as shown in the Fig. 3.21. This circuit subtracts the noise signals superimposed on the original signal generated by the encoder, thus a pure signal is obtained. Fortunately the PCI-Quad04 DAQ provides built-in differential circuits that solve the noise problems, eliminating the need for such a circuit. More information about this amplifier, internal circuits, technical specifications and connections are available at [15].

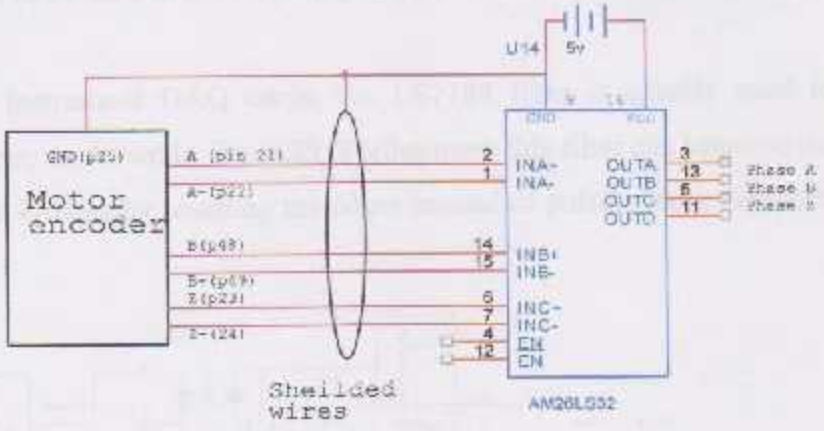

Figure 3.21 Differential amplifier connected with the encoder of servo motor.

In this project, the hardest environmental conditions, in terms of noise, is faced by the servomotor encoder, due to the electromagnetic field generated by the motor. So it is necessary to use the differential mode of the PCI_QUAD04 for this encoder, to get rid of noise problems.

- **Vibration**

If the encoder disk is not rotating, but is vibrating back and forth enough to cause active transitions on Channel A, then each movement will be incorrectly counted. The effect of this dither motion is illustrated in Fig.3.22. As the encoder disk moves back and forth across A2, Channel B remains low but the DAQ counter continues to increment the count, resulting in an incorrect position readings.

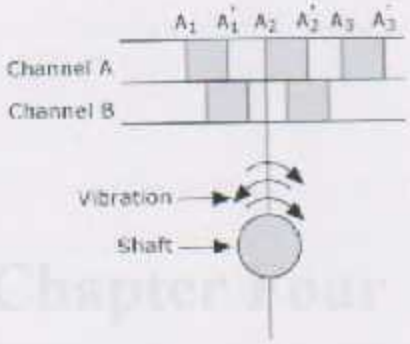

Figure 3.22 The vibration occurred at the edge of A which counted as a valid state.

The PCI-QUAD04 has a special digital noise filter which has the ability to handle situations such as those described earlier; thus readings obtained from it are reliable and accurate enough to be used in the control system.

With National Instrument DAQ cards, the LS7184 filter is usually used to solve the vibration problem, as shown in Fig. 3.23. Furthermore this filter can improve the resolution of encoder up to 4 times by counting the edges instead of pulses. More details are available at [14].

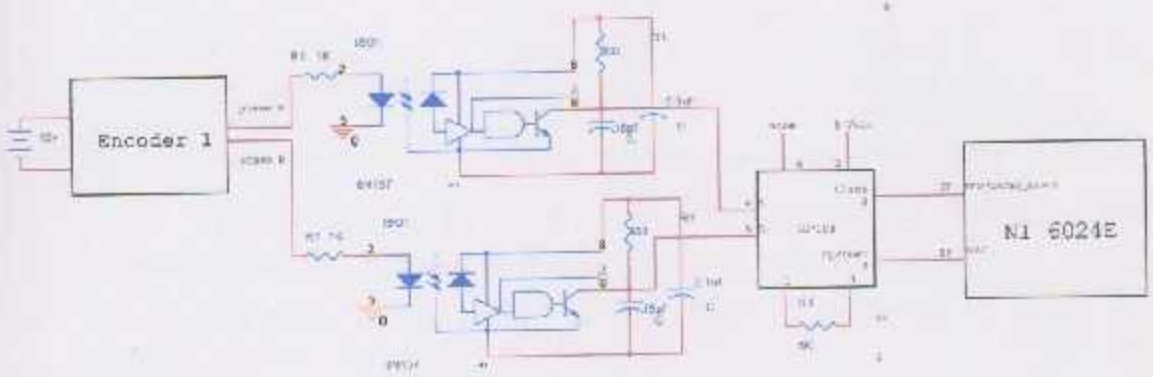

Figure 23 Interfacing encoder to NI DAQ using LS7184.

Chapter Four

Computer and Information System

4.1 Introduction

In mechatronic systems computers, microcontrollers and software packages are of significant importance during different design phases up to the final implementation of the system, which is especially true for the DIPC system. The availability of suitable software tools facilitates testing different design configurations and iterating certain design. This plays an important role in reducing the length of design cycle and can be considered as one way for rapid prototyping. Software packages are needed in design, simulation, and testing as well as managing the controller implementation. For the DIPC system, the controller should be implemented with a flexible platform with high real-time abilities required for dealing with such rapid dynamic system. So that, a special purpose software tool (xPC target technology) is used, as discussed in the coming sections.

4.2 Software environment

In DIPC system, software packages are used for design, analysis, and simulation purposes for both the mechanical and control parts of the system. MATLAB and Simulink, provides a wide variety of functions, and toolboxes that help not only to design and simulate the control system, but also to build an executable real-time applications. For the purposes of mechanical design and analysis, software packages such as CATIA and ANSYS are helpful to create three dimensional mechanical models, specify the constraints for each part, define the relations between different parts, in addition to apply loads to the system and study their effects.

4.3 MATLAB and Simulink

MATLAB is a high-performance language for technical computing, that integrates computation, visualization, and programming in an easy-to-use environment where problems and solutions are expressed in familiar mathematical notation. MATLAB provides many functions, numerical algorithms and toolboxes that help significantly to design the desired controller.

Simulink is a software package for modeling, simulating, and analyzing dynamic systems. It supports linear and nonlinear systems, modeled in continuous time, sampled time, or a hybrid of the two.

4.4 xPC target

The double inverted pendulum on a cart (DIPC) systems are usually used for educational and research purposes as test-beds for controllers and control techniques. Such systems have fast dynamic behavior, which implies that high real time control abilities are required; limiting in turn the possibility of using ordinary PCs for implementing control functions. On the other hand, the use of microcontrollers will not be suitable, since the ease with which changes in control logic are applied is an important performance criterion in such systems. One solution for such a case is the xPC target technique.

The xPC target is a solution for prototyping, testing, and deploying real-time systems using standard PC hardware and its peripheral such as DAQ cards. In this technique two PCs are used, host and target. With the host PC, one can design the controller, simulate it, and download it to the target PC. The target PC, which is connected to the controlled plant, is just used to run control functions in real-time and monitor the controlled application.

xPC target technique is considered as an excellent solution for educational and rapid prototyping purposes due to the following facts:

- Changes and modifications in controller design are easily introduced to the host PC, and the modified controller is downloaded to the target PC almost with no effort. Furthermore, online tuning of some parameters is also possible.
- Hard real time requirements can be satisfied since the target PC processor is fully dedicated for running the controller.
- Host and target PCs can be connected serially, through network or even through the internet. In addition, the target PC can operate alone without any connection with the host.

- xPC target technique supports a wide range of DAQ cards and I/O boards, which gives the designer a high level of flexibility to choose the suitable hardware.

All of that make xPC target technique an attractive solution for implementing control functions for the DIPC system, and other rapid prototyping and hardware-in-the-loop simulation purposes.

4.4.1 Rapid prototyping using xPC target technique

xPC target technique is a powerful tool for rapid prototyping processes. With the help of MATLAB, Simulink and xPC target technique, one can design, simulate and easily modify the controller for target application, and run that controller in real time. The rapid prototyping process using xPC target technique can be divided into the following sequence of steps:

1- Design the control system: MATLAB and Simulink provide a wide variety of functions and toolboxes that greatly help the designer throughout the design phases.
2- Simulate the model: after the controller has been designed, or even during the design process, it is possible to simulate that controller and check its response; thus any necessary improvements can be introduced before applying that controller to the real application.
3- Create the target application: by combining the real time workshop, xPC target and a C- compiler, an executable target application (control algorithm) is built, without any need for writing low level language programs for realizing the real-time controller.
4- Execute the target application in real time: the target PC is fully dedicated for running control algorithm for the controlled plant, resulting with high real-time abilities.
5- Monitor the target application: using xPC target scopes, it is possible to monitor the running application either on host or target PCs. Saving the signal data to a file for later use is also possible.

6- Tune parameters: after the controller has been built and downloaded to the target PC, xPC target technique permits an online modification of some controller's parameters, such as gain values, and sampling time, with no need for rebuilding that controller.

4.4.2 Hardware and Software environment

In xPC target technique, two computers are used, host and target. Furthermore a serial or network connection between those computers is necessary to build the Simulink model, monitor it, and control its operation. The hardware and software requirements for both host and target PCs are as follows:

1. Host PC requirements

- **Hardware requirements**

Any PC runs a Microsoft Windows platform supported by The MathWorks can be used as the host PC. It must also contain a 3.5-inch floppy disk drive, and a free serial port or an Ethernet adapter card as shown in Fig. 4.1.

- **Software requirement**

Table 4.3 summarizes the basic software requirements that should be satisfied by the host PC to be used in xPC target technique.

Table 4.3 Host PC requirements

Software	Description
Operating system MATLAB Simulink Real-Time Workshop	Microsoft Windows platform supported by The MathWork MATLAB Version 7.0.1 Simulink Version 6.1 Real-Time Workshop Version 6.1
C language compiler	Microsoft Visual C/C++ Professional Edition Versions 5.0, 6.0, or 7.0 Watcom C/C++ Versions or 11.0
xPC Target	xPC Target Version 2.6.1
Active X controls	Includes the .dll files to achieve the connection using network.

2. Target PC requirements

- **Hardware requirements**

The xPC Target supports up to 64 target PCs with one host. A target PC can be almost any PC with an Intel 386, 486, Pentium, or AMD K5 or K6/Athlon processor or any industrial PC, including that it has:

- 3.5 inch floppy drive.
- Free serial port or a special Ethernet card.
- The necessary I/O boards to communicate with the controlled application.

- **Software requirements.**

No operating system is required. All operations are performed using the xPC target kernel, which can be thought of as a real-time operating system, booted from the target boot disk. The xPC Target kernel has no effect on any operating system installed on the target PC, which means that the target PC can be reused directly as a normal PC after the control process ends.

Figure 4.1 summarizes the basic hardware and software components for both host and target PCs.

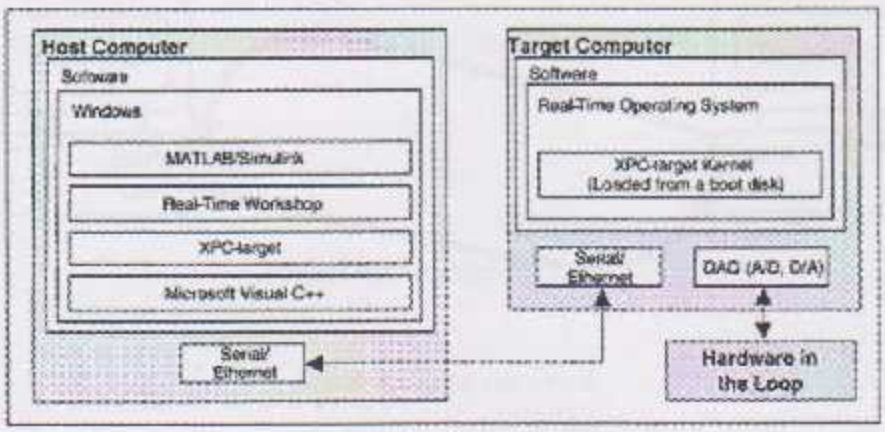

Figure 4.1 xPC target components.

4.5 xPC target operating modes

xPC target technique provides three basic modes of operation: boot disk, DOS loader and stand alone options.

4.5.1 Boot disk mode

In this mode the target PC is booted from a floppy disk that contains the xPC target kernel, while the target application, which is built in Simulink, is downloaded, controlled and monitored directly by the host PC. One major specification determined within the xPC target kernel is the communication type between the host and target PCs. xPC target technique provides two ways of host-to-target communication, which are serial and network communication.

1- Serial connection

The host and target computers are connected directly with a serial cable using their RS-232 ports. This cable is wired as a null modem link that can be up to 5 meters long and with a transfer rate between 1200 and 115200 baud Rate. Figure 4.2 shows the serial connection between the host and target PCs; while Fig. 4.3 illustrates the wiring for the cable used in serial communication for a 9-pin DB9 connector.

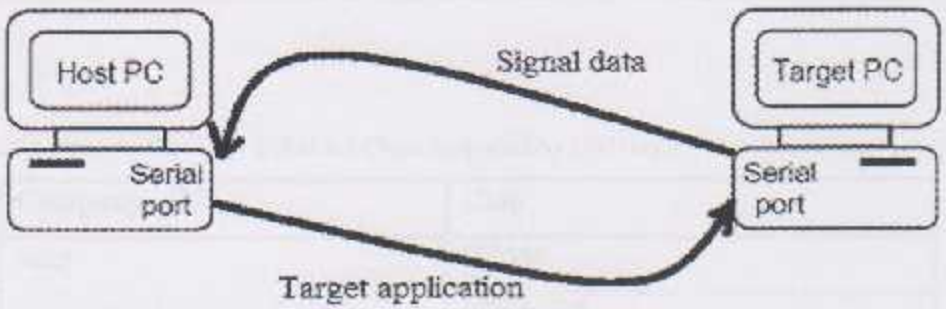

Figure 4.2 Serial connection.

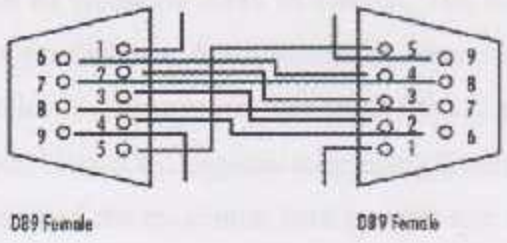

Figure 4.3 Null Model Cable connection

2- Network connection

With the network communication, the host and target PCs can be connected through a local area network (LAN), or even through internet. In this case both PCs need to have network cards. Host PC has no limitations on the card type to be used, while the target PC network card should be xPC target compatible. The following tables lists the network cards compatible with the xPC technique and the parameter needed to be select in the xPC target explorer to set the network connection.

Table 4.1 Boards supported by xPC target

Board	Identification	Setup Parameter
SME 1208BT	Card includes both BNC RJ45 connectors and an SMC label on the packaging.	NE2000
Intel Pro/100S	Card has only an RJ45 connector and an Intel label on the back of the card.	I82559

Table 4.2 Chips supported by xPC target

Company	Chip
Intel	I82559
	I82559ER
	I82550
AMD	79C97x family
	SMC91C9X

Communication cable can be crossover RJ45 or coaxial. The coaxial is better than RJ45 since it supports much longer distance. A host-to-target connection using network TCP/IP communication has the following advantages over serial RS-232 communication:

- Higher data throughput: Network communication using Ethernet can transfer data up to 100 Mbit/second instead of the maximum data transfer rate of 115 kBaud with serial communication.
- Longer distances between host and target computer: By using repeaters and gateways the distance between the host and target computers will not be restricted to the length of the connecting cable. Communication over the Internet is also possible.

4.5.2 DOS loader mode

In this mode the target PC can be booted from devices other than a floppy disk, such as a flash memory or a hard disk, while the target application is still downloaded from the host PC either by serial or network communication. Unlike the boot floppy mode, DOS loader mode needs DOS copy to be installed to the target PC boot device; in order to load and run the xPC target kernel.

4.5.3 Stand alone mode

This mode combines both the target application and the xPC target kernel on the target boot device, which can be a floppy disk, flash memory or a hard disk. Thus both the application and kernel files are booted together on the target PC, eliminating any need for the connection between the host and target PCs. The target boot device in this mode will contain the following files:

- DOS files.
- *.rtb: This file contains the xPC Target kernel.
- xpcboot.com: This file executes the Target application in addition to the *.rtb file, which represents the real-time operating system.
- autoexec.bat: calls the xpcboot.com to boot the xPC Target kernel.

4.6 xPC target procedures

During the work with the DIPC system serial, network and internet host-to-target connections are successfully achieved. Monitoring the target application using host and target scopes and data logging are also performed according to the following procedures:

4.6.1 Target boot disk

The target boot disk includes the xPC target kernel specific for either serial or network communication. To create a target boot disk for the current xPC target environment, the following procedure can be followed:

- In command window type:

  xpcsetup

  A dialog box as that in Fig. 4.4 opens, in this box the communication type between the host and target PCs can be specified to be either serial or TCP/IP communication. Selecting serial communication does not need any additional settings. While the TCP/IP needs the following parameters to be specified:

  - TCP/IP Target Address
  - TCP/IP Target port number
  - TCP/IP Target Gateway Address
  - TCP/IP subnet mask

  If the connection is performed between two networks as it the case in the internet, set the IP and Gateway address which are taken from the administrator.

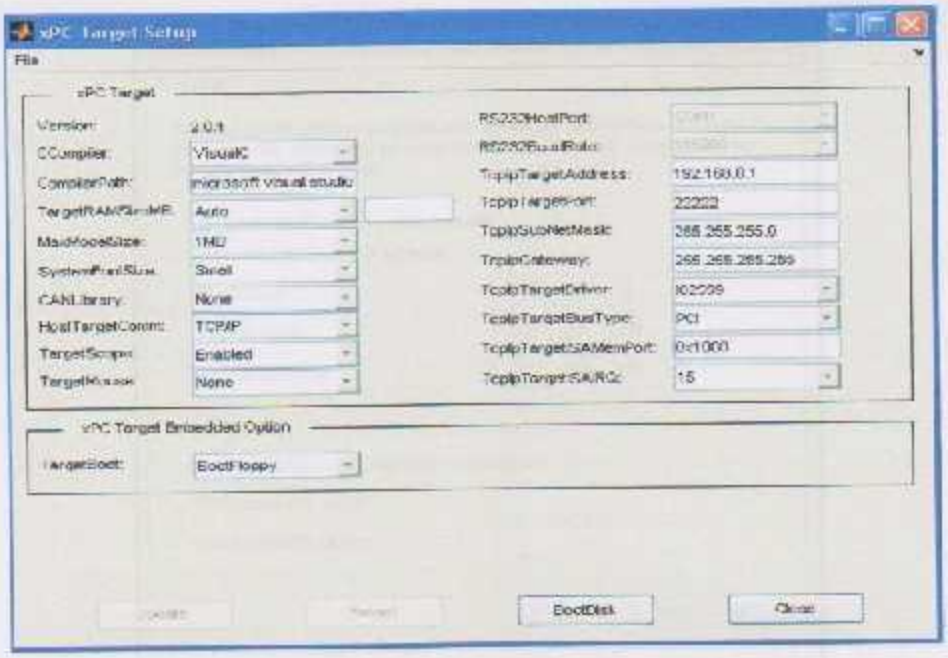

Figure 4.4 xPC Target setup.

- click update then insert a formatted floppy disk to create boot disk by clicking on "boot disk" icon.

4.6.2 Running the model using network connection

In order to run and monitor the target application using network connection using the xPC target explorer, the following procedures should be followed:

1. Setting the IP address to the host PC.

1- Select control panel.
2- Double click to Network connection.
3- Enter to the properties of network icon.
4- Enter to the internet protocol TCP/IP.
5- Choose "use the following IP address ".
6- Set 192.168.0.1 as a standard IP address.

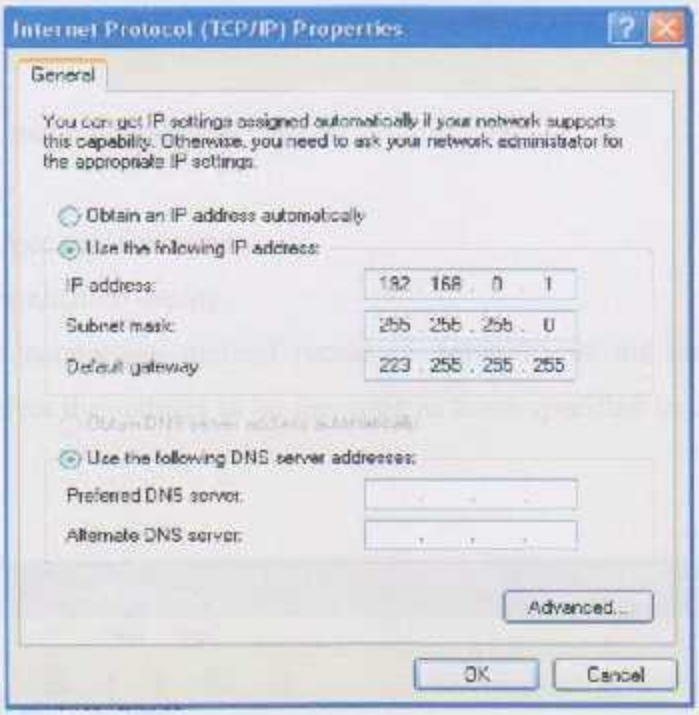

Figure 4.5 Setting IP address.

2. Registering MATLAB's active X controls

In order to make the host PC ready for communication with the target by network connection; active X controls are to be registered first. This can be achieved as follows:

1- In MATLAB command window type:

xpc_register_ocx

This function registers the Active X controllers that xPC Target Explorer requires.

2- Type

Rehash_toolbox

3- Close xPC Target Explorer.

4- Close MATLAB.

5- Restart MATLAB.

6-Restart xPC Target Explorer.

4.6.3 Running the target application:

1- In MATLAB command window type:

xpcexplr

The xPC target explorer opens.

2- Select communication setting.

3- Specify the connection method (serial or network). If the choice is through a network, select the settings to be the same as those specified in the boot disk being created.

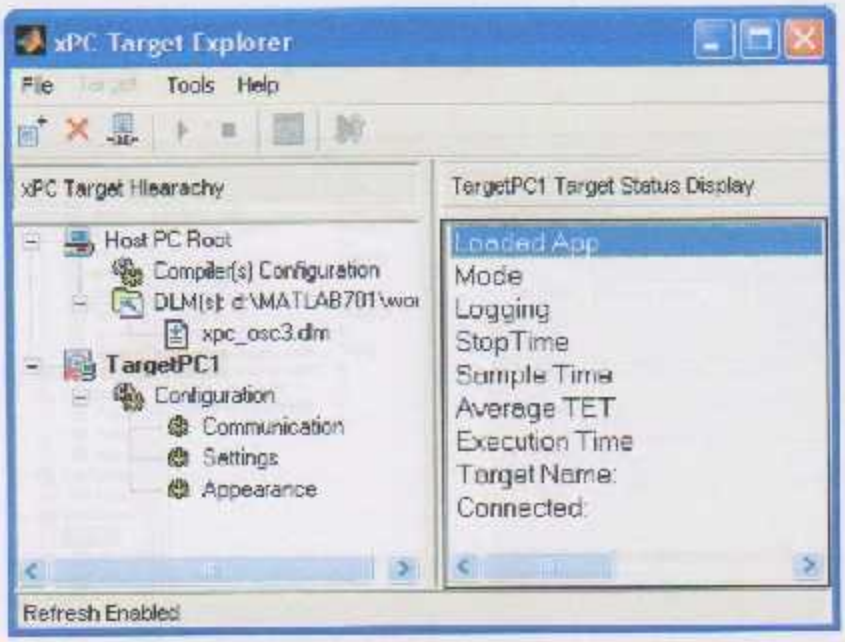

Figure 4.6 xPC target explorer

4- Right click on the targetPC1 icon, select connect.

5- From Simulink window that contains the desired application to be downloaded on the target PC, select Tools, Real-Time Workshop, and then select Build model, as shown in Fig. 4.7.

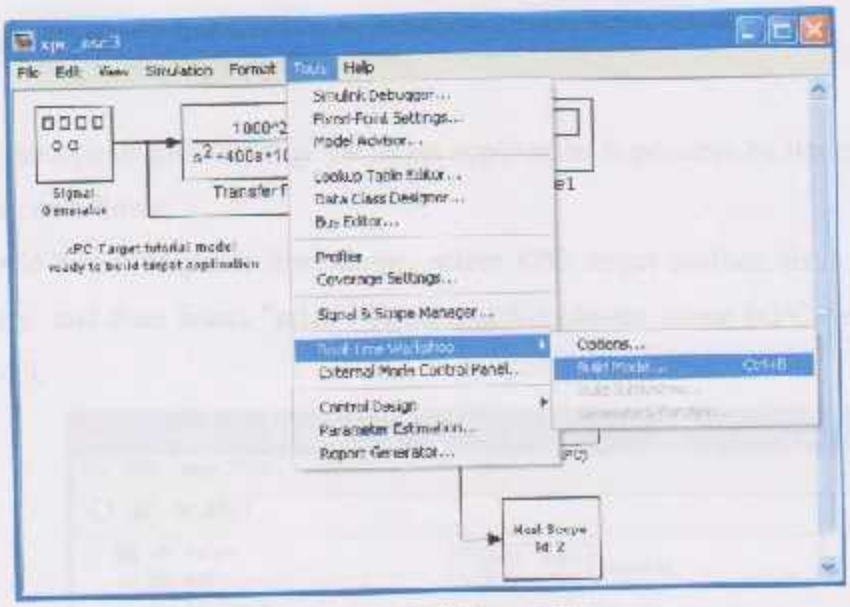

Figure 4.7 Building model.

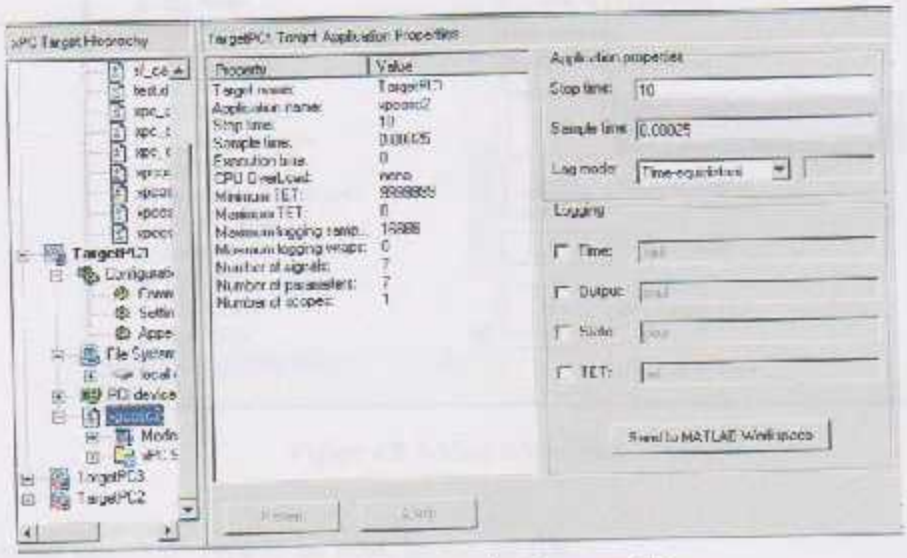

Figure 4.8 Target application properties

6- From the xPC Target Explorer toolbar, click the start application button ▶. The target application begins running on the target PC, and stops when it reaches the stop time.

7- To set the stop time, from Simulink go to configuration, choose solver , and set the final time. To have an infinity running time, type "inf" thus the target application runs until stopping it by the user, clicking the "Stop Application" button ■.

4.6.4 Monitoring target application

Monitoring the signals generated by the target application is possible by the use of host and target scopes, as follows:

1- To add target scope or host scope, select xPC target toolbox from the Simulink library, and then select "misc". From that list choose scope (xPC) as show in the Fig.4.9.

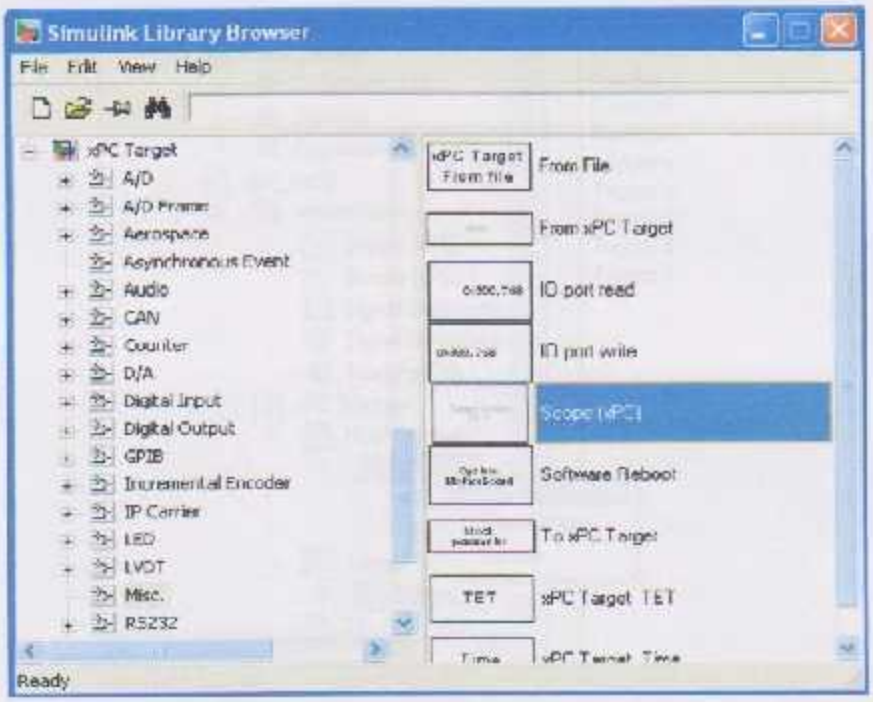

Figure 4.9 Adding xPC scopes.

2- Choose the scope type to be host, target, or file.

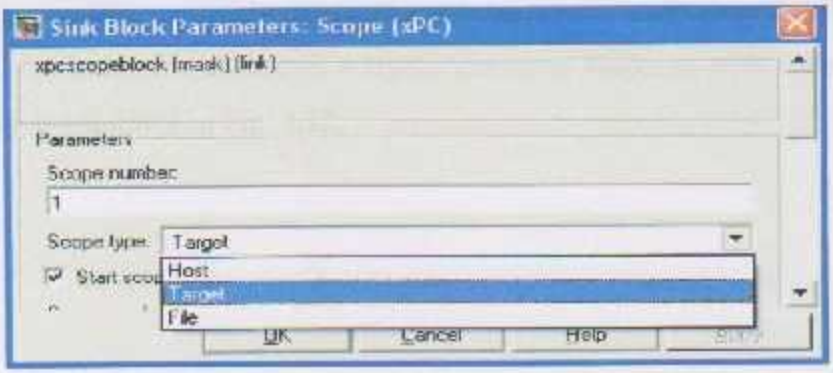

Figure 4.10 Selection of scope type.

3- From the scope properties choose the scope mode, which specifies the scope output forms, like graphical redraw or numerical.

4- Target scopes will be created automatically at the target monitor, while host scopes need to be started first. To start host scopes, from the xPC explorer select host scope node, then select view scope, start it, as shown in Fig. 4.11, after that run the model, then a graphical drawing will be displayed on the host PC monitor.

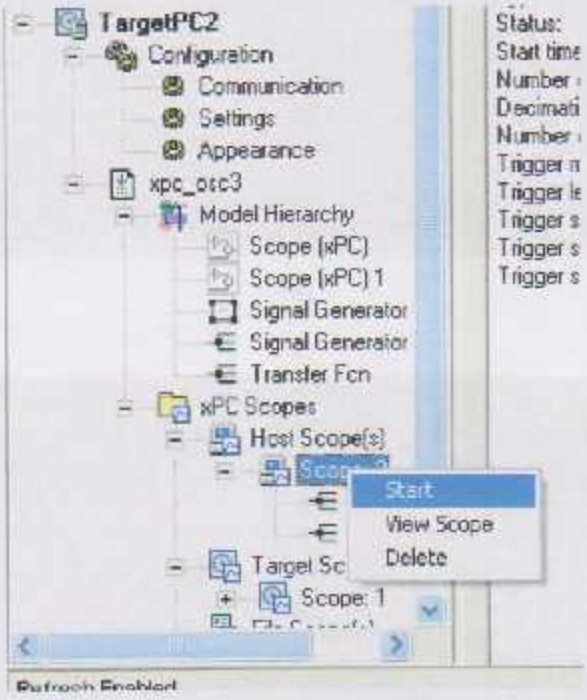

Figure 4.11 Starting Host scope.

With xPC explorer, it is possible to modify some parameters of the target application, such as the stop time, gain values, signals amplitude and frequency, switching threshold, and other parameters. An example that shows a signal generator response with different stop time and frequency is exhibited in Fig. 4.12.

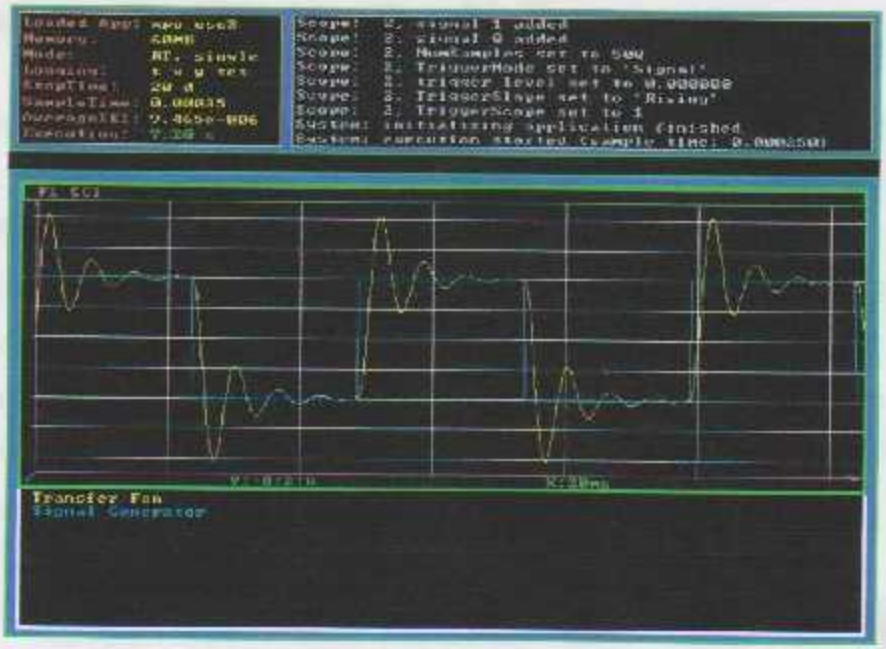

(a)

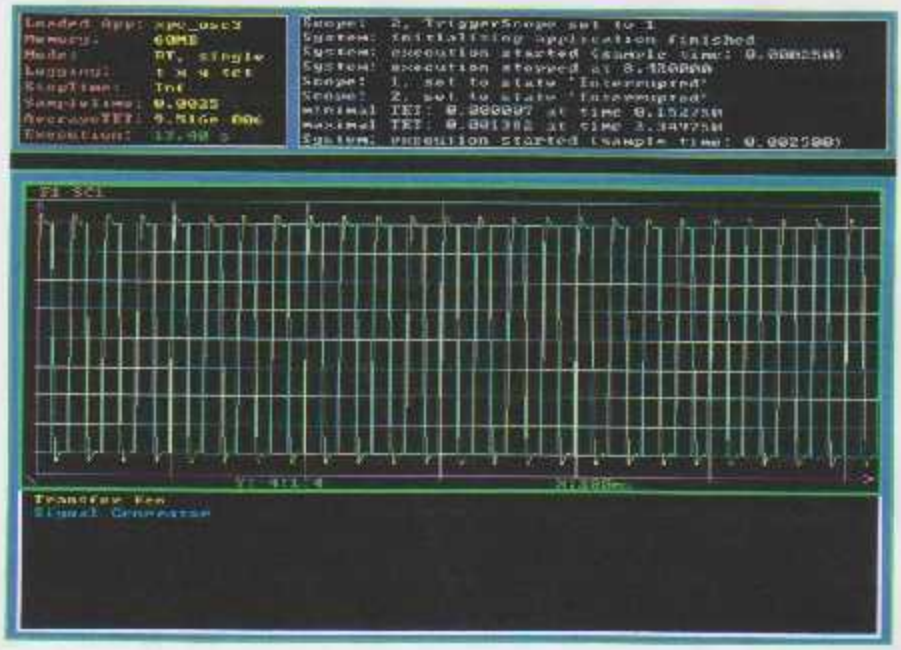

(b)

Figure 4.12 Parameter tuning using xPC target explorer.

a) With 20 sec. stop time and 25Hz signal frequency.

b) With infinite stop time and 50Hz signal frequency.

4.6.5 Data logging

xPC target technique is used for implementing real-time control systems for experimental, educational, and hardware-in-the-loop simulation purposes. This use requires in many cases acquiring the experimental results and storing them for plotting, analysis, or later use, which is achieved using the data logging feature provided by xPC target technique. Data logging is achieved using the following procedure:

- from configuration parameters, select Data Import/Export, check the boxes as shown in the figure, and select the value of "Limit data points", this value depend on the target PC memory resources.

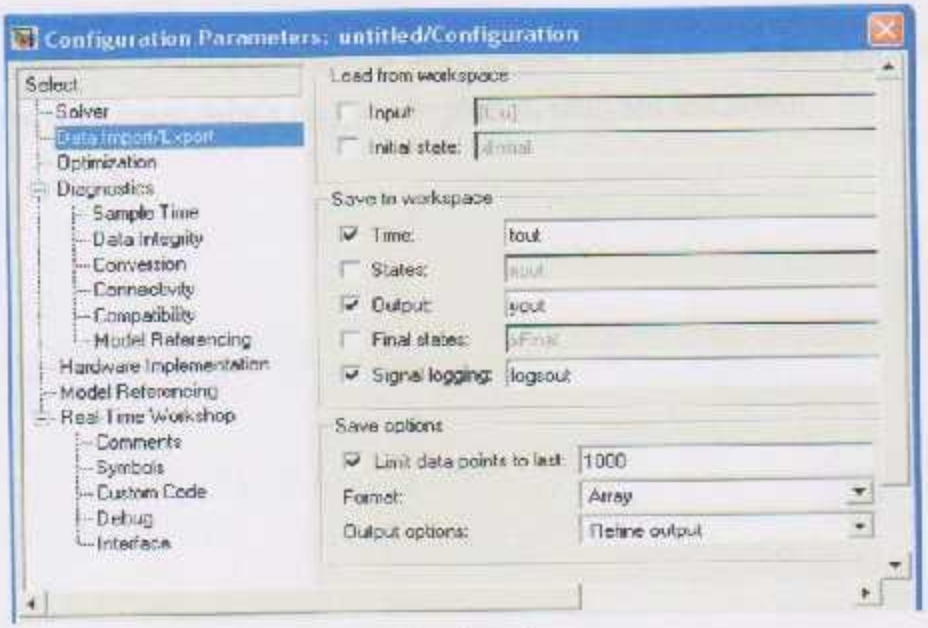

Figure 4.13 Data logging options

- In the Simulink model, put an "out" port at the desired signals.
- After building the model, and finishing the running time, mark the boxes representing the data to be acquired, as shown in Fig. 4.14, and then click "Send to Matlab Workspace".

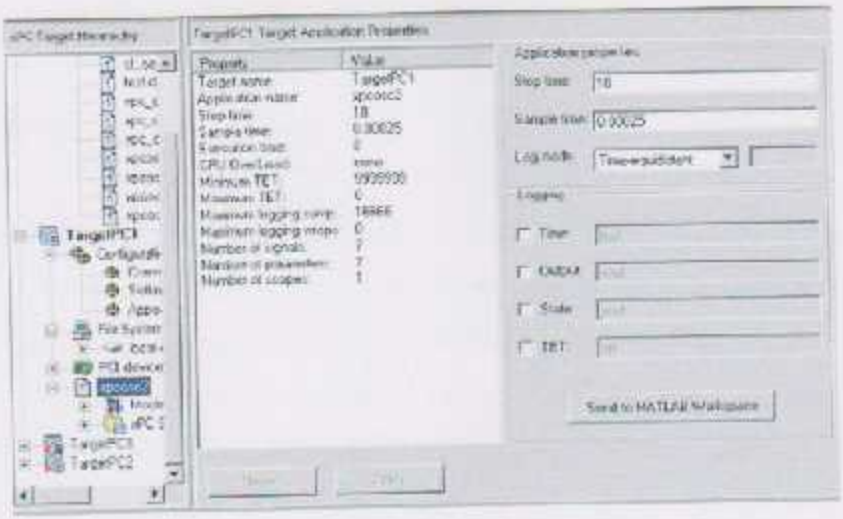

Figure 4.14 sending the outputs and states to work space

Then data signals representing the running time, system's states and outputs are stored as arrays in the work space, where they can be plotted, analyzed and saved.

Chapter Five

Control System Design and Simulation

5.1 Introduction

Inverted pendulum systems, in general, are used in control laboratories as test-beds for various control theories, including the classical linear control theories, and can be extended to the modern nonlinear fields. The control problem of inverted pendulum systems can be divided into two major branches: stabilization, and self erecting. The former deals with the problem of making the cart track a desired position along the rail, while keeping the links stable at their vertical position. Furthermore such a controller should reject, within certain limits, disturbances acting on the cart or each of the two links. On the other hand, self erecting problem tends to swing the links from their stable lower position up to the upright vertical point, and then a switching mechanism is used to activate the stabilization controller.

As stated earlier, inverted Pendulum systems present a number of complications and challenges in terms of their control, due to the following facts:

- Inverted pendulum systems are under-actuated mechanical systems, which means that the number of control inputs is less than that of the controlled outputs (and also less than the number of degrees of freedom), thus some of the system outputs are not directly affected by the input signal applied to the system.
- Inverted pendulum systems are inherently open-loop unstable at the desired operating point, which is the upper vertical position, due to the destabilizing naturally-generated gravitational force.
- Such systems have high nonlinear dynamics. These nonlinearities appear in the form of centrifugal and dry friction forces, and need to be handled by the linear controller.
- External disturbances that act on the system are not directly measurable.
- All of the states (outputs) are dynamically coupled, thus a change in any state will affect all other states.
- Some states in the system, i.e. the velocities, are not measured. These states should be accurately estimated, considering the existing noise problems.

Furthermore, from a practical point of view, when applying controllers to such systems, more limitations and constraints are faced, such as:

- Limited driving torque generated by the motor.
- Limited rail length, which means that motion beyond these limits is not possible.
- Limited motor bandwidth, which limits the reversal speed of the driving torque generated by the motor.

These underlying complications make for a control problem which is both interesting and challenging.

In the upcoming sections, control theory and strategies used for inverted pendulum systems control problem are demonstrated. Then these theories are applied to the single and double inverted pendulum systems respectively. Finally simulation results are demonstrated and discussed.

5.2 Control strategy

In this section state feedback control theories, including robust tracking and disturbance rejection controller design, and extended observer for nonlinearities and disturbances estimation are discussed. These theories are used to design a stabilization controller, described at the introduction of this chapter, for both single and double inverted pendulum system.

5.2.1 State-space representation

In control engineering, a state space representation is a mathematical model of a physical system as a set of input, output and state variables related by first-order differential equations. To abstract from the number of inputs, outputs and states, the variables are expressed as vectors and the differential and algebraic equations are written in matrix form. The state space representation (also known as the "time-domain approach") provides a convenient and compact way to model and analyze systems with multiple inputs and outputs. Unlike the frequency domain approach, the use of the state space representation is

not limited to time-invariant systems with linear components and zero initial conditions. "State space" refers to the space whose axes are the state variables.

To obtain the state-space representation for any system, the state variables of that system, its inputs, outputs, in addition to the state and output equations are to be determined. The general linear time invariant state space model that is used through out this chapter is:

$$\begin{aligned} \dot{x} &= Ax + Bu + B_d F_d \\ y &= Cx + Du \end{aligned} \tag{5-1}$$

Where:

$x \in R^{n_s}$: The state vector.

$u \in R^{n_i}$: The input vector, where n_i equals 1 for the inverted pendulum systems.

$y \in R^{n_o}$: The output vector.

$F_d \in R^{n_d}$: The disturbances vector.

A $n_s \times n_s$: The system matrix.

B $n_s \times n_i$: The input matrix.

B_d $n_s \times n_d$: The disturbance matrix.

C $n_o \times n_s$: The output matrix.

D $n_o \times n_i$: The feed-forward matrix. In the case of single and double inverted pendulum systems, this matrix is a zero matrix, since all the transfer functions relating the outputs to the input are strictly proper rational functions.

5.2.2 Robust tracking and disturbance rejection controller

The problem in this section is to design a state feedback controller that is able to track a desired reference input of the cart position, while keeping the links balanced in their

vertical position, even with the presence, to some extent, of disturbances and changes in plant parameters. The function of such a controller is divided into two main parts:

1- Regulation: this part tends to keep the links stabilized at their inverted position, which is the desired operating point around which the system is linearized. This requires overcoming the effects of disturbances and nonzero initial conditions.
2- Cart position tracking: which deals with the problem of making the cart tracks a desired reference signal. This function is also divided into two branches:
    a. Asymptotic (Stepoint) tracking: where the reference signal to be tracked is constant. i.e. $r(t)=a \quad \forall t \geq t_o$.
    b. Servo mechanism problem: where the reference signal to be tracked is a function of time, not a constant.

To achieve these functions robustly, the internal model control method is used to design the required controller. Referring to the state space model given in Eq. (5-1), and repeated here:

$$\begin{aligned} \dot{x} &= Ax + Bu - B_d F_d \\ y &= Cx \end{aligned} \tag{5-2}$$

Let the disturbances acting on the system be modeled by the following state and output equations:

$$\begin{aligned} \dot{x}_d &= A_d x_d \\ F_d &= C_d x_d \end{aligned} \tag{5-3}$$

While the reference signal to be tracked is modeled as follows:

$$\begin{aligned} \dot{x}_r &= A_r x_r \\ r &= C_r x_r \end{aligned} \tag{5-4}$$

Given that the Eq. (5-3) and Eq. (5-4) are the minimal realization of the proper rational functions that describes the disturbances and reference input respectively, in other words, the pairs (A_d, C_d) and (A_r, C_r) are observable.

To design a controller that is able to track the desired input signal, and at the same time, reject disturbances acting on the system, a "Θ" function is to be found, such that:

$$\Theta = s^q + \alpha_1 s^{q-1} + \cdots + \alpha_{q-1} s + \alpha_q \tag{5-5}$$

Which represents the least common multiple of the minimal polynomials of A_d and A_r .

It should be noted that the maximum number of signals that can be tracked equals the number of independent inputs of the system (the rank of matrix B). In the case of inverted pendulum systems, there is only one actuator acting on the system; it is possible for only one output to track a desired input signal, which is the cart position, while other outputs are just regulated.

Based on the previous discussion, the controller is chosen as follows [8]:

$$\dot{x}_c = A_c x_c + B_c e$$
$$y_c = C_c x_c \qquad (5\text{-}6)$$

Where:

- $A_c = \begin{bmatrix} 0 & 1 & 0 & \cdots & 0 \\ 0 & 0 & 1 & \cdots & 0 \\ \vdots & \vdots & \vdots & \ddots & \vdots \\ 0 & 0 & 0 & \cdots & 1 \\ -\alpha_q & -\alpha_{q-1} & -\alpha_{q-2} & \cdots & -\alpha_1 \end{bmatrix}$

- $B_c = \begin{bmatrix} 0 \\ 0 \\ \vdots \\ 1 \end{bmatrix}$

- $C_c = I_q$

- e : the error signal, which is the difference between the desired cart position and the actual one.

Figure 5.1 shows the control system configuration, where the models of the reference input, disturbances and controller are demonstrated with respect to the controlled plant.

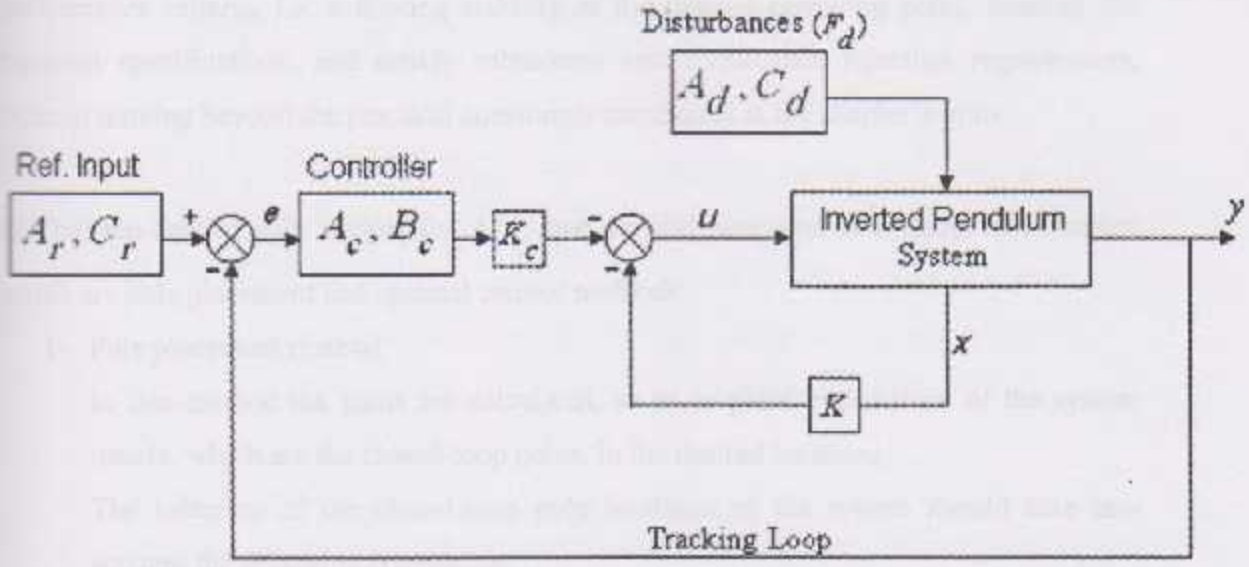

Figure 5.1 Robust tracking and disturbance rejection state feedback controller.

The augmented system, according to [8], is given as follows:

$$\begin{bmatrix} \dot{x} \\ \dot{x}_c \end{bmatrix} = \underbrace{\begin{bmatrix} A & 0 \\ -B_c C_{track} & A_c \end{bmatrix}}_{A_a} \begin{bmatrix} x \\ x_c \end{bmatrix} + \underbrace{\begin{bmatrix} B \\ 0 \end{bmatrix}}_{B_a} u \tag{5-7}$$

Where:

$C_{track} = [1 \quad zeros]$, which corresponds to the cart position.

To check the possibility for the closed loop poles of the system, which are the eigenvalues of (A_a) matrix, to be placed arbitrarily; so as to achieve stability and the desired transient response, the controllability of the system is checked. This can be done by finding that the matrix $[A_a - \lambda I \quad B_a]$ has a full row rank for every eigenvalue, λ, of the system. Alternatively, the controllability of the pair (A_a, B_a) is checked by calculating the controllability matrix (C_M), such that:

$$C_M = \left[B_a \quad A_c B_a \quad A_a^2 B_a \quad \cdots \quad A_a^{n-1} B_a \right]$$

If the controllability matrix has a full row rank, then the system is controllable, and it is possible to find a gain vector $[K \quad K_c]$, shown in Fig. 5.1, so that to obtain the desired

performance criteria, i.e. achieving stability at the desired operating point, meeting the transient specifications, and satisfy robustness and disturbance rejection requirements, without moving beyond the practical constraints mentioned at the chapter's intro.

To find the desired gain vector $[K \quad K_e]$, two methods are used throughout this chapter, which are pole placement and optimal control methods.

1- Pole placement method:

In this method the gains are calculated, so as to place eigenvalues of the system matrix, which are the closed-loop poles, in the desired locations.

The selection of the closed-loop pole locations of the system should take into account the following constraints:

- The location of the open-loop zeros and poles.
- The imaginary part of the poles should be small enough in order to reduce the oscillation frequency of system response.
- The real part of the poles should not be placed far away from the imaginary axis, since a choice like this will result in large gain values, which will in turn require a large driving torque to be generated by the motor, thus the motor will saturate and the resulting response will significantly deviate from that expected.
- The location of system poles should achieve an acceptable transient response in terms of settling time and percent overshoot, thus a tradeoff between the system speed and control effort is to be made.
- The bandwidth frequency of the system should be kept small enough, so as to make the system less susceptible to noise.

After determining the desired poles locations, MATLAB function (*place*) can be used to calculate the necessary gain values.

2- Optimal control method:

In this method, the gains $[K \quad K_e]$ are determined to minimize the quadratic performance index

$$J = \int_0^\infty (x^T Q x + u^T R u) dt \tag{5-8}$$

Where:

- **Q**: is a positive semidefinite symmetric matrix that represents the importance of the states relative to each other. Such a matrix is selected to be diagonal, where its elements are selected to be inversely proportional to the square of the maximum value of their corresponding states, as follows:

$$Q_i = \frac{q_i}{\left(x_{i,\max}\right)^2} \tag{5-9}$$

  Where q_i reflects the importance of the sate.

- **R**: is positive definite matrix that represents the relative importance of control inputs. Since there is only one control input in the case of inverted pendulum systems, this matrix is a (1×1) matrix, with its value is selected to represent the penalty of consuming the control effort.

After determining the Q and R matrices, MATLAB function (*lqr*) is used to solve the Riccati equation and obtain the optimal gain values, and the corresponding eigenvalues of the system.

5.2.3 Nonlinearities and disturbances estimation

As stated earlier, one of the challenges that face the control problem of the inverted pendulum systems is their nonlinear dynamics, in addition to the immeasurable external disturbances acting on the system. These nonlinearities are omitted from the system when deriving the linearized model, which latter formed the base on which the robust tracking state feedback controller was designed, as shown in the previous subsection.

In order to improve the overall response of the system, and enhance system's immunity against disturbances, the effects of nonlinearities and disturbances are taken into consideration. Referring to Eqs. (2-13) and (2-43) that describe the motion of single and

double inverted pendulum systems respectively. It is possible to collect all the nonlinear terms in a vector (n),such that:

$$M\ddot{x} + D\dot{x} + Kx = BT_m + Nn \tag{5-10}$$

Where the matrices *M, D, K, B* constitute the linear model, while the vector (n)describes the difference between the nonlinear model and the linearized one, including friction force, centrifugal forces, external disturbances, and other nonlinearities.

Since these nonlinearities and disturbances (n) are not directly measurable; an extended observer is needed. Extended observers are basically classical observers where the nonlinearities and external disturbances(n), are assumed to be regular states. Since these states are originally extraneous to the system, one can not write down their corresponding differential equations governing their behavior in the time domain, which is necessary for completing the state-space model. A practical solution would be to assume that they are step-wise constant, thus their derivatives are set to zero.

Based on the previous discussion, and referring to Eq. (5-10), the extended state-space representation is:

$$\begin{bmatrix} \dot{x} \\ \ddot{x} \\ \dot{n} \end{bmatrix} = \underbrace{\begin{bmatrix} 0 & I & 0 \\ -M^{-1}K & -M^{-1}D & M^{-1}N \\ 0 & 0 & 0 \end{bmatrix}}_{Ae} \begin{bmatrix} x \\ \dot{x} \\ n \end{bmatrix} + \underbrace{\begin{bmatrix} 0 \\ M^{-1}B \\ 0 \end{bmatrix}}_{Be} T_m \tag{5-11}$$

$$y = \underbrace{I}_{Ce} \begin{bmatrix} x \\ \dot{x} \\ n \end{bmatrix}$$

To check the possibility for the disturbances and nonlinearities to be estimated by the extended observer with the available measurements, the condition:

$$rank \begin{bmatrix} sI - A & N \\ C & 0 \end{bmatrix} = \dim(x) + \dim(n) \tag{5-12}$$

should be satisfied for all complex numbers s. This requires that the number of nonlinearities may not exceed the number of measurements, which is the case here. Alternatively the observability of the pair (A_e, C_e) can be checked by the observability matrix (O_M), such that:

$$O_M = \begin{bmatrix} C_e \\ C_e A_e \\ \vdots \\ C_e A_e^{n-1} \end{bmatrix}$$

This matrix can be calculated with *(obsv)* MATLAB function, and then its rank is found. If the observability matrix has a full column rank, then system is fully observable and the nonlinearities and external disturbances can be estimated with the extended observer.

Figure 5.2 shows the basic concept of observer design. The measured outputs of the system are compared to those estimated, and then error signal is fed back to the observer. In order to increase the convergence speed of the error signal, i.e. to make the observer outputs match those measured as fast as possible, the dynamics of the observer should be made much faster than that of the controlled system.

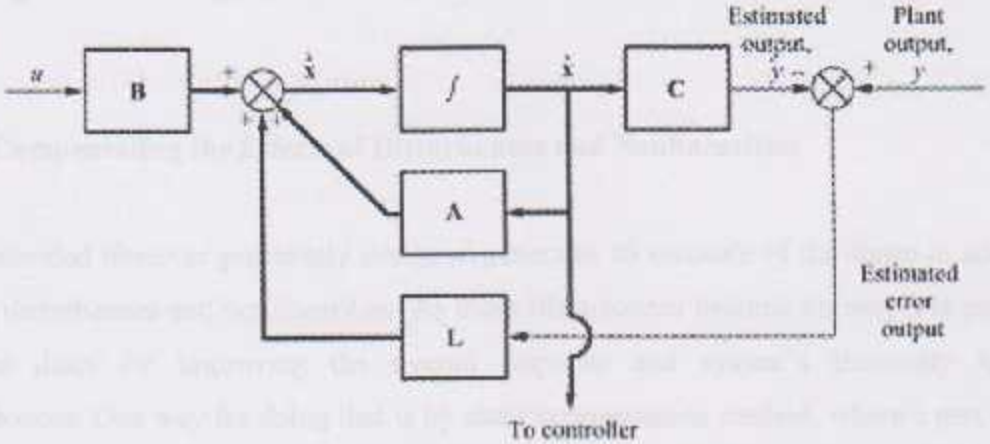

Figure 5-2 Observer design process.

The state equation of the observer is found from Fig. 5.2 as follows:

$$\dot{\hat{x}} = A\hat{x} + Bu + LC(x - \hat{x}) \qquad (5\text{-}13)$$

While that of the linear real system is:

$$\dot{x} = Ax + Bu \tag{5-14}$$

The error signal between the measured output and the observer output is:

$$\hat{e} = x - \hat{x} \tag{5-15}$$

Subtracting Eq.(5-13) from (5-14); the error dynamic equation is:

$$\dot{\hat{e}} = (A - LC)\hat{e} \tag{5-16}$$

Thus by choosing an appropriate gain vector (**L**), the poles of the error characteristic equation can be placed far to the left from those of the controlled system, so as to achieve the desired speed of the observer.

The gain vector (**L**) is obtained in a similar way to the feedback gains, either by pole placement method, where observer's poles are selected to be 4 to 10 times of those of the controlled plant, or by using optimal control method previously discussed.

Based on the separation property [4], it is very legal to design the controller and observer independently, and also feedback the estimated states instead of the original ones without affecting the selected eigenvalues of neither the controller nor the observer.

5.2.4 Compensating the Effects of Disturbances and Nonlinearities

The extended observer previously designed generates an estimate of the states in addition to the disturbances and nonlinearities. As these disturbances become known, it is possible to use them for improving the overall response and system's immunity against disturbances. One way for doing that is by static compensation method, where a part of the control effort is dedicated to cancel the effects of disturbances on the system. In fact, this method can be used only to compensate for the disturbances and nonlinearities acting on the cart. This is due to the fact that the applied motor torque acts directly on the cart whereas it affects the links motion indirectly. Thus the control signal (u) becomes:

$$u = -kx - k_a x_a - r_p n_1 \tag{5-17}$$

Figure 5.3 shows the complete controller-observer configuration with disturbance compensation, used for controlling the DIPC system.

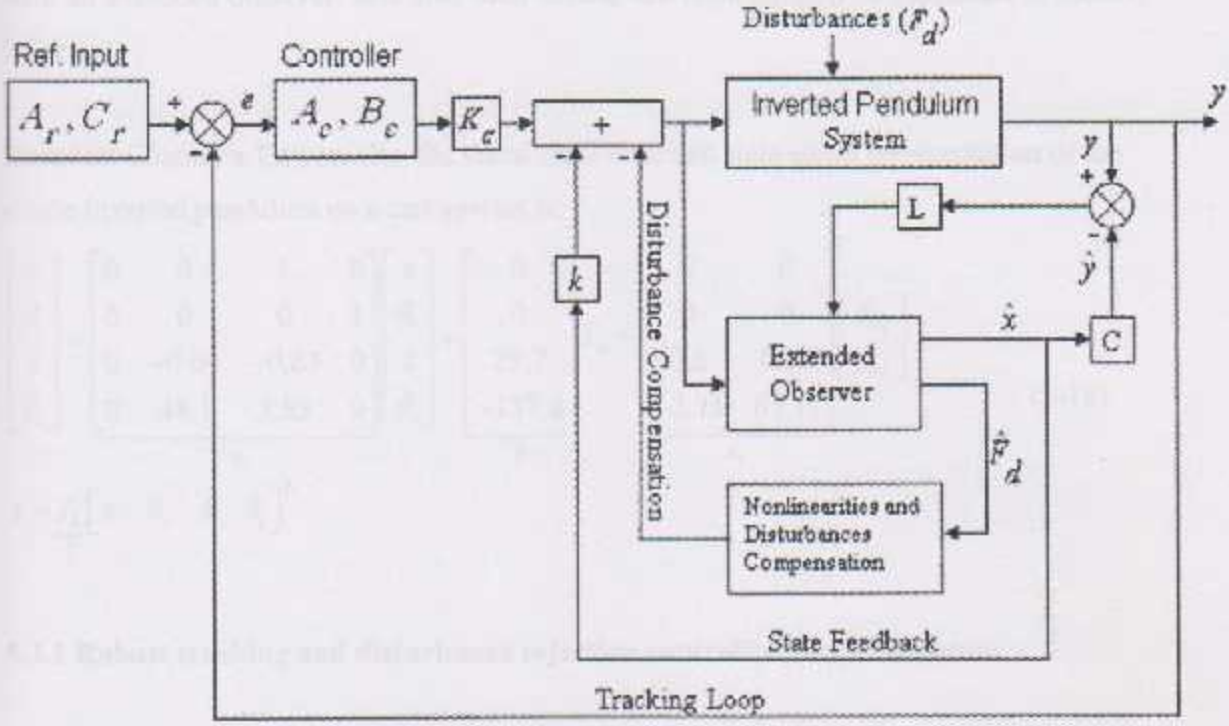

Figure 5.3 Using the extended observer outputs to compensate for the nonlinearities and disturbances effects in the inverted pendulum system.

5.3 Control system design for SIPC system

In this section, theories previously demonstrated are applied to the single inverted pendulum on a cart system. At first, a robust tracking and disturbance rejection controller is designed, after that the nonlinearities and disturbances acting on the system are estimated with an extended observer, and then their effects are compensated as explained in section 5.2.4.

Based on Chapter's Two results, the linear time-invariant state space representation of the single inverted pendulum on a cart system is:

$$\begin{bmatrix} \dot{x} \\ \dot{\theta}_1 \\ \ddot{x} \\ \ddot{\theta}_1 \end{bmatrix} = \underbrace{\begin{bmatrix} 0 & 0 & 1 & 0 \\ 0 & 0 & 0 & 1 \\ 0 & -0.64 & -0.85 & 0 \\ 0 & 48.1 & 3.93 & 0 \end{bmatrix}}_{A} \begin{bmatrix} x \\ \theta_1 \\ \dot{x} \\ \dot{\theta}_1 \end{bmatrix} + \underbrace{\begin{bmatrix} 0 \\ 0 \\ 29.7 \\ -137.8 \end{bmatrix}}_{B} T_m + \underbrace{\begin{bmatrix} 0 & 0 \\ 0 & 0 \\ 0.6 & 0.32 \\ -2.75 & 67.11 \end{bmatrix}}_{B_d} \begin{bmatrix} f_{d1} \\ f_{d2} \end{bmatrix} \tag{5-18}$$

$$y = \underbrace{I_4}_{C} \begin{bmatrix} x & \theta_1 & \dot{x} & \dot{\theta}_1 \end{bmatrix}^T$$

5.3.1 Robust tracking and disturbance rejection controller for SIPC system

Based on the SIPC state-space model, and referring to the discussion in section 5.2.2, it is desired to design a robust tracking and disturbance rejection controller that will be able to stabilize the link in its upper vertical position, while tracking a sine wave cart position command

First, the reference signal to be tracked is characterized as follows:

$$r(t) = A \sin(\omega t) \tag{5-19}$$

The Laplace transform for such a signal is:

$$R(s) = A \frac{\omega}{s^2 + \omega^2} \tag{5-20}$$

This signal is realized by the following zero-input state-space model:

$$\begin{bmatrix} \dot{y}_r \\ \ddot{y}_r \end{bmatrix} = \underbrace{\begin{bmatrix} 0 & 1 \\ -\omega^2 & 0 \end{bmatrix}}_{A_r} \begin{bmatrix} y_r \\ \dot{y}_r \end{bmatrix}$$

$$y_r = \underbrace{\begin{bmatrix} \omega & 0 \end{bmatrix}}_{C_r} \begin{bmatrix} y_r \\ \dot{y}_r \end{bmatrix} \tag{5-21}$$

Where the initial conditions of (A_r) determine the sine wave amplitude.

Assuming that the disturbances acting on the system are also *sine* waves with the same frequency but different amplitudes, then:

$$A_d = A_r \qquad and \qquad C_a = C_r \tag{5-22}$$

This means that the least common multiple of the minimal polynomials of A_d *and* A_r is:

$$\Theta = s^2 + \omega^2 \tag{5-23}$$

Applying Eq. (5-6), the required controller is:

$$A_c = \begin{bmatrix} 0 & 1 \\ -\omega^2 & 0 \end{bmatrix}$$

$$B_c = \begin{bmatrix} 0 \\ 1 \end{bmatrix} \tag{5-24}$$

$$C_c = I_2$$

It is clear that A_c is equivalent to A_r, because A_d and A_r are the same, which explains why this method is called internal model control.

Referring to Eq. (5-7), the augmented system is given as follows:

$$\begin{bmatrix} \dot{x} \\ \dot{x}_c \end{bmatrix} = \underbrace{\begin{bmatrix} A & 0 \\ -B_c C_{track} & A_c \end{bmatrix}}_{A_a} \begin{bmatrix} x \\ x_c \end{bmatrix} + \underbrace{\begin{bmatrix} B \\ 0 \end{bmatrix}}_{B_a} u \tag{5-25}$$

Where:

$$C_{track} = \begin{bmatrix} 1 & 0 & 0 & 0 \end{bmatrix}^T$$

To check the controllability of the pair (A_a, B_a), first the controllability matrix is calculated, and then its rank is found. This is performed using MATLAB as follows:

Cm = ctrb(Aa,Ba)

rank(Cm)

Which is found to be 6, full row rank, meaning that the augmented system is fully controllable, and a gain vector $[K \quad K_e]$ can be calculated to achieve the desired response. Referring to section 5.2.2, these gains can be found either by pole-placement or optimal-control methods. In this section the former method is applied, and the gain vector is obtained to place the closed-loop poles of the system in the desired locations.

The open-loop poles and zeros are found to be:

Open-loop poles:	0	6.93	-6.93	-0.016
Open-loop zeros:	0	0	6.72	-6.72

Then a possible selection of the closed-loop poles, tacking into account the open-loop poles and zeros, the desired transient response, and motor saturation limits, is:

$$\text{Poles} = [-1.8 \quad -1.85 \quad -4.5 \quad -4.6 \quad -30 \quad -35]$$

Let the frequency of the sine wave to be tracked is 0.5 rad/sec. With MATLAB the gains required to achieve the desired closed-loop poles are found as follows:

gains = place (Aa,Ba,poles).

K=gains(1:4)

$$K = [-50.53 \quad -25.48 \quad -14.64 \quad -3.75]$$

Kc=gains(5:6)

$$K_e = [41.3 \quad 82.5]$$

5.3.2 Extended observer design and disturbance compensation

Based on the previous discussion, it is worth trying to design an extended observer for the SIPC system, which is able to estimate the disturbances and nonlinearities acting on the system. These nonlinearities and disturbances appeared clearly during the derivation of the SIPC mathematical model, and are described by Eq. (2-13). This equation is rearranged here as follows:

$$\underbrace{\begin{bmatrix} M+m_1+J/r_p^2 & m_1 l_1 \\ m_1 l_1 & m_1 l_1^2+J_1 \end{bmatrix}}_{M}\begin{bmatrix}\ddot{x}\\ \ddot{\theta}_1\end{bmatrix}+\underbrace{\begin{bmatrix} d/r^2 & 0\\ 0 & 0\end{bmatrix}}_{D}\begin{bmatrix}\dot{x}\\ \dot{\theta}_1\end{bmatrix}+\underbrace{\begin{bmatrix}0 & 0\\ 0 & -m_1 g l_1\end{bmatrix}}_{K}\begin{bmatrix}x\\ \theta_1\end{bmatrix}=\underbrace{\begin{bmatrix}1/r_p\\ 0\end{bmatrix}}_{b}T_m+ \underbrace{\begin{bmatrix} f_{d1}+f_{d2}-m_1 l_1\dot{\theta}_1^2\sin\theta_1-F_{fric}+m_1 l_1(1-\cos\theta_1)\ddot{\theta}_1 \\ f_{d2}l_1\cos\theta_1+m_1 l_1(1-\cos\theta_1)\ddot{x}-m_1 g l_1(\theta_1-\sin\theta_1)\end{bmatrix}}_{n} \quad (5\text{-}26)$$

where the vector (n) represents the difference between the nonlinear model and the linearized one.

To obtain the extended-state-space model, with the nonlinearities and disturbances (n) are considered to be regular states of the system, the idea expressed in section 5.2.3 is applied here. Thus these nonlinearities are assumed to be step-wise constants, so that their derivatives are set to zero. Applying Eq. (5-11), the resulting extended state space model is:

$$\begin{bmatrix}\dot{x}\\ \dot{\theta}_1\\ \ddot{x}\\ \ddot{\theta}_1\\ \dot{n}_1\\ \dot{n}_2\end{bmatrix}=\underbrace{\begin{bmatrix}0 & 0 & 1 & 0 & 0 & 0\\ 0 & 0 & 0 & 1 & 0 & 0\\ 0 & -0.64 & -0.85 & 0 & 0.6 & -2.76\\ 0 & 48.1 & 3.9 & 0 & -2.76 & 208.5\\ 0 & 0 & 0 & 0 & 0 & 0\\ 0 & 0 & 0 & 0 & 0 & 0\end{bmatrix}}_{A_e}\begin{bmatrix}x\\ \theta_1\\ \dot{x}\\ \dot{\theta}_1\\ n_1\\ n_2\end{bmatrix}+\underbrace{\begin{bmatrix}0\\ 0\\ 29.7\\ -136.8\\ 0\\ 0\end{bmatrix}}_{B_e}T_m \quad (5\text{-}27)$$

$$y=\underbrace{I_6}_{C_e}\begin{bmatrix}x & \theta_1 & \dot{x} & \dot{\theta}_1 & n_1 & n_2\end{bmatrix}^T$$

Checking the observability of the system based on the two direct measurements $(x \quad and \quad \theta_1)$, the rank of the observability matrix is found as follows:

Ce=[eye(2), zeros(2,4)]

Om= obsv(Ae,Co)

rank(Om)

Which is found to be 6, i.e. full column rank. Thus the extended system is fully observable and an extended observer is able to estimate all the nonlinearities in the system based on the measured outputs.

To make the error of the observer die out much faster than the system dynamics, such that the controller will receive the true estimates instantaneously, the gain vector (L) is selected to place the poles of the observer ten times further to the left than those of the controlled plant, as follows:

Obs_poles = 10[-1.8 -1.85 -4.5 -4.6 -40 -50]*

Le = place(Ae',Co',Obs_poles)'

Le=

*1.0e+005 **

0.0034 -0.0000

-0.0000 0.0028

0.1165 -0.0005

-0.0010 0.0962

1.5647 0.0032

0.0206 0.0035

Applying Eq. (5-17), the nonlinear terms and disturbances acting on the cart are compensated directly by dedicating a part of the control signal to cancel the effect of the estimated (n_1), as follows:

$$u = -kx - k_e x_e - r_p n_1 \qquad (5\text{-}28)$$

Where: r_p (the motor pulley's radius) = 0.02 m.

5.3.3 Simulation results

The next step in controller design process is simulation. This step is of significant importance to check whether the resulted system response meets the design specifications or not. Using the controller and observer design results obtained in the previous sections, with the system nonlinear model derived in Chapter Two of this report, MATLAB and Simulink are used to simulate system performance. The nonlinear model of the system is used to build an s-function block that represents the actual SIPC system including the disturbances acting on it, thus the model will be as representative as possible.

The model used in simulation process is shown in Fig 5.4, this model includes the followings:

- A subsystem that contains the s-function block representing the actual system, this subsystem has three inputs which are the actuating torque and the two disturbances acting on the cart and the link. Six outputs are obtained from the system, these are the four states (x, θ_1, $\dot{x}$, $\dot{\theta}_1$) representing the measurable outputs of the real system. The other two outputs are the nonlinear and disturbance terms that are used to check the observer results.
- A robust tracking and disturbance rejection state feedback controller.
- An extended observer for nonlinearities and disturbances estimation.

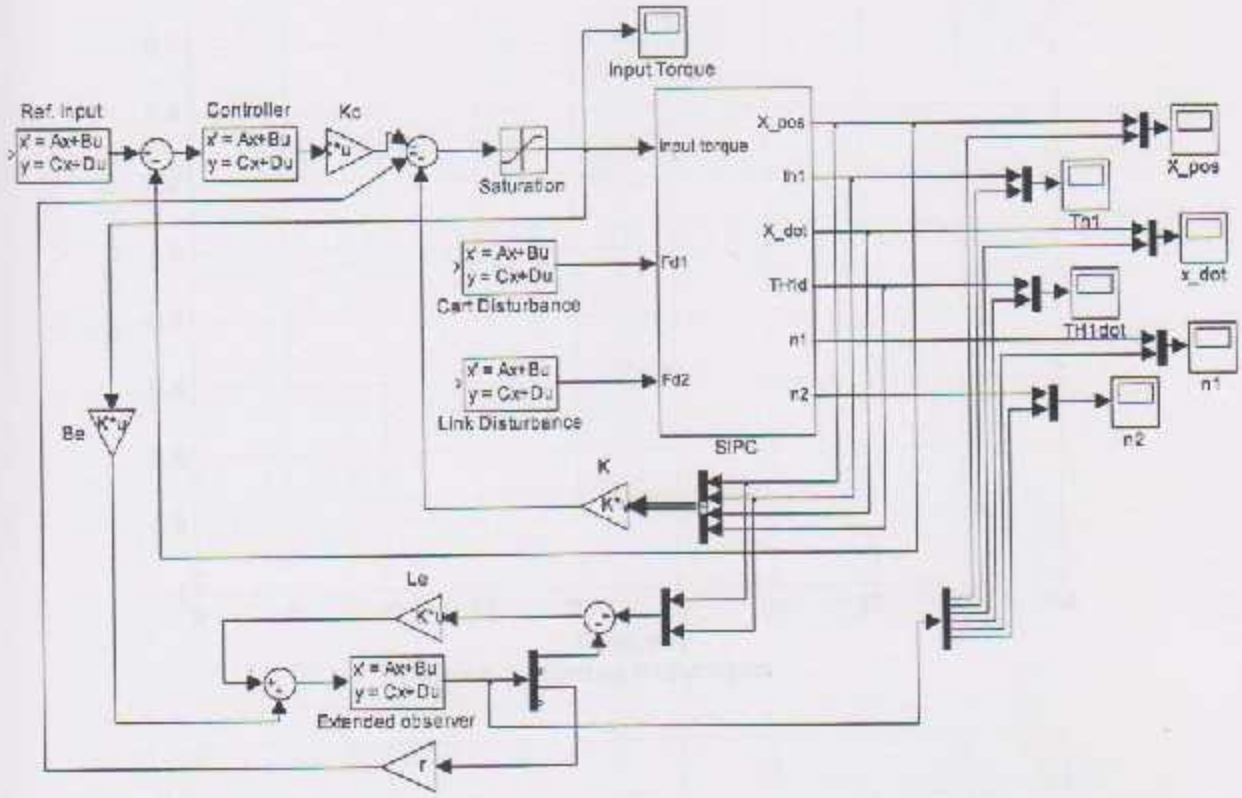

Figure 5-4 Simulink model for SIP control system.

The initial conditions, desired input, and disturbances acting on the system are supposed to be:

- Initial cart position = 0 m.
- Initial angle of the link = 0 rad.
- Desired cart position = $0.5\sin(0.5t)$ m.
- The link should be stabilized at the upright equilibrium position.
- There is a disturbing force equal $0.05\sin(0.5t)$ N acting on the cart.

Simulation results were as follows:

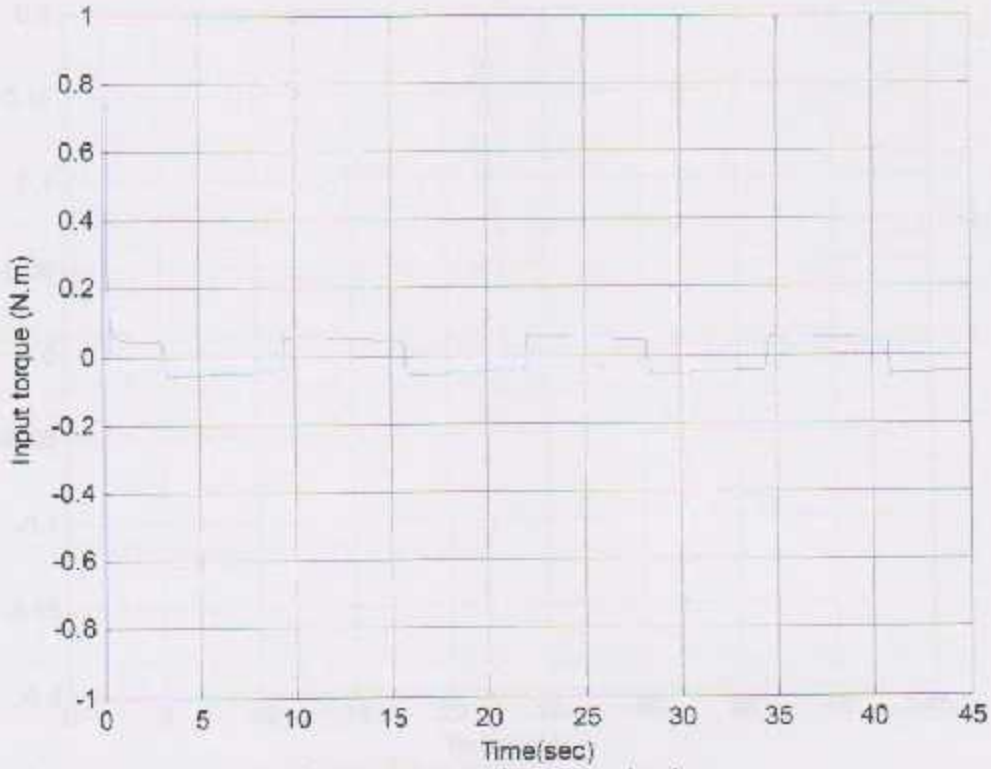

Figure 5-5 Actuating torque signal.

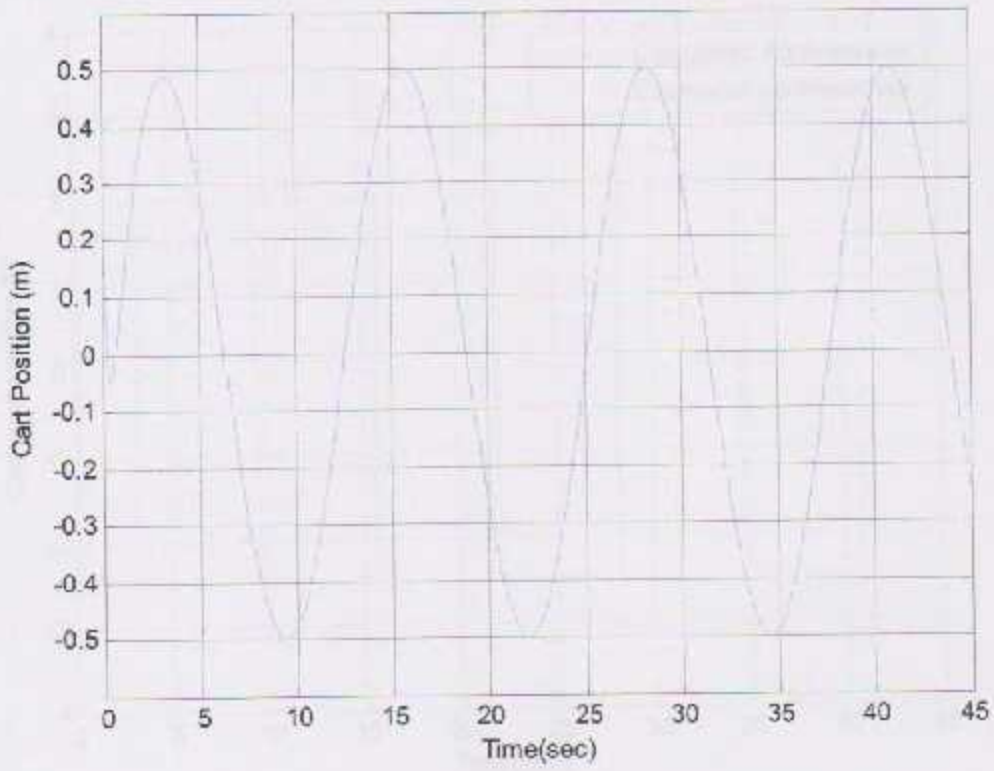

Figure 5-6 Cart position with time.

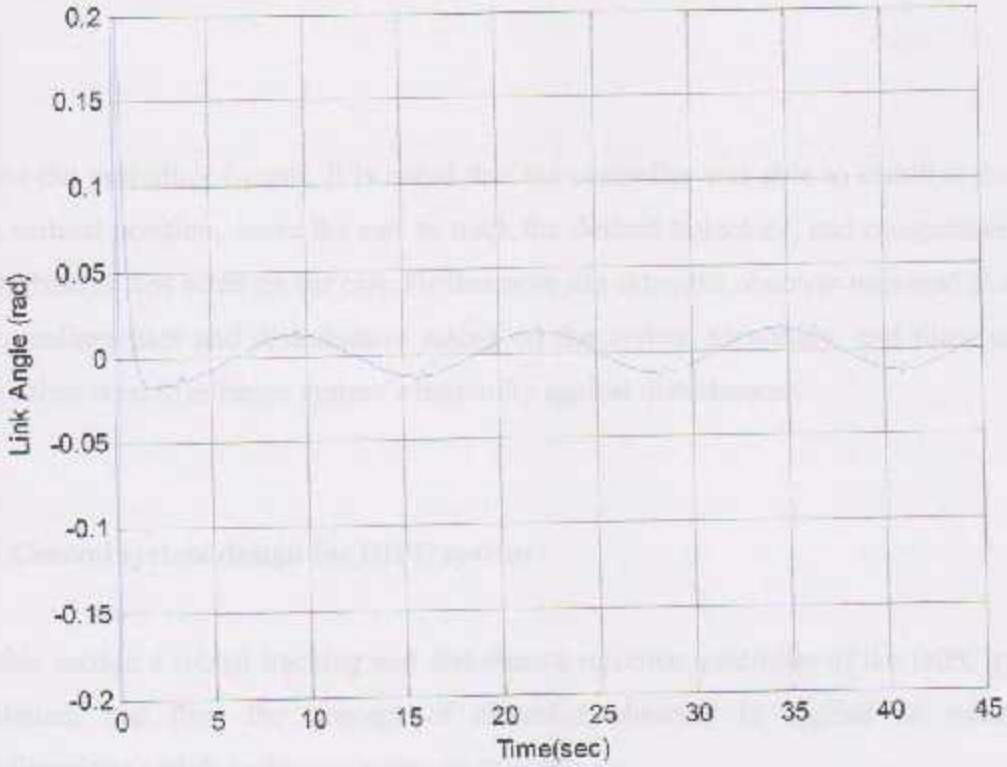

Figure 5-7 Link angular displacement.

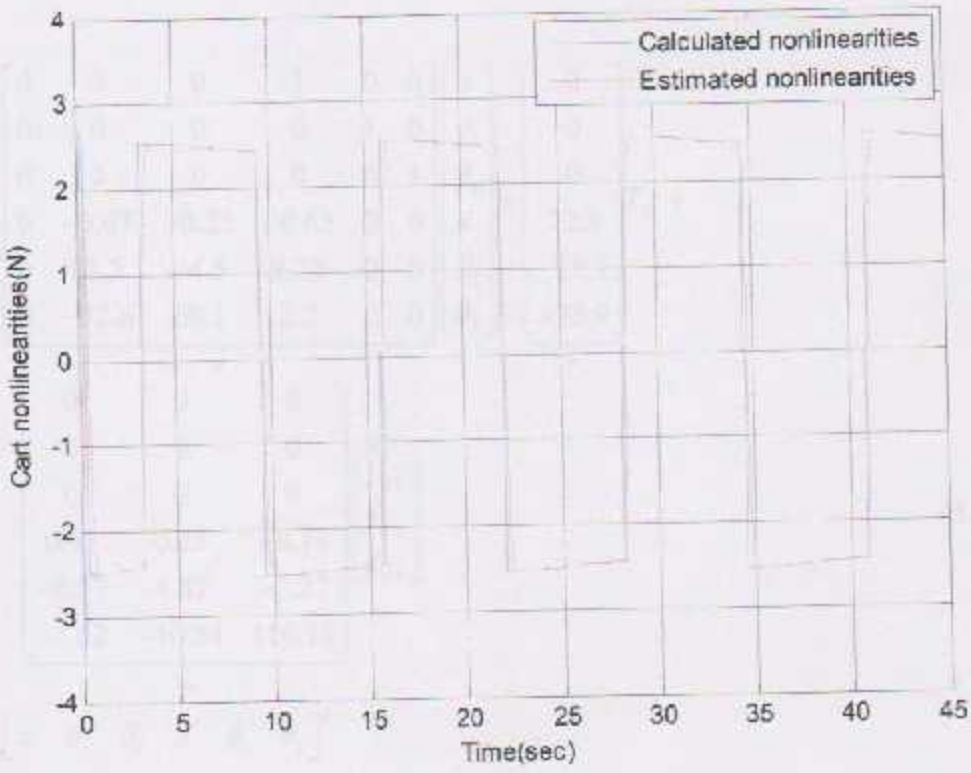

Figure 5-8 Cart nonlinearity (n_1).

From the preceding figures, it is noted that the controller was able to stabilize the link in the vertical position, move the cart to track the desired trajectory, and compensate for the disturbances that acted on the cart. Furthermore the extended observer managed to estimate the nonlinearities and disturbances acting on the system accurately, and these estimates were then used to enhance system's immunity against disturbances.

5.4 Control system design for DIPC system

In this section a robust tracking and disturbance rejection controller of the DIPC system is designed, and then the concept of extended observer is applied to estimate the nonlinearities and disturbances acting on the system.

The state space model for the DIPC given in Eq. (2-54) and Eq. (2.55), and repeated here:

$$\begin{bmatrix} \dot{x} \\ \dot{\theta}_1 \\ \dot{\theta}_2 \\ \ddot{x} \\ \ddot{\theta}_1 \\ \ddot{\theta}_2 \end{bmatrix} = \underbrace{\begin{bmatrix} 0 & 0 & 0 & 1 & 0 & 0 \\ 0 & 0 & 0 & 0 & 1 & 0 \\ 0 & 0 & 0 & 0 & 0 & 1 \\ 0 & -0.67 & -0.25 & -0.65 & 0 & 0 \\ 0 & 18.3 & -4.5 & 8.32 & 0 & 0 \\ 0 & -32.6 & 69.1 & 2.2 & 0 & 0 \end{bmatrix}}_{A} \begin{bmatrix} x \\ \theta_1 \\ \theta_2 \\ \dot{x} \\ \dot{\theta}_1 \\ \dot{\theta}_2 \end{bmatrix} + \underbrace{\begin{bmatrix} 0 \\ 0 \\ 0 \\ 22.3 \\ -28.7 \\ -75.9 \end{bmatrix}}_{B} T_m +$$

$$\underbrace{\begin{bmatrix} 0 & 0 & 0 \\ 0 & 0 & 0 \\ 0 & 0 & 0 \\ 0.45 & 0.25 & -0.18 \\ -0.57 & 4.67 & -3.27 \\ -1.52 & -10.84 & 110.78 \end{bmatrix}}_{B_d} \begin{bmatrix} f_{d1} \\ f_{d2} \\ f_{d3} \end{bmatrix} \qquad (5\text{-}29)$$

$$y = \underbrace{I_3}_{C} \begin{bmatrix} x & \theta_1 & \theta_2 & \dot{x} & \dot{\theta}_1 & \dot{\theta}_2 \end{bmatrix}^T$$

5.4.1 Robust tracking and disturbance rejection controller for DIPC system

Based on the DIPC state space model, and referring to the discussion in section 5.2.2, it is desired to design a robust tracking and disturbance rejection controller that will be able to stabilize the two links in the upper vertical position, reject step disturbances, while tracking a step cart position command. Since the signal to be tracked is a step, then the servomechanism problem discussed for the SIPC will reduce to a simple asymptotic tracking problem. Figure 5.9 shows the control system configuration for the DIPC, In order to have a robust controller that is able to track any desired step input for the cart position with zero steady-state error, even if disturbances act on the system, a unity feed-back from the cart position in addition to an integrator is used as shown in Fig.5.9. The integrator increases the system type, adds a new state to the system, and reduces the steady-state error to zero. This can be also obtained by applying Eq. (5-3) to Eq. (5-6), since the least common multiple for step input and disturbances is just $\Theta = s$, thus the matrices A_e and B_e reduces to [0] and [1] respectively, which is equivalent to adding an integrator $\left(\frac{1}{s}\right)$ shown in Fig. 5.9.

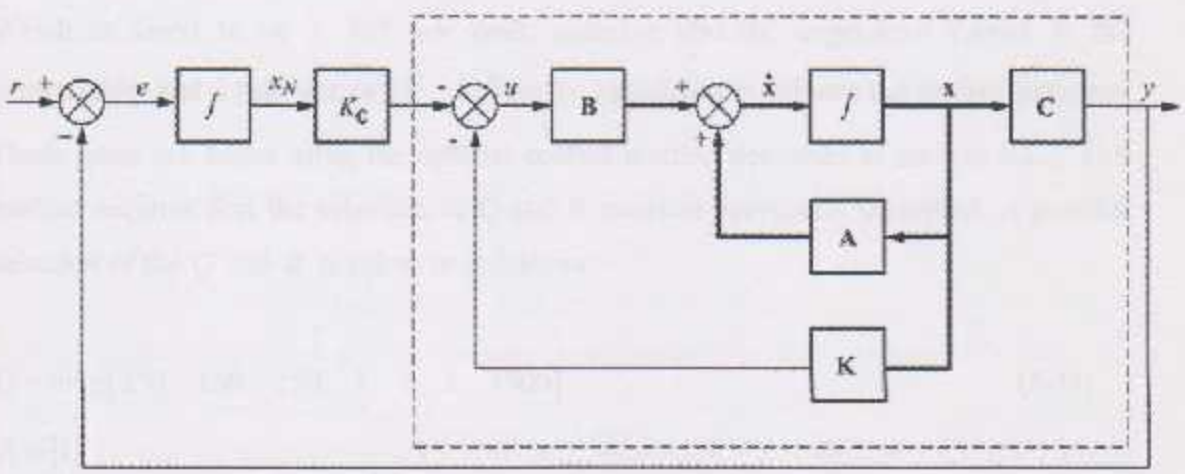

Figure 5.9 Augmented system with state feedback controller.

The Augmented model that describes the system in Fig. 5.9 is given as follows:

$$\begin{bmatrix} \dot{x} \\ \dot{x}_a \end{bmatrix} = \underbrace{\begin{bmatrix} A & 0 \\ -C_{track} & 0 \end{bmatrix}}_{Aa} \begin{bmatrix} x \\ x_a \end{bmatrix} + \underbrace{\begin{bmatrix} B \\ 0 \end{bmatrix}}_{Ba} r$$

$$y = \underbrace{\begin{bmatrix} C & 0 \end{bmatrix}}_{Ca} \begin{bmatrix} x \\ x_a \end{bmatrix} \qquad (5\text{-}30)$$

Where:

x_a represents the new (augmented) state.

$C_{track} = [1 \quad zeros(1,5)]$, since the tracking loop is established only to obtain a zero steady state error for any step cart position command.

To check the controllability of the pair (A_a, B_a), first the controllability matrix is calculated, and then its rank is found. This is performed using MATLAB as follows:

Cm = ctrb(Aa,Ba)

rank(Cm)

Which is found to be 7, full row rank, meaning that the augmented system is full controllable, and a gain vector $[k \quad k_a]$ can be calculated to achieve the desired response. These gains are found using the optimal control method described in section 5.2.2. This method requires first the selection of Q and R matrices previously described. A possible selection of the Q and R matrices is as follows:

$$Q = \text{diag}[250 \quad 150 \quad 150 \quad 1 \quad 1 \quad 1 \quad 1500] \qquad (5\text{-}31)$$

$$R = [1]$$

The selection of Q matrix entries is based on Eq. (5-9); it is desired to have small changes in cart position and links' angles, so that their corresponding entries are selected to be relatively large. At the same time the rate of change of these variables (the velocities) are

allowed to have large changes, so that their corresponding entries are selected to be small. Finally, it is not desired to have a large error in the cart position, so that Q_1 is selected to be 1500.

For the R matrix, since there is only one input to the system, this matrix is (1×1), and it is selected to have a value of 1.

Using MATLAB function *(lqr)*, the Riccati equation is solved, and the optimal gains corresponding to the selected Q and R matrices are found as follows:

```
[gains ,s ,poles] =lqr(Aa,Ba,Q,R)
k=gains(1:6)
kc=gains(7)
```

The resulting optimal gains are:

```
k =   53.5344   257.5289   -122.7357   33.7715   54.9161   -12.3106
kc =  -38.7298
```

While the corresponding eigenvalues of the system, the closed loop poles, are:

$$Poles = [-2.44 \quad -3.42 \quad -5.58+j0.33 \quad -5.58-j0.33 \quad -5.18+j3.6 \quad -5.18-j3.6 \quad -84.57]$$

5.4.2 Extended observer design and disturbance compensation

In this section an extended observer for the DIPC system is designed. This observer aims to estimate the disturbances and nonlinearities acting on the system using the measured outputs. These nonlinearities and disturbances are described in Eq. (2-43), which is rearranged here as follows:

$$\underbrace{\begin{bmatrix} M+m_1+m_2+J/r_p^2 & (m_1l_1+m_2L_1) & m_2l_2 \\ (m_1l_1+m_2L_1) & m_1l_1^2+m_2L_1^2+J_1 & m_2L_1l_2 \\ m_2l_2 & m_2L_1l_2 & m_2l_2^2+J_2 \end{bmatrix}}_{M} \begin{bmatrix} \ddot{x} \\ \ddot{\theta}_1 \\ \ddot{\theta}_2 \end{bmatrix} + \underbrace{\begin{bmatrix} d/r_p^2 & 0 & 0 \\ 0 & 0 & 0 \\ 0 & 0 & 0 \end{bmatrix}}_{D} \begin{bmatrix} \dot{x} \\ \dot{\theta}_1 \\ \dot{\theta}_2 \end{bmatrix} +$$

$$\underbrace{\begin{bmatrix} 0 & 0 & 0 \\ 0 & -(m_1l_1+m_2L_1)g & 0 \\ 0 & 0 & -m_2l_2g \end{bmatrix}}_{K} \begin{bmatrix} x \\ \theta_1 \\ \theta_2 \end{bmatrix} - \underbrace{\begin{bmatrix} 1/r_p \\ 0 \\ 0 \end{bmatrix}}_{B} T_m$$

$$+ \underbrace{\begin{bmatrix} (m_1l_1+m_2L_1)(\cos\theta_1-1)\ddot{\theta}_1+m_2l_2(\cos\theta_2-1)\ddot{\theta}_2+ \\ \dot{\theta}_1^2(m_1l_1+m_2L_1)\sin\theta_1+\dot{\theta}_2^2m_2l_2\sin\theta_2+f_{d1}+f_{d2}+f_{d3}-F_{fric} \\ (m_1l_1+m_2L_1)(\cos\theta_1-1)\ddot{x}+m_2L_1l_2\left(\cos(\theta_1-\theta_2)-1\right)\ddot{\theta}_2 \\ -\dot{\theta}_2^2m_2L_1l_2\sin(\theta_1-\theta_2)-(m_1l_1+m_2L_1)g\sin\theta_1+L_1\cos\theta_1(f_{d2}-f_{d3}) \\ m_2l_2(\cos\theta_2-1)\ddot{x}+m_2L_1l_2\left(\cos(\theta_1-\theta_2)-1\right)\ddot{\theta}_1 \\ +\dot{\theta}_1^2m_2L_1l_2\sin(\theta_1-\theta_2)-m_2l_2g\sin\theta_2+f_{d3}L_2\cos\theta_2 \end{bmatrix}}_{n}$$

(5-32)

Based on the previous equation, and referring to section 5.2.3, an extended state-space model for the DIPC system is:

$$\underbrace{\begin{bmatrix} \dot{x} \\ \ddot{x} \\ \dot{n} \end{bmatrix} = \begin{bmatrix} zeros(3) & I_3 & zeros(3) \\ -M^{-1}K & -M^{-1}D & M^{-1}N \\ & zeros(3,9) & \end{bmatrix}}_{Ae} \begin{bmatrix} x \\ \dot{x} \\ n \end{bmatrix} + \underbrace{\begin{bmatrix} zeros(3,1) \\ M^{-1}B \\ zeros(3,1) \end{bmatrix}}_{Be} T_m \qquad (5\text{-}33)$$

$$y = \underbrace{I_9}_{Ce} \begin{bmatrix} x \\ \dot{x} \\ n \end{bmatrix}$$

Where:

$$N = I_3$$

$$\boldsymbol{x} = [\mathrm{x} \quad \theta_1 \quad \theta_2]^{\mathrm{T}}$$

To check the possibility for the observer to estimate these nonlinearities $(n_1, n_2 \text{ and } n_3)$ using the measured outputs, which are the cart position, the two angles, and the calculated

velocities. The observability of the pair (Ac, Ce) is checked by calculating the rank of the observability matrix (O_M) as follows:

Co = [eye(6), zeros(6,3)]

Om= obsv(Ae,Co)

rank(Om)

Which is found to be 9, i.e. full column rank. Thus the extended system is fully observable and an extended observer is able to estimate all the nonlinearities in the system based on the measured outputs. To obtain the desired speed of the observer, the gain vector (**L**) is chosen to place the observer's poles 10 times to the left from those of the control law. This is achieved using MATLAB's (*place*) function, as follows:

```
Observer_poles=10*[poles (1:6)' -70 -80 -90]
L=place(Ae',Ce', Observer_poles)'
```

And the resulting (**L**) vector is:

```
L =

  1.0e+004 *
    0.0233    0.0009   -0.0298    0.0074    0.0061   -0.0026
    0.0009    0.0707    0.0005    0.0012   -0.0009    0.0032
   -0.0297    0.0005    0.0662    0.0048    0.0022    0.0024
    0.0131    0.0012    0.0078    0.0585    0.0355   -0.0050
    0.0108    0.0005    0.0040    0.0369    0.0370    0.0073
   -0.0011    0.0011    0.0114    0.0025   -0.0033    0.0938
    1.2717    0.1114    0.7412    5.0925    3.2623   -0.7569
    0.0916    0.0042    0.0517    0.3451    0.2512    0.0104
    0.0103    0.0017    0.0072    0.0417    0.0267    0.0097
```

As in the case of SIPC, the first term of the estimated nonlinearities and disturbances is fed back to the controller so as to improve the overall response, and enhance system's immunity against disturbances.

5.4.3 Simulation results

The next step in controller design process is simulation. This step is very important to check whether the resulted system response meets the design specifications or not. The controller and observer design results obtained in the previous sections, and the system nonlinear model derived in Chapter Two are used with MATLAB and Simulink to simulate system's performance, as shown in Fig. 5.10. This figure contains the DIPC nonlinear model in s-function form, in addition to the robust tracking and disturbance rejection controller with the extended observer for nonlinearities and disturbances estimation.

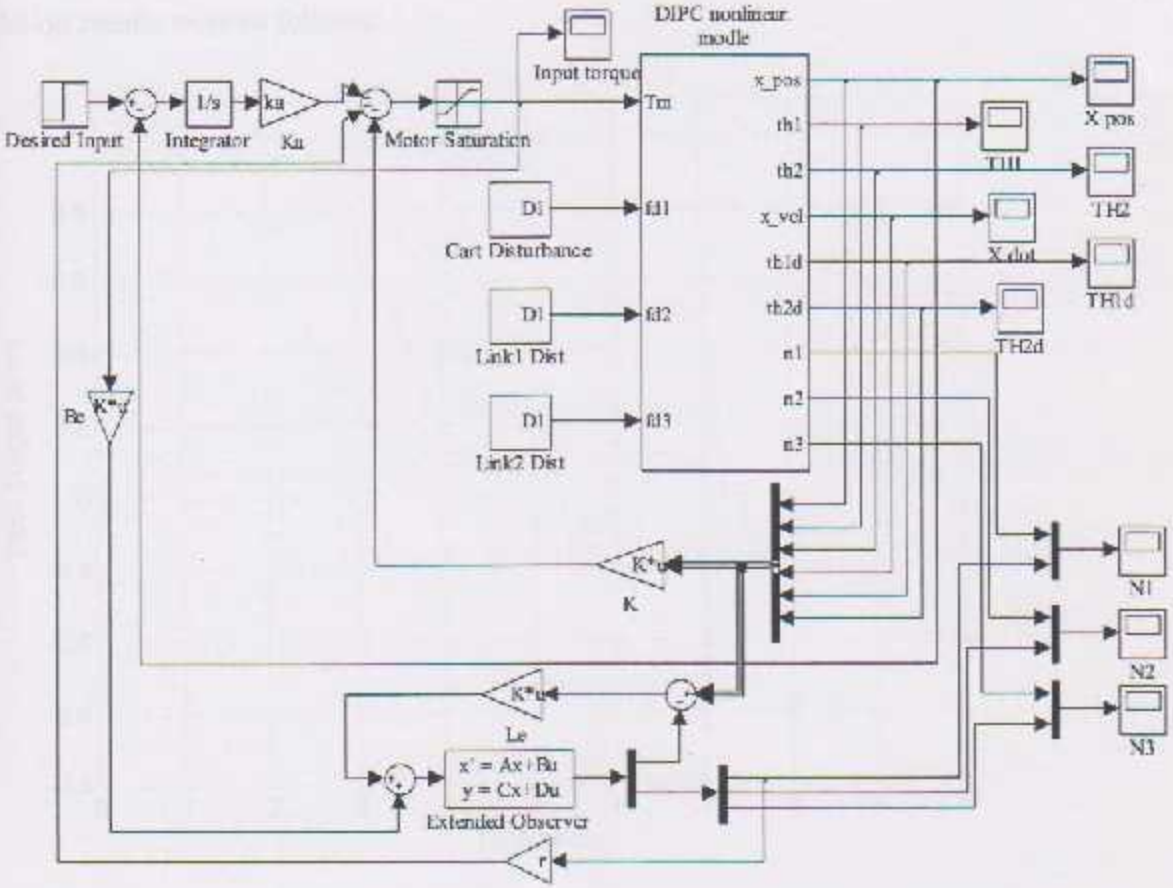

Figure 5.10 DIPC Simulink model.

The initial conditions, desired input, and disturbances acting on the system are supposed to be:

- Initial Conditions = 0.
- Desired cart position = 0.25 m.
- The two links should be stabilized at their vertical position, i.e. the final angle of each link must be forced to zero.
- There is a disturbing force acting on the cart at the interval (2 – 2.1) sec. with a value of 2 N.
- There is a disturbing force acting on the first link at the interval (5 – 5.1) sec. with a value of 0.2 N.
- There is a -0.05 N disturbing force acting on the second link at the interval (7 – 7.05) sec.

Simulation results were as follows:

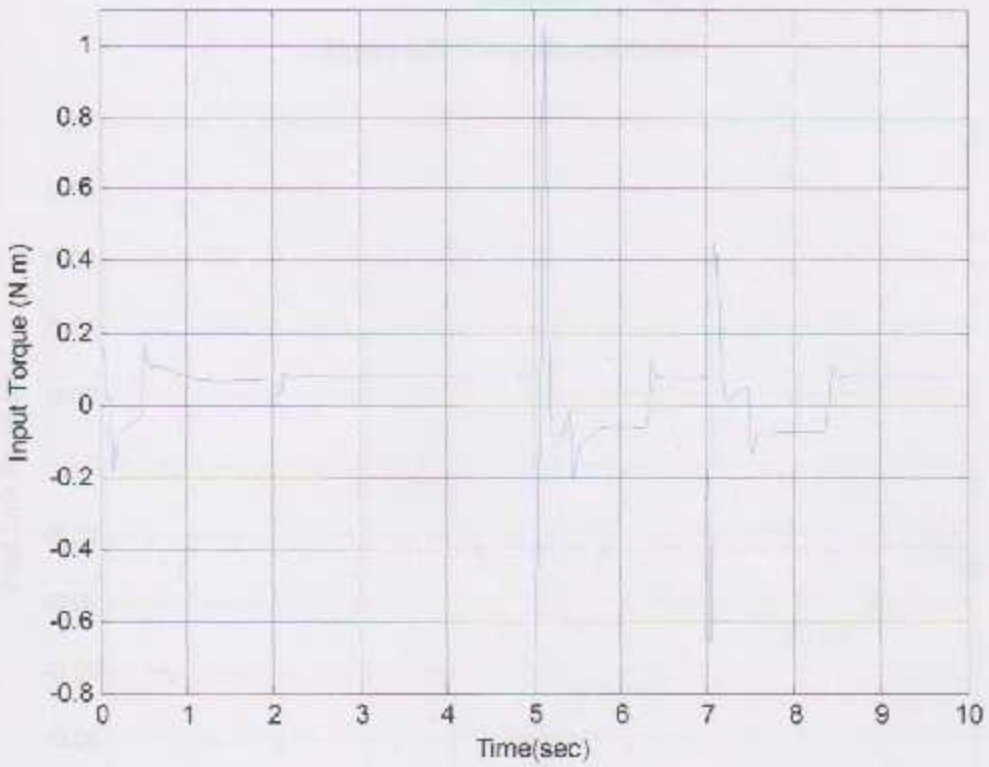

Figure 5.11 Deriving Torque signal.

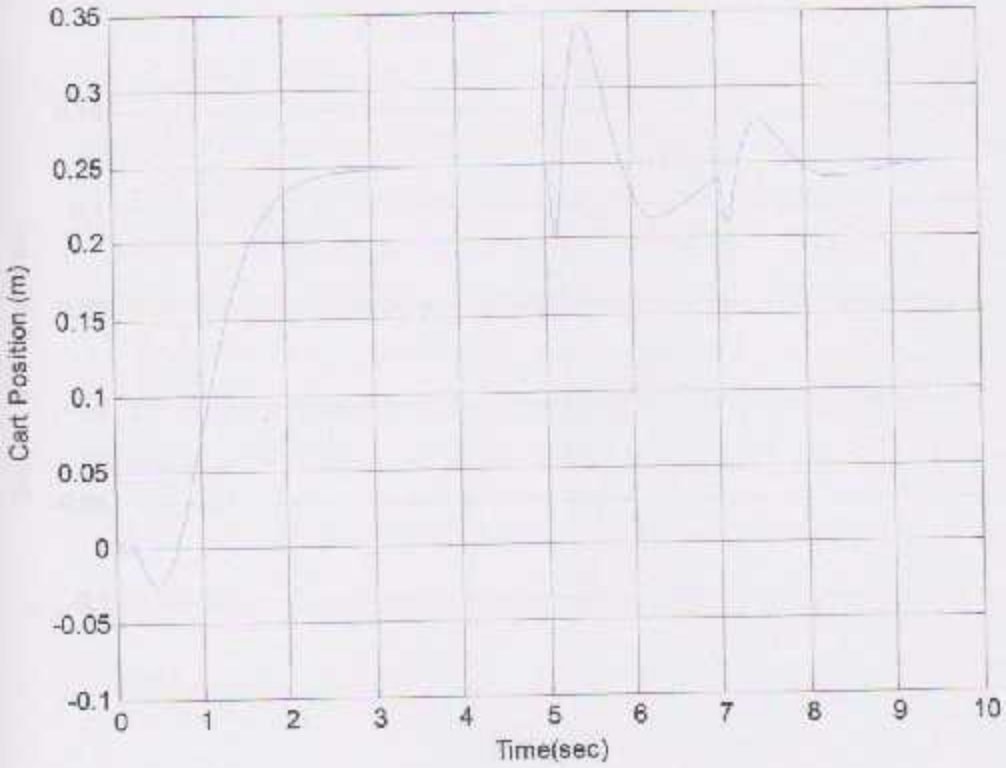

Figure 5.12 Cart position with time.

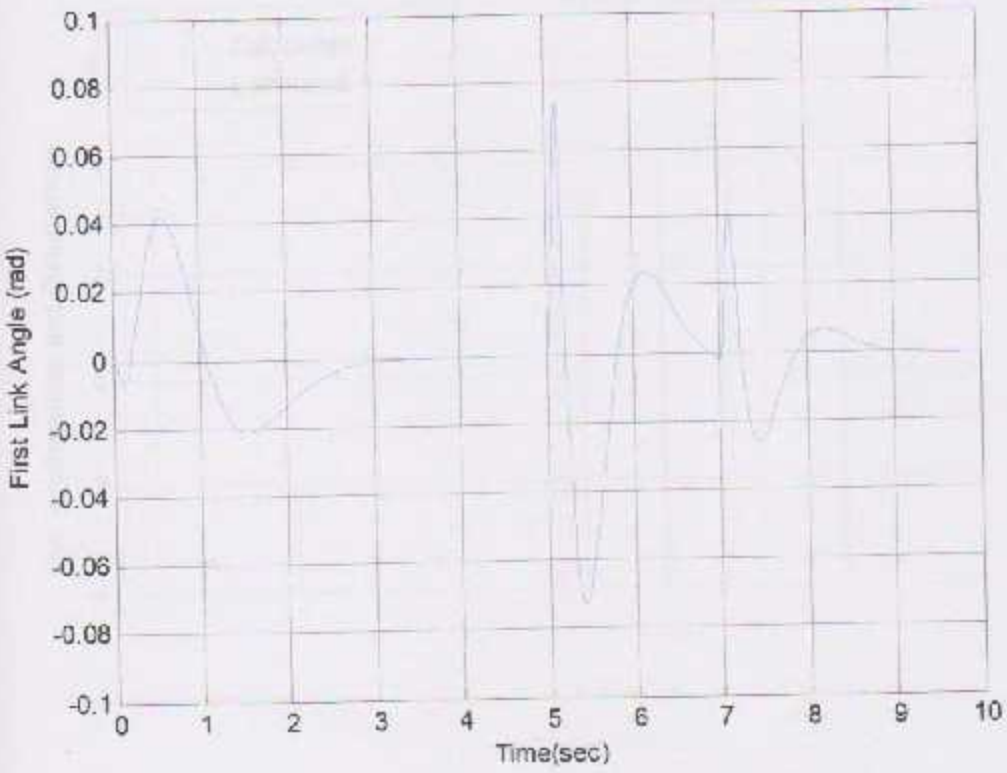

Figure 5.13 First link angular displacement.

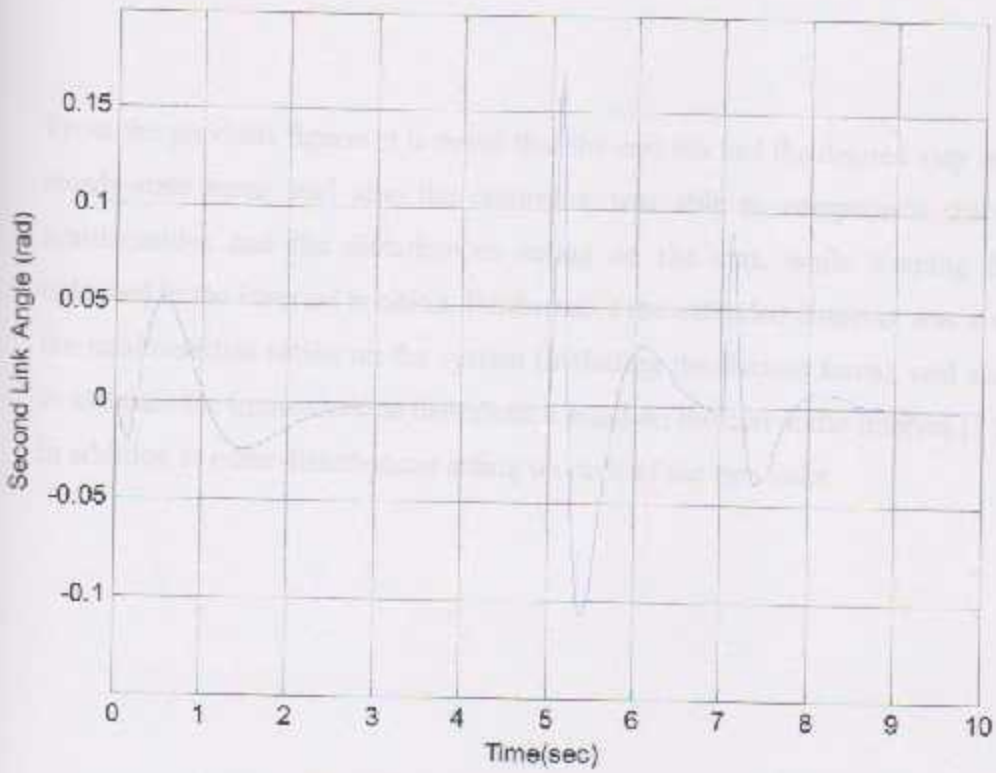

Figure 5.14 Second link angular displacement.

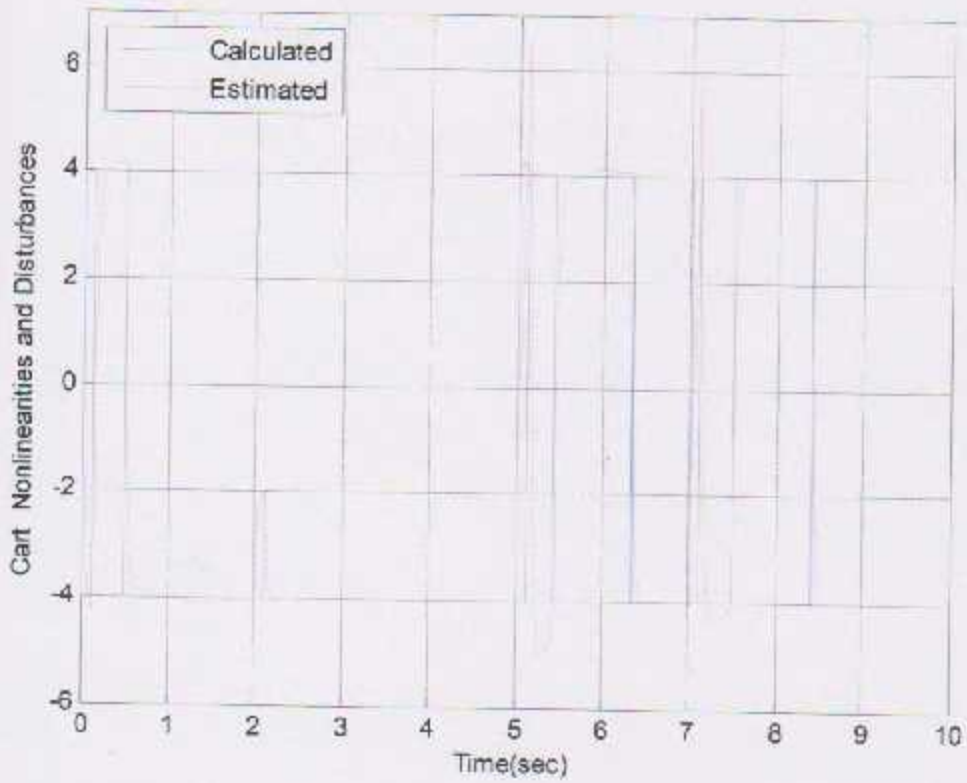

Figure 5.15 Estimated nonlinearity 1 (n_1).

From the previous figures it is noted that the cart tracked the desired step input with zero steady-state error, and also the controller was able to compensate the effect of the nonlinearities and the disturbances acting on the cart, while keeping the two links balanced in the inverted position. Furthermore the extended observer was able to estimate the nonlinearities acting on the system (including the friction force), and also it manages to estimate the immeasurable disturbance acted on the cart at the interval [2 2.1] seconds, in addition to other disturbances acting on each of the two links.

Chapter Six

Experimental Results

6.1 Introduction

The main objective of developing the double inverted pendulum on a cart system is to use it as a control test-bed. With such a system various controllers and control theories including state feedback, optimal control, neural networks, fuzzy logic, and nonlinear control theories can be studied and tested via a set of performance criteria such as:

- Links stabilization at the upright inverted position.
- Cart position tracking.
- Disturbance rejection.

Comparison between these control theories depends on:

1- The maximum links' angle that can be regulated.
2- Controller robustness.
3- Disturbance rejection ability.
4- Transient and steady state responses.
5- Energy consumption.

Figure 6.1 shows the developed double inverted pendulum system. This system consists of the mechanical components that construct the physical structure of the system, the AC servomotor and the servo driver, two incremental optical encoders for measuring links' angles, in addition to the interfacing circuits that connect the sensors and the actuator with the target PC, on which the real-time controller is implemented using xPC target technique. The target PC is equipped with two DAQ cards, NI6024E and PCI-Quad04. The former is a general purpose card that is used for:

- Generating an analog voltage signal representing the torque command for the servo driver.
- Receive the velocity and torque feedback signals coming from the servo driver.
- Receive a digital input signal used for switching between controller layers, as shown in section 6.3.3.

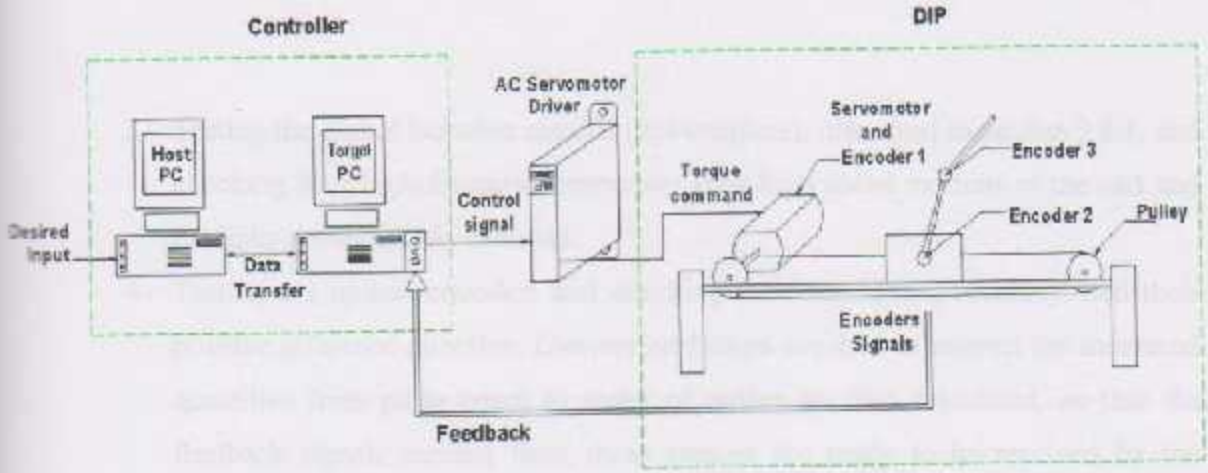

Figure 6.1 Hardware-in-the-loop simulation environment for DIP system.

The PCI-Quad04 DAQ, as stated in section 3.4.2, is a special DAQ used for interfacing quadrature incremental encoders. This DAQ is used to receive the feedback signals generated by the three encoders; so that cart position and links angle are determined.

Before starting experiments with the developed inverted pendulum system, it is necessary to perform some tests and modifications on some system components; so as prepare the system for being controlled. Such modifications and tests include:

1- Mechanical system modification, including :
   a. Aligning motor shaft with the pulley and the mounted bearings. This is important to eliminate vibration generated by misalignment, and protect the shaft of the motor and its bearings.
   b. Reduce the friction at the carriage and the two mounted bearings; so that less driving torque is required to overcome these friction forces.

   Further details related to the mechanical system are demonstrated at appendix A.
2- Testing the analog isolation circuit, described in section 3.6.1. These tests aim to ensure that the output voltage, i.e. that after isolation, equals the original input signal. After several testes it is found that a 0.02 volt offset between the input and output signals exists regularly, so that a correction constant is included within the Simulink model.

3- Testing the digital isolation circuits (opt-couplers), discussed in section 3.6.1, and checking their high-frequency response. Thus high speed motions of the cart and the links are accurately detected.

4- Testing the optical encoders and checking their resolution, accuracy, and their positive reference direction. Conversion factors required to convert the measured quantities from pulse count to meter or radian are also calculated, so that the feedback signals coming from these sensors are ready to be received by the controller.

5- Preparing the servomotor for torque control mode by installing the required parameters to the servo driver, as shown in section 3.2.4.

6- Installing the limit switches at the cart, so that motions beyond the predetermined limits are inhibited. This is necessary for protecting the mechanical structure and the driving motor form over-travel damages.

7- Preparing the connection between the host and target PCs using xPC target technique, according to the procedures demonstrated in section 4.6.

8- Modifying the Simulink models and making them ready for being converted to an accessible real-time application using MATLAB's real-time workshop, xPC target toolbox, and C++ compiler. This process includes:

   a. Replacing the s-function blocks, used in simulation models shown in sections 5.3.3 and 5.4.3, by the DAQ cards driving blocks. Such blocks enable the controller to communicate directly with the DAQ ports (the inputs and outputs) without any need for writing a low-level language programs.

   b. Using the "rate transition" blocks for matching between the discrete time DAQ ports and the continuous time controller.

In this chapter, state feedback control theories, discussed in Chapter Five, are applied and tested with the developed inverted pendulum system. With such a system the effects of poles location, gain values, input saturation, sampling time, nonlinearities and disturbances are studied and experimented with the cart alone, single and double inverted pendulum systems respectively.

As sated in earlier chapters, one of the challenges that face the control problem of inverted pendulum systems is that some of system's states are not directly measured. Thus, and in order to be able to implement the state feedback controller practically, the unmeasured states, which are those related to the velocity of the cart and the two links, should be estimated. This can be achieved by using either state observers, or numerical differentiation methods. The former is possible based on the fact that the system is fully observable. Such a method suffers from estimation errors due to system parameters uncertainty, and initial conditions of the system. Such errors will cause problems when dealing with sensitive applications as inverted pendulum. The second approach uses only the position measurement for velocity estimation.

As it is known, pure derivative operators link the position and the velocity, and the simplest method for differentiating a signal numerically is backward difference. This is the most common approach used to obtain the velocity from the position measurement. Unfortunately, this solution produces noisy estimations due to the combination of the following reasons:

- The position obtained by an optical encoder is a discrete-time, quantized signal; hence quantization noise is superimposed to the real value.
- Backward difference operator has a noise-amplifying characteristic, which is inversely proportional to the sampling time.

To solve these noise problems, a low pass filter is used. The filter's bandwidth is selected to compromise between noise rejection ability, and the relatively large control bandwidth necessary for high speed motions and quick reversals. Figure 6.2 shows the main idea used for velocity estimation using a filtered backward difference method.

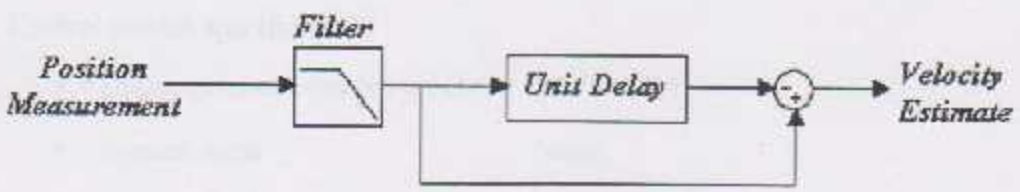

Figure 6.2 Velocity estimation method.

In the upcoming sections, robust tracking and disturbance rejection state feedback controllers, discussed in Chapter Five, are applied practically to the cart, and then to the single and double inverted pendulum systems respectively. Experiments results are also demonstrated and discussed for each case.

6.2 Cart experiments

In this section, two experiments performed on the cart are demonstrated and discussed in details. In the first, a robust tracking and disturbance rejection controller is used to robustly track a step reference cart position command, while an extended observer is used to estimate the nonlinearities acting on the system. The second experiment deals with the servo mechanism problem, where it is desired to make the cart track sine inputs with different frequencies.

Due to their simplicity, in comparison to the single and double inverted pendulum cases, the cart mathematical modeling and controller design processes are not detailed here, but only the final results are shown and used within m-files to calculate the desired feedback and observer gains.

6.2.1 Robust tracking and disturbance rejection controller with extended observer

In this experiment, it is desired to track a step cart position command robustly using state feedback control theories discussed in Chapter Five. Nonlinearities, including friction force, and external disturbances acting on the cart are also estimated with an extended observer, these estimates are then used with a static compensation loop to enhance system's ability for rejecting disturbances.

Control system specifications

- Uncompensated system poles $[0 \quad -0.721]$
- System zeros None
- Controlled system poles $[-7.03 \quad -7.05 \quad -25]$

- Feedback gains $[k \quad k_e] = [14.8 \quad 1.4 \quad -45.6]$
- Observer's poles 6* Sys. Poles
- Observer gains

$$L = \begin{bmatrix} 42 & 1 \\ -0.79 & 192 \\ -1 & 11586 \end{bmatrix}$$

Here, the closed-loop poles are selected to obtain an over damped transient response, with performance specifications as shown in Table 6.1. The m-file and Simulink model used for this experiment are available at Appendix B.1.

Table 6.1 Performance specifications

	Designed	Simulated	Actual
%OS	0	0	0
Settling time	0.57	0.68	0.91
Steady state error	0	0	0

Experimental results are shown in the following figures, including input torque command, cart position and velocity, in addition to the estimated nonlinearities.

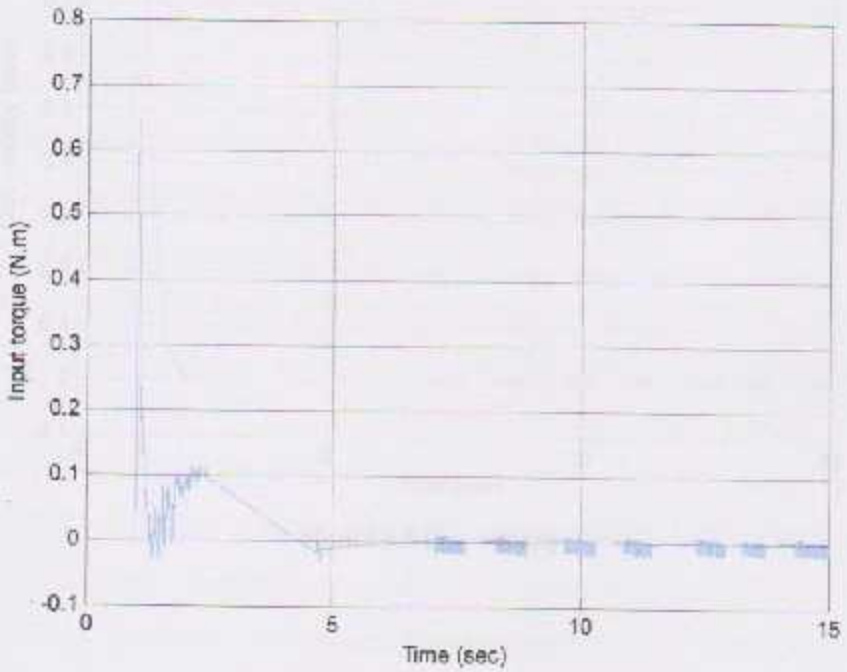

Figure 6.3 Actuating torque signal.

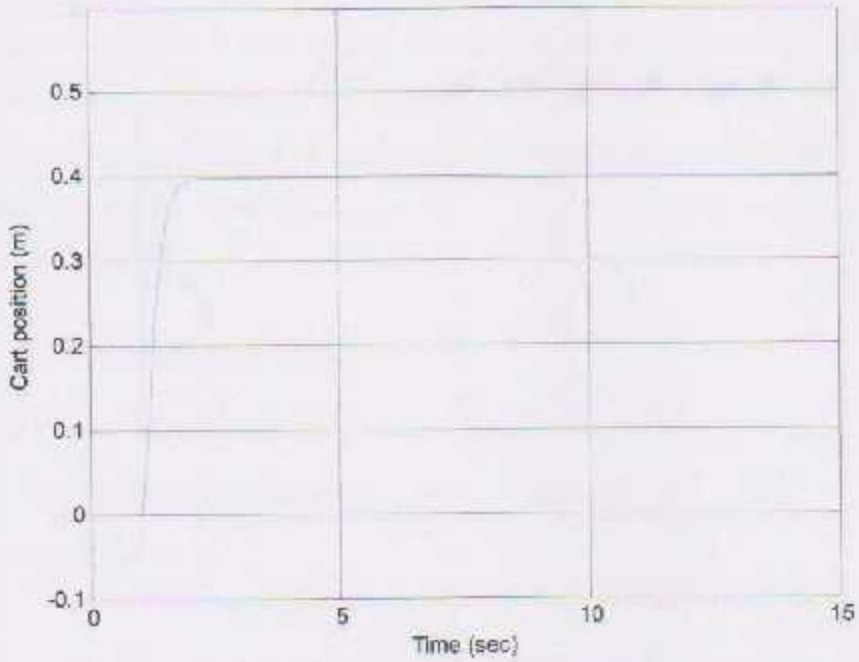

Figure 6.4 Cart position, the actual value (experimentally).

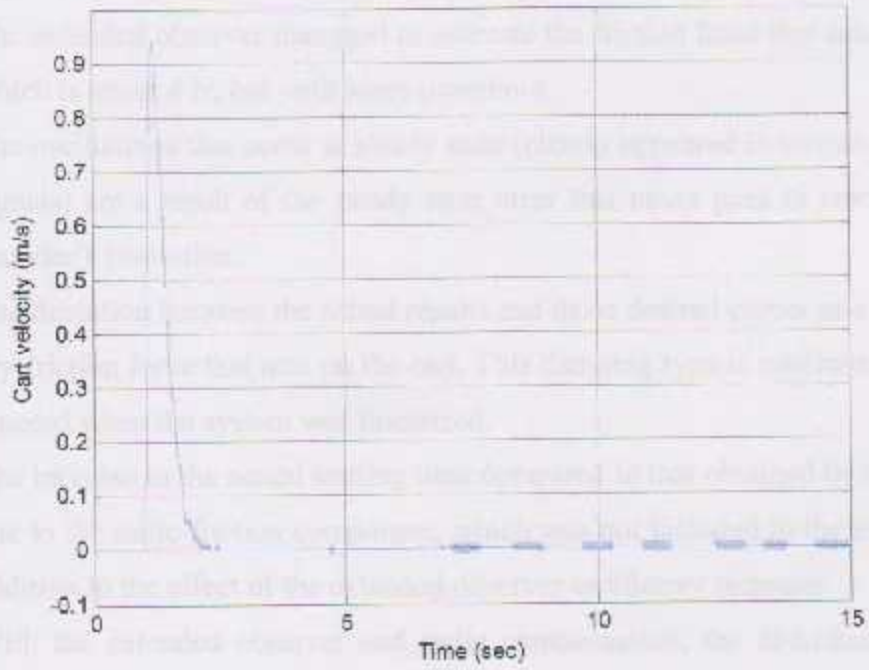

Figure 6.5 Cart velocity.

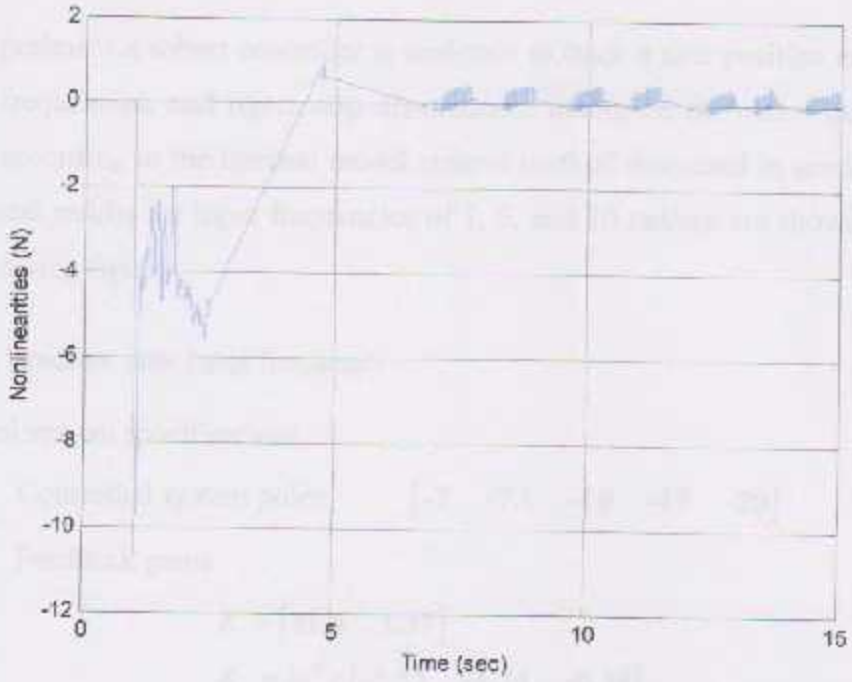

Figure 6.6 Estimated nonlinearities.

From the previous results, it could be noted that:

- The extended observer managed to estimate the friction force that acts on the cart, which is about 4 N, but with some overshoot.
- The oscillations that occur at steady state (clearly appeared in torque and velocity signals) are a result of the steady state error that never goes to zero; due to the encoder's resolution.
- The deviation between the actual results and those desired comes as a result of the dry friction force that acts on the cart. This damping type is nonlinear, and it was ignored when the system was linearized.
- The increase in the actual settling time compared to that obtained by simulation is due to the static friction component, which was not included in the simulation, in addition to the effect of the extended observer oscillatory response.
- With the extended observer and static compensation, the disturbance rejection ability of the system is much improved compared to that obtained with the robust controller alone. Furthermore, with this feature it is possible to obtain a high disturbance rejection performance independently of the controlled system poles location.

6.2.2 Sine tracking controller

In this experiment a robust controller is designed to track a sine position command with different frequencies, and reject step disturbances acting on the cart. The controller is designed according to the internal model control method discussed in section 5.2.1. The experimental results for input frequencies of 1, 5, and 10 rad/sec are shown respectively in the following figures.

1) With a 1 rad/sec sine input frequency

Control system specifications

- Controlled system poles $[-7 \quad -7.1 \quad -10 \quad -15 \quad -20]$
- Feedback gains

$$K = [31.6 \quad 1.37]$$

$$K_c = 1e^3 \times [-3.53 \quad -1.74 \quad -0.34]$$

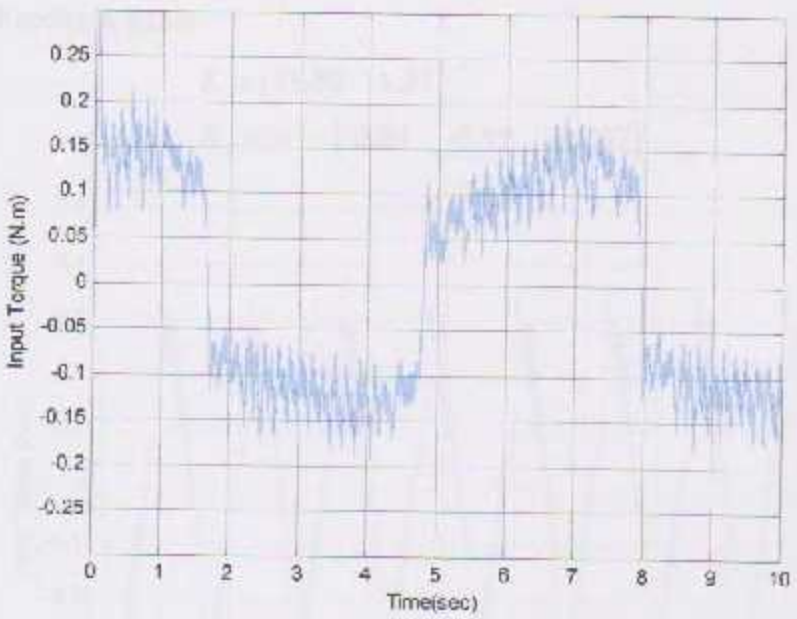

Figure 6.7 Torque command signal.

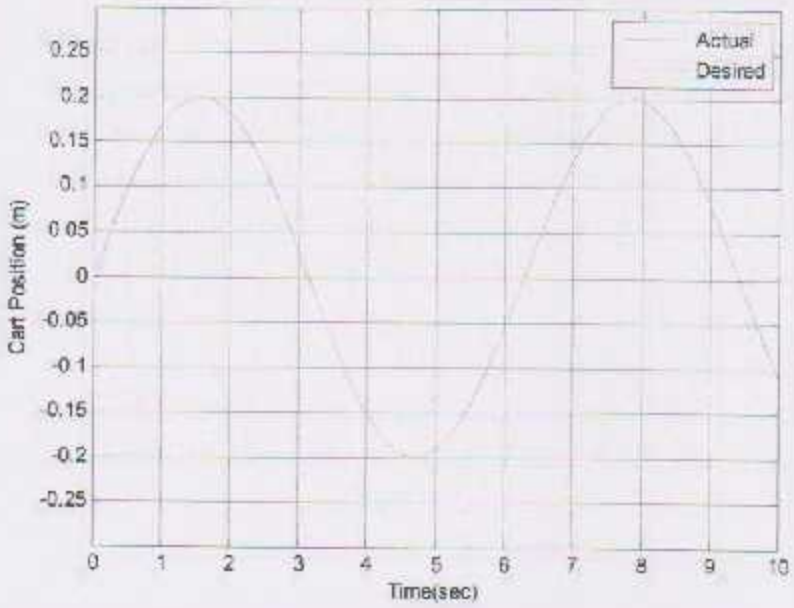

Figure 6.8 Cart position, the desired command and the actual response..

2) With a 5 rad/sec sine input frequency

- Controlled system poles $[-7 \quad -7.1 \quad -10 \quad -15 \quad -20]$
- Feedback gains

$$K = [31.05 \quad 1.37]$$

$$K_e = 1e^3 \times [-3.54 \quad -0.99 \quad -0.307]$$

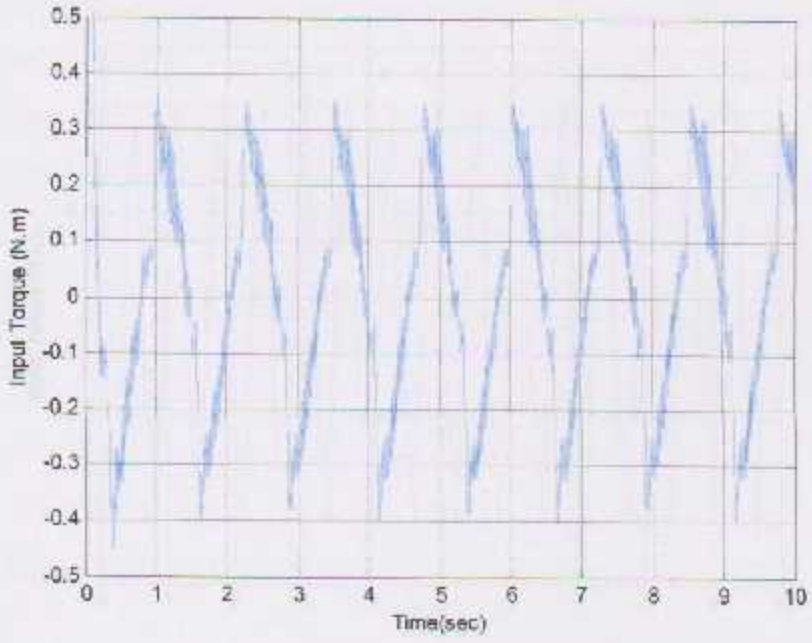

Figure 6.9 Torque command signal.

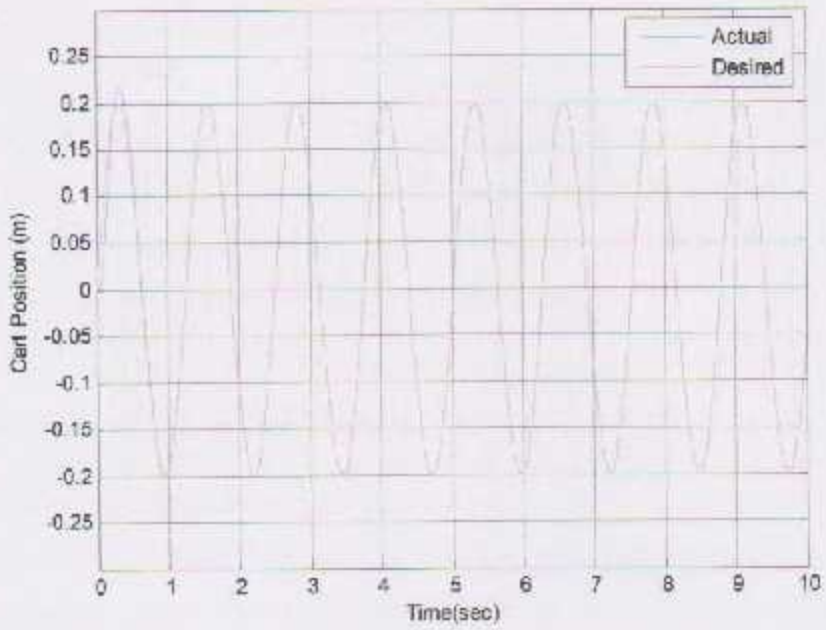

Figure 6.10 Cart position, the desired command and the actual response.

3) With a 10 rad/sec sine input frequency

- Controlled system poles $\quad [-7 \quad -7.1 \quad -10 \quad -15 \quad -20]$
- Feedback gains

$$K = [29.28 \quad 1.37]$$

$$K_e = 1e^3 \times [-3.54 \quad -1.16 \quad -0.201]$$

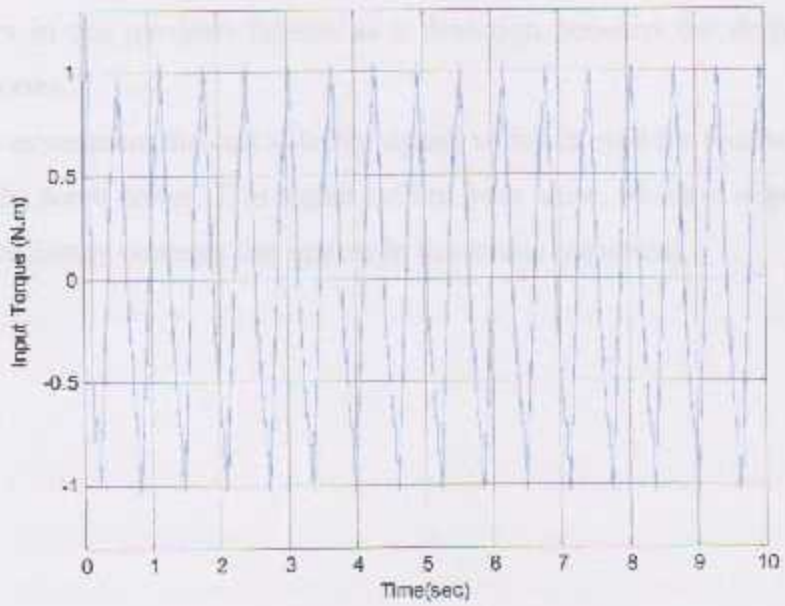

Figure 6.11 Torque command signal.

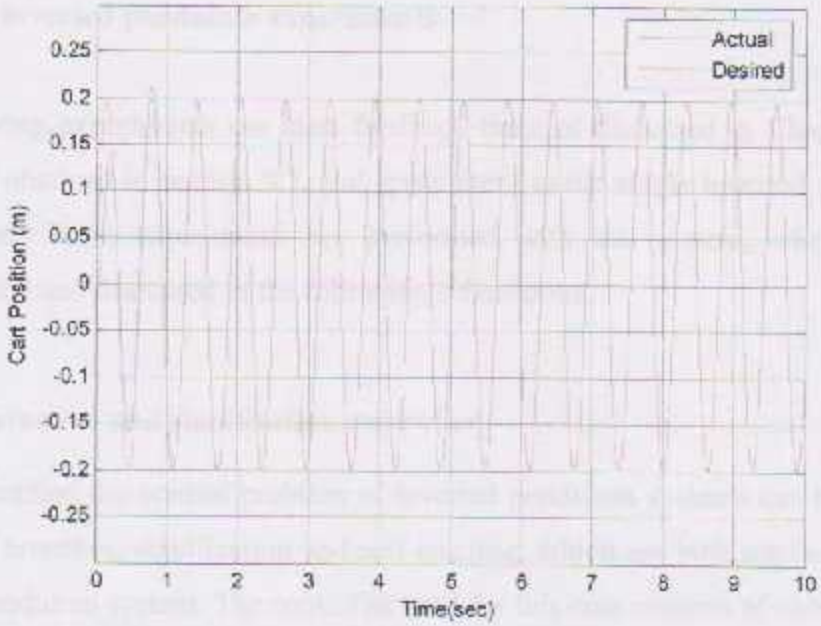

Figure 6.12 Cart position, the desired command and the actual response.

From the previous results it could be noted that:

- The controller managed to track the desired trajectories with zero steady-state error.
- The higher is the input frequency, the more is the required torque.
- By increasing the gain values, it is possible to obtain a faster transient response, but this will require more torque to be used. The transient response in this case appears in the previous figures as a deviation between the desired and actual trajectories.
- In this experiment the cart velocity signal, which is used for feedback, is obtained from the servo driver. This signal suffers from noise, which is responsible for the high frequency contents that appear in the torque command.

6.3 Single inverted pendulum experiments

The following experiments use state feedback theories discussed in Chapter Five, with the results obtained in section 5.3, and apply them to the single inverted pendulum on a cart system. Three experiments are performed with this system, whose results are demonstrated and discussed in the following subsections.

6.3.1 Self erection and stabilization controller

As stated earlier, the control problem of inverted pendulum systems can be divided into two major branches, stabilization and self erecting, which are both applied to the single inverted pendulum system. The controller used for this case consists of two parts:

1- Self erection controller

This is a bang-bang controller that aims to swing the link up to the inverted position by means of cart motion. With this controller, energy is added to the system such that its final energy approximates that at the upright vertical position. The main difficulties that face such a controller are:

- The limited rail length, such that the back and forth motion of the cart may not exceed certain limits.
- The link's velocity when it reaches the inverted position must be low enough, so that the stabilization controller will be able to keep the link stable at the desired position.

2- Stabilization controller:

This is responsible for keeping the link at the upright vertical position, tracking a desired step cart position command, and rejecting disturbances may act on the cart or the link.

Furthermore, a switching criterion is required for transmission from the first controller to second, when the link angle reaches the stabilization region. This switching uses the link angle measurements to determine which controller to be activated. The Simulink model

and the m-file for this experiment are available in Appendix B.2, while the following figures shows the torque command, cart position and link angle for a self erecting and regulation experiment.

Control system specifications

1. Self erecting
   - Controlled system poles $[-15.5 \quad -16 \quad -25]$
   - Controller gains $[k \quad k_c] = [33.96 \quad 1.83 \quad -203.36]$
2. Stabilization controller
   - Controlled system poles $[-0.45 \quad -0.5 \quad -6 \quad -6.1 \quad -70]$
   - Controller gains $[k \quad k_c] = [-2.13 \quad -8.47 \quad -2.78 \quad -1.26 \quad 0.47]$

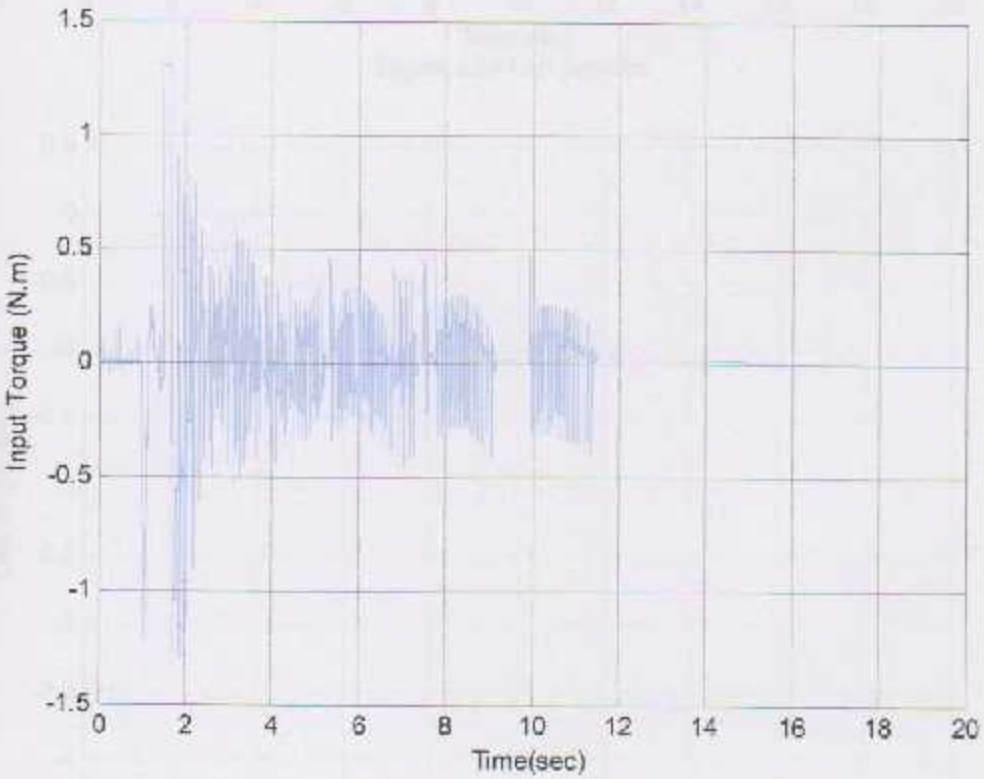

Figure 6.13 Actuating torque signal.

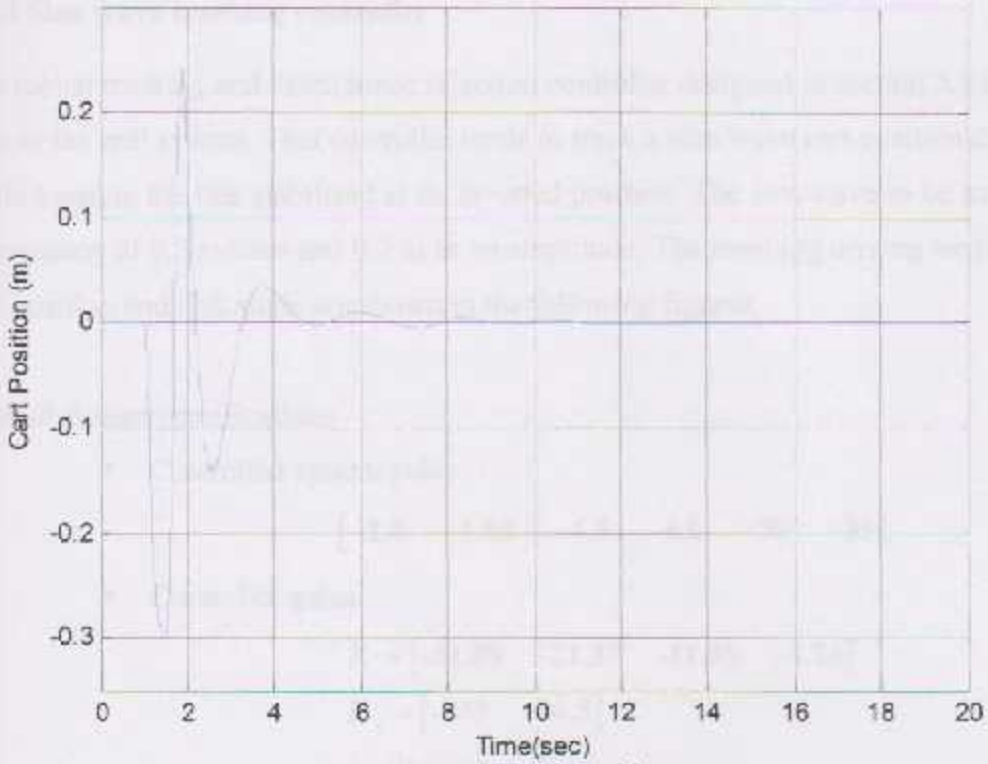

Figure 6.14 Cart position.

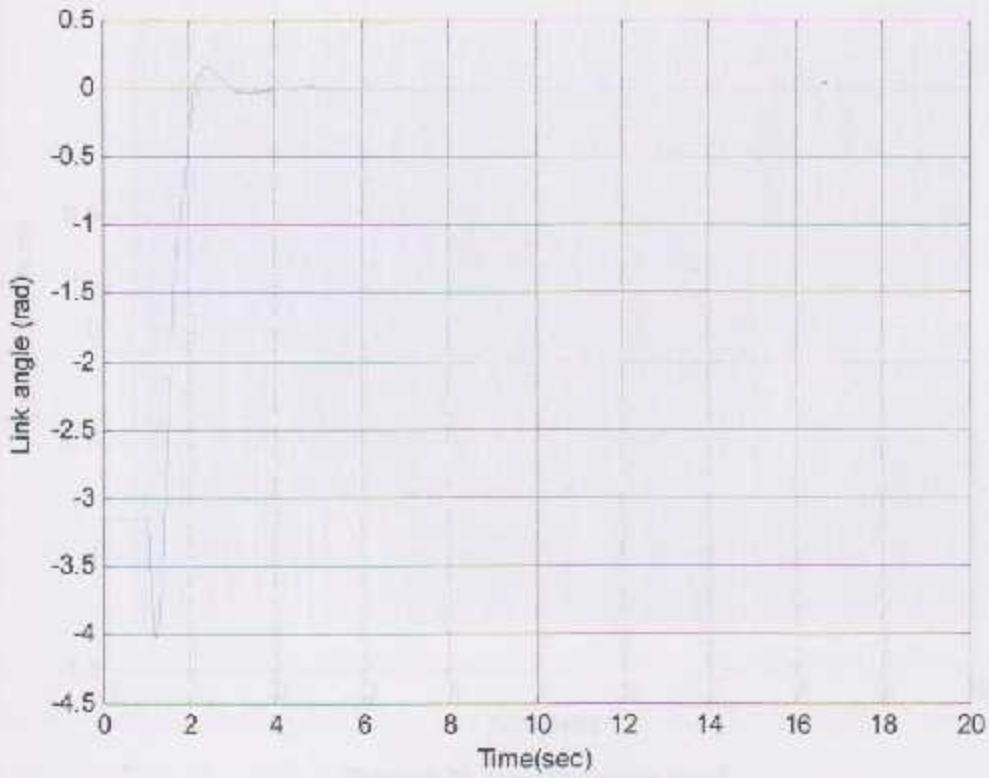

Figure 6.15 First link angle.

6.3.2 Sine wave tracking controller

The robust tracking and disturbance rejection controller designed in section 5.3 is applied here to the real system. This controller tends to track a sine wave cart position command, while keeping the link stabilized at its inverted position. The sine wave to be tracked has a frequency of 0.5 rad/sec and 0.2 m as an amplitude. The resulting driving torque signal, cart position and link angle are shown in the following figures.

Control system specifications

- Controlled system poles

$$[-1.8 \quad -1.85 \quad -4.5 \quad -4.6 \quad -30 \quad -35]$$

- Controller gains

$$K = [-31.89 \quad -21.37 \quad -11.85 \quad -3.14]$$
$$K_e = [-233 \quad -20.5]$$

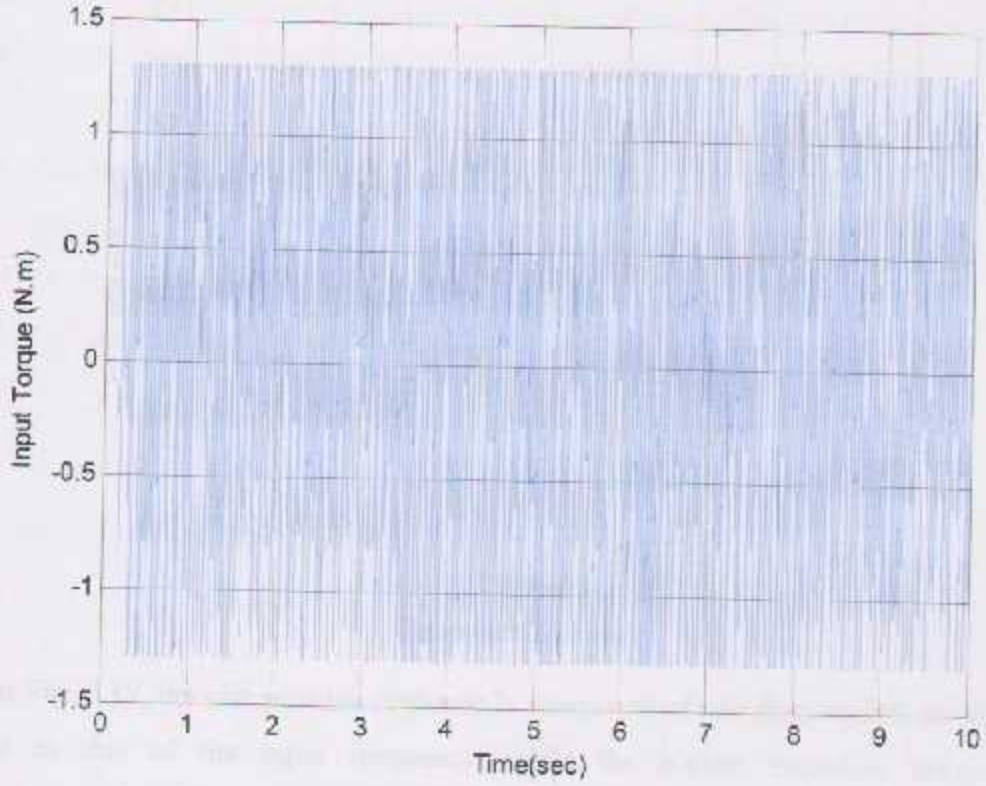

Figure 6.16 Actuating torque signal.

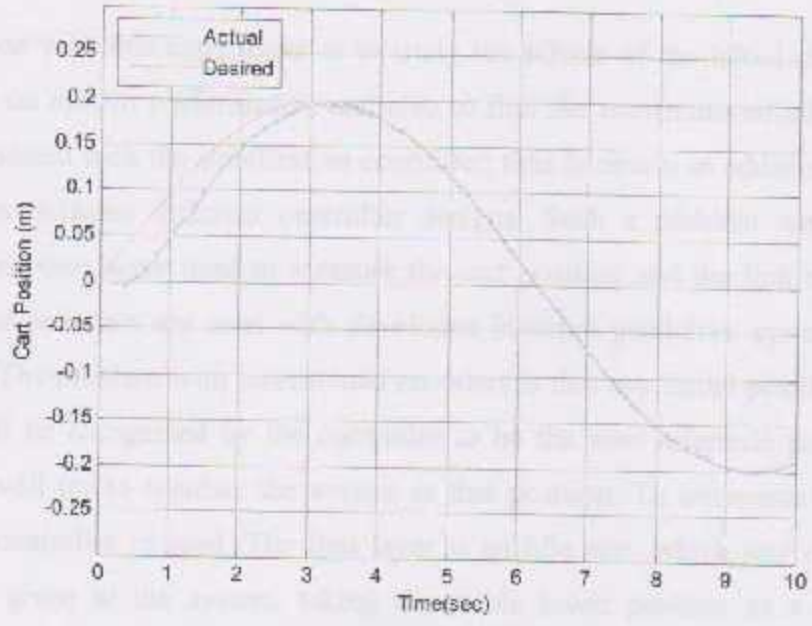

Figure 6.17 Cart position.

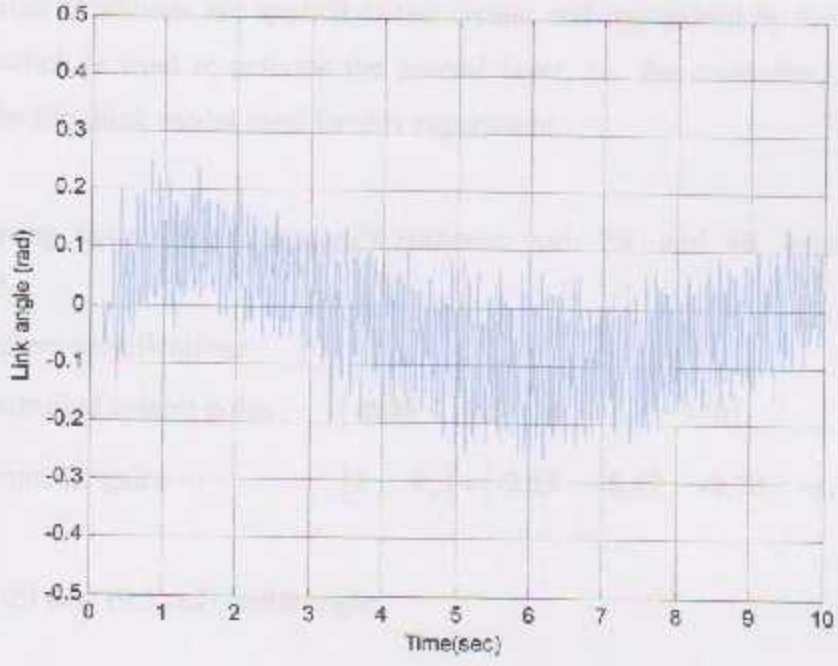

Figure 6.18 Link angle.

From Fig. 6.17, the cart position response is composed of two frequencies, the first is the same as that of the input frequency, while the higher frequency component is superimposed on the main one, and it is responsible for keeping the link stable at the upright vertical position.

6.3.3 Multi layers SIPC controller

The purpose with this experiment is to study the effects of the initial cart position and link angle on system performance, and also to find the maximum-initial link angle that can be regulated with the stabilization controller; thus to obtain an additional criterion for comparison between different controller designs. Such a problem would be easy if absolute encoders were used to measure the cart position and the link angle, but since incremental encoders are used with developed inverted pendulum system, a challenge will arise. The problem with incremental encoders is that any initial position given to the system will be recognized by the controller to be the zero reference position, and the controller will try to regulate the system at that position. To overcome this problem a two-layer controller is used. The first layer is an idle one, which just reads the initial conditions given to the system, taking the stable lower position as a reference. The second one is a stabilization controller, similar to that used with experiment 6.3.1. As the desired initial conditions are applied to the system and recognized by the first layer, an external switch is used to activate the second layer, i.e. the controller. Appendix C.3 includes the Simulink model used for this experiment.

The following figures shows system's response with 29° and 40° initial link angles respectively.

Control system specifications

- Controlled system poles $\begin{bmatrix}\mathbf{-0.45} & \mathbf{-0.5} & \mathbf{-6} & \mathbf{-6.1} & \mathbf{-70}\end{bmatrix}$
- Controller gains $\begin{bmatrix}k & k_e\end{bmatrix} = \begin{bmatrix}\mathbf{-2.13} & \mathbf{-8.47} & \mathbf{-2.78} & \mathbf{-1.26} & \mathbf{0.47}\end{bmatrix}$

1) With a -29 deg. (0.5 rad) initial angle.

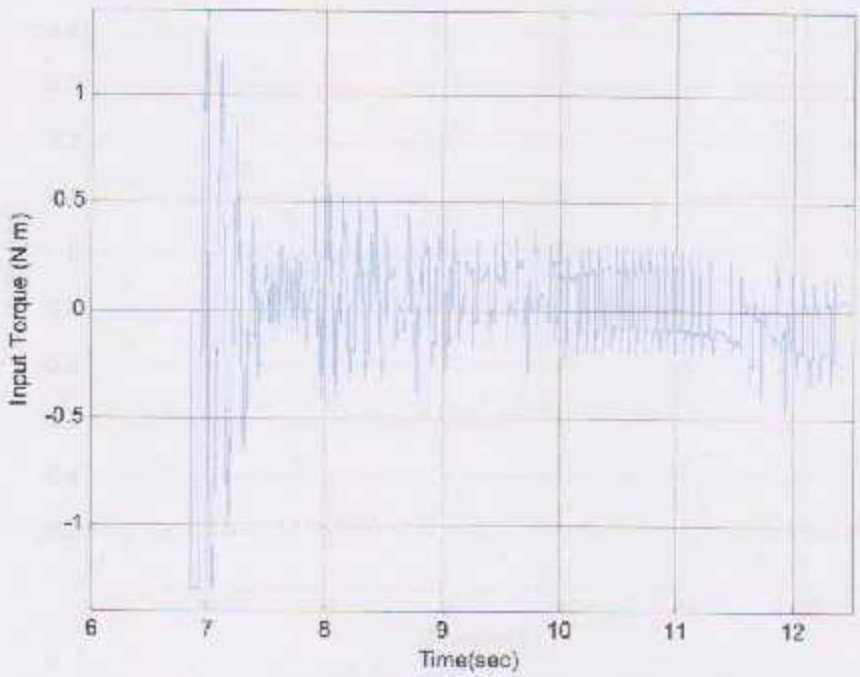

Figure 6.19 Torque command.

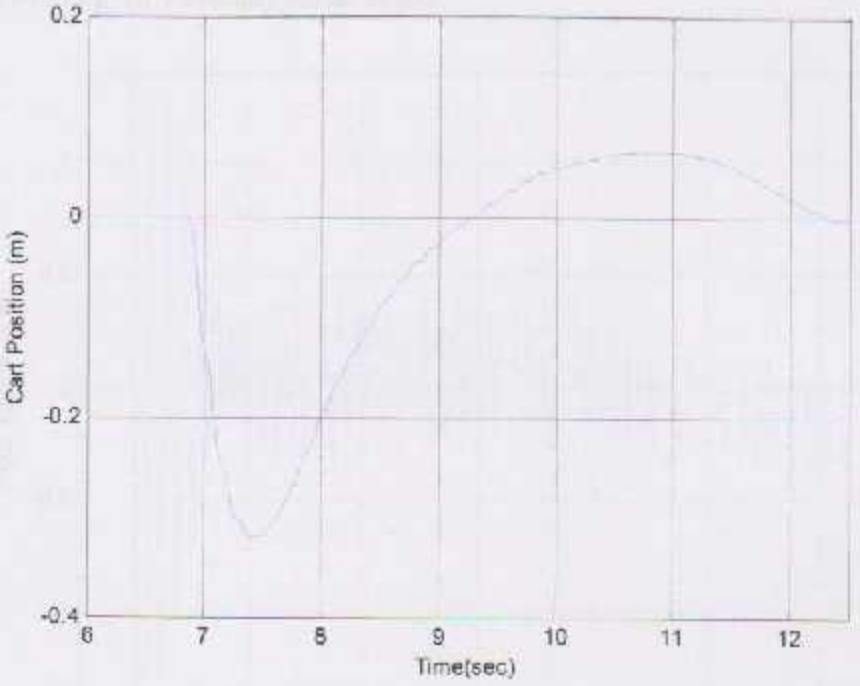

Figure 6.20 Cart position.

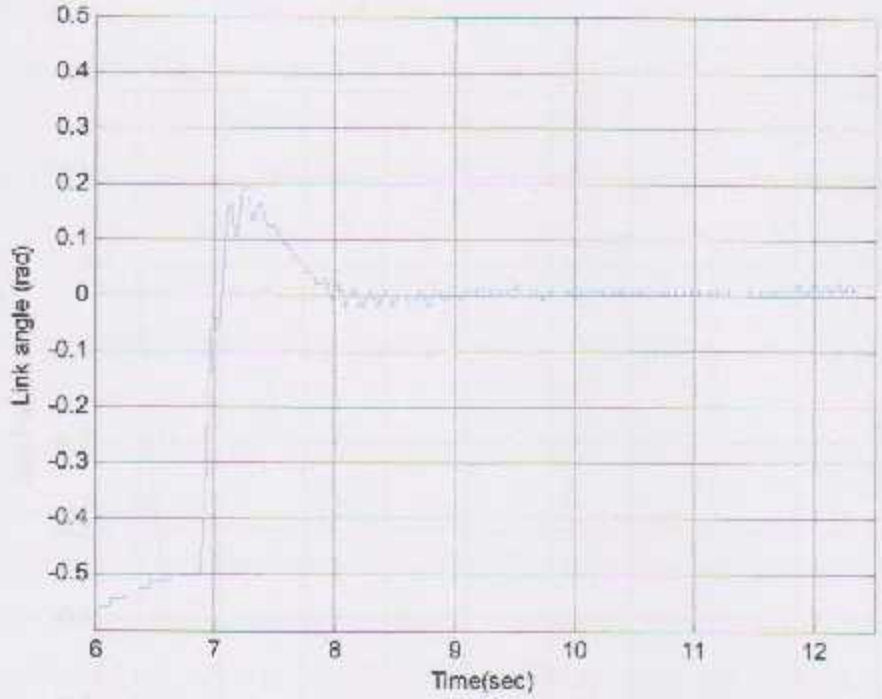

Figure 6.21 Link angle.

2) With a -40 deg. (0.7 radian) initial angle.

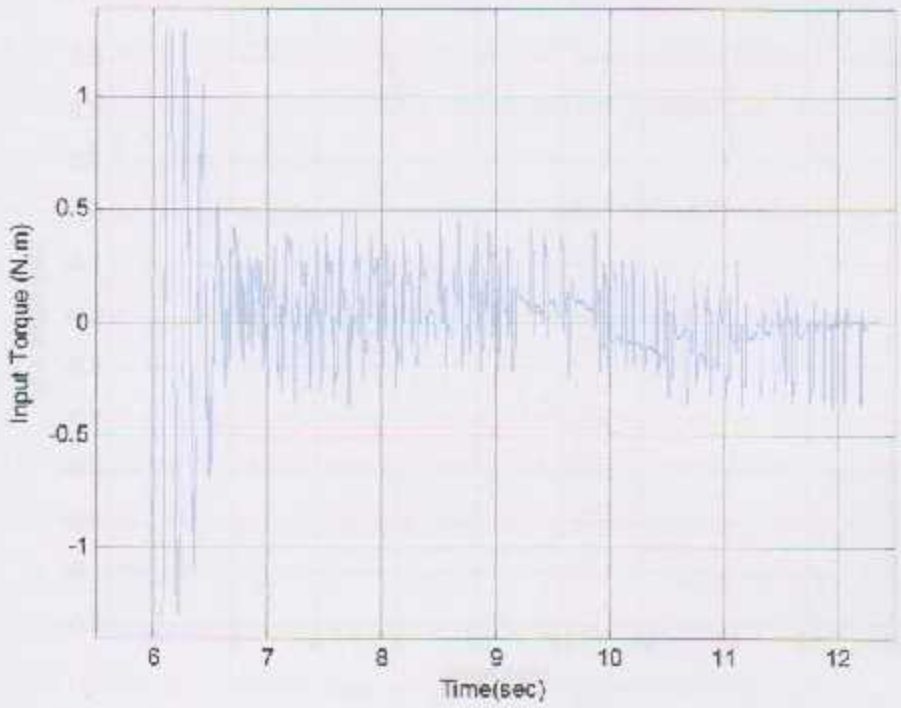

Figure 6.22 Torque command.

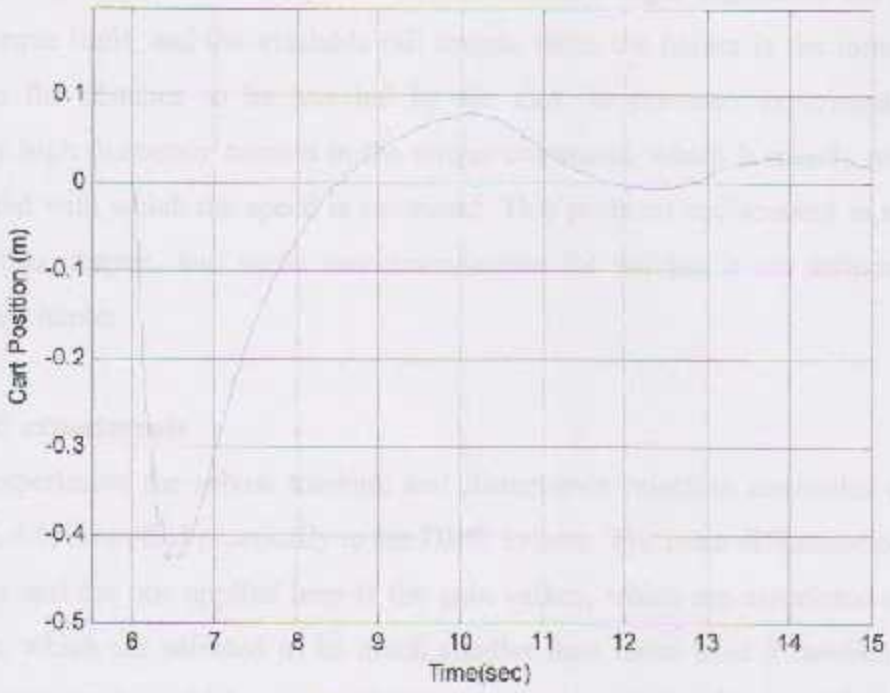

Figure 6.23 Cart position.

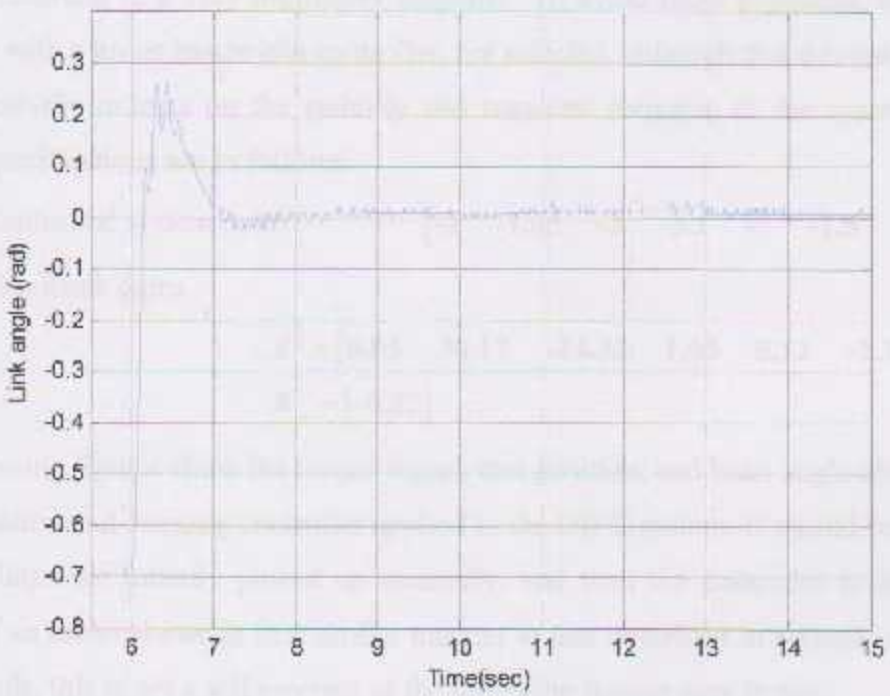

Figure 6.24 Link angle.

From these experiments it is found that the maximum initial angle that can be regulated is about 40 degrees. The main constraints that face the angle regulation are the driving motor torque limit, and the available rail length, since the higher is the initial angle the longer is the distance to be traveled by the cart. In previous experiments, there is relatively high frequency content in the torque command, which is mainly resulted from the method with which the speed is estimated. This problem is discussed in more details later in this chapter, and some recommendations for solving it are introduced in the upcoming chapter.

6.4 DIPC experiments

In this experiment the robust tracking and disturbance rejection controller designed in section 5.4.1, is applied practically to the DIPC system. The main difference between that controller and the one applied here is the gain values, which are associated to the poles locations, which are selected to be much smaller than those used in section 5.4.1. The problem with applying high gains to the practical system is that the unmodeled dynamics of the cable, which is used for power transition between the pulley and the cart, are excited; resulting in a very oscillatory response. To avoid these problems, lower gains, resulting with a lower bandwidth controller, are selected, although that this gain reduction will negatively reflects on the stability and transient response of the system. Control system specifications are as follows:

- Controlled system poles $[-1 \quad -1.05 \quad -3 \quad -3.1 \quad -7 \quad -7.5 \quad -15]$
- Feedback gains

$$K = [0.95 \quad 30.17 \quad -24.43 \quad 1.05 \quad 5.12 \quad -2.77]$$

$$K_r = [-0.32]$$

The following figures show the torque signal, cart position, and links angle obtained with a stabilization and tracking controller applied to the DIPC system. It should be noted that the two links are initially picked up manually, and then the controller is activated by means of an external switch in a similar manner to that described in experiment 6.3.3, in other words, this is not a self erection as the following figures may imply.

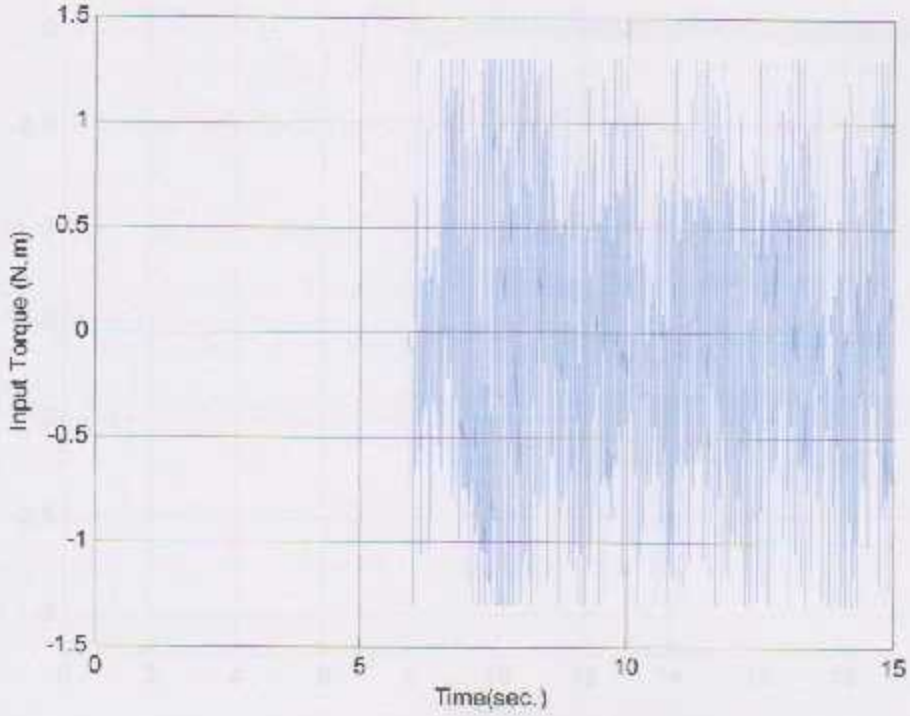

Figure 6.25 Torque command.

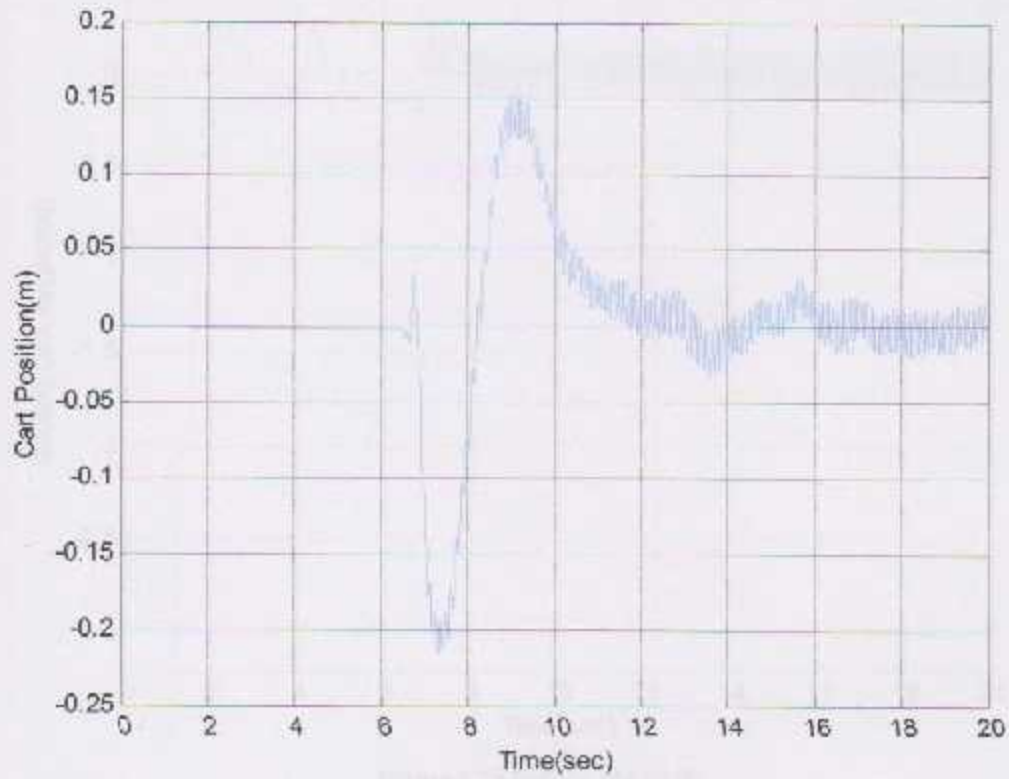

Figure 6.26 Cart position.

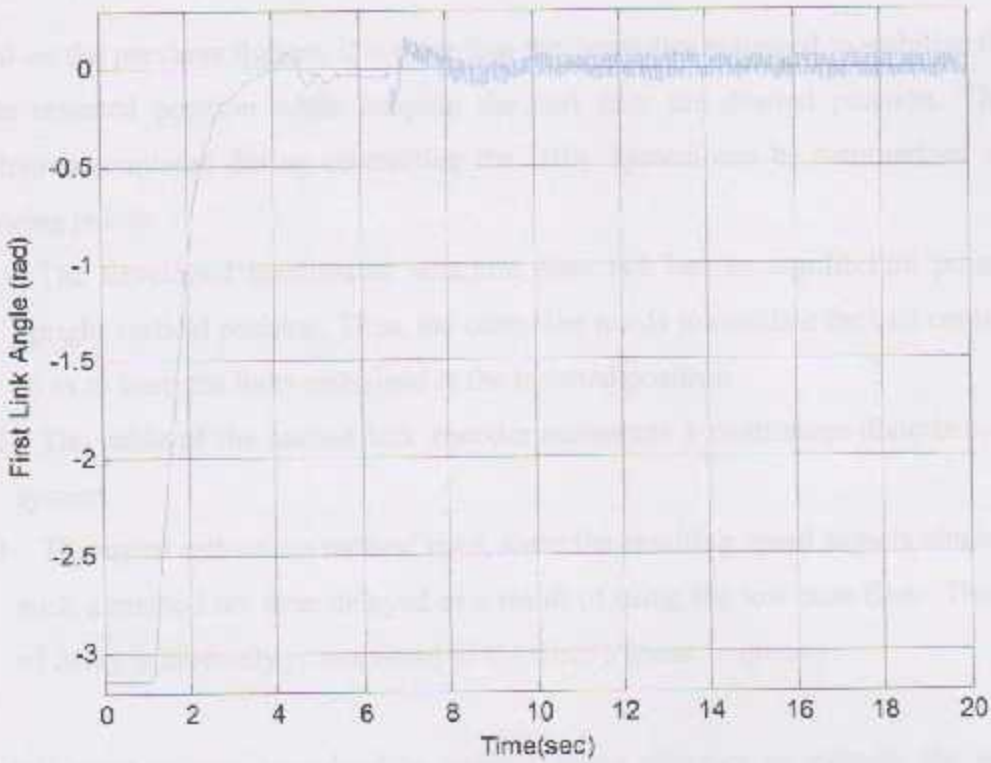

Figure 6.27 First link angle.

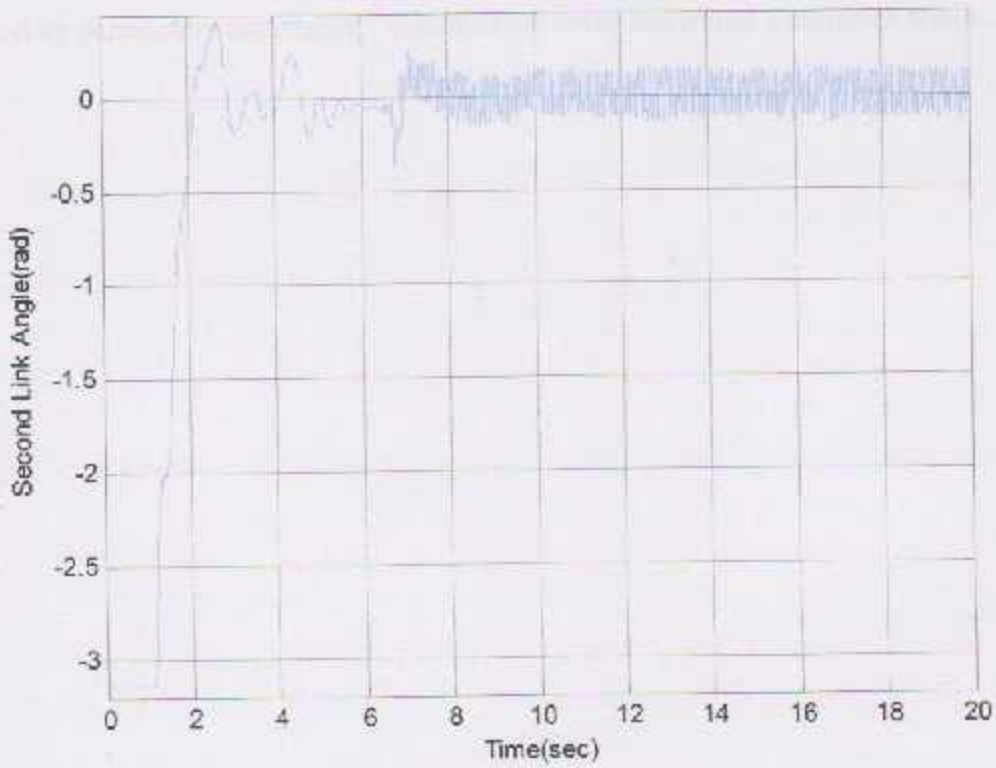

Figure 6.28 Second link angle.

Based on the previous figures, it is clear that the controller managed to stabilize the links at the inverted position while keeping the cart near the desired position. The main problem encountered during controlling the DIPC system can be summarized with the following points:

1- The developed mechanical structure dose not has an equilibrium point at the upright vertical position. Thus, the controller needs to oscillate the cart continuously so as to keep the links stabilized at the inverted position.

2- The cable of the second link encoder represents a continuous disturbance to the system.

3- The speed estimation method used, since the resulting speed signals obtained with such a method are time delayed as a result of using the low pass filter. The amount of delay is inversely proportional to the filter's break frequency.

The last problem may be solved by using a states observer to estimate the necessary unmeasured states, but this solution requires overcoming the existing estimate errors caused by parameters uncertainty, quantization noise and initial conditions effects.

6.5 Internet based self erection controller for the single inverted pendulum

In this section a self erection controller for the single inverted pendulum is applied, but this time with an internet host-to-target connection. In this experiment the controller is designed and simulated with a host PC located any where in the world, and then this controller is downloaded on the target PC located in the lab. With the host PC it is possible to tune some parameters on line, such as cart position command, gain values, etc. without any need for rebuilding or restarting the controller. Finally, the results are obtained from the target PC, as an Excel data file. Figure 6.29 shows the torque command, cart position and link angle during self erection, performed over the internet.

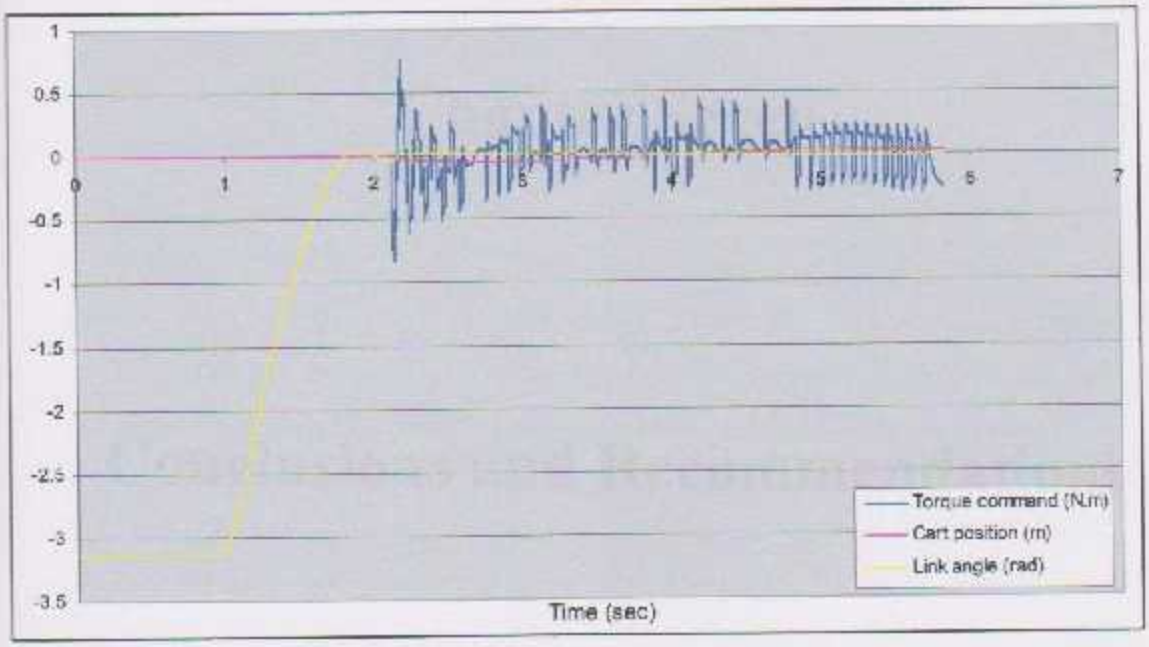

Figure 6.29 Internet-self-erection controller for single inverted pendulum

Chapter Seven

Conclusions and Recommendations

7.1 Discussions and conclusions

In this project a double inverted pendulum on a cart system is developed, tested and controlled. With such a system, several results related to the mechanical, electrical and computer parts, in addition to control theory, interfacing and real-time control implementation are obtained.

Starting with the mechanical part of the system, the existing structure is modified so as to make the system ready for being controlled. These modifications concentrate mainly on obtaining lower friction between moving components, and achieving the most possible alignment between those directly coupled components, i.e. the motor shaft and the pulley. This is important to protect these components, and to reduce the vibrations generated by misalignment.

Related to the electrical part, the AC servomotor used in the system is operated in torque control mode, which is essential for applying the designed controllers. Safety and protection features provided by the servo driver are also activated, while a noise filter is used to eliminate the effects of the harmonic content in the main power lines.

In order to measure the cart position and links angle, incremental optical encoders are installed. Accurate readings for these measurements, required to establish closed-loop controllers, are obtained using a DAQ specially designed for interfacing quadrature incremental optical encoders.

Interfacing, signal conditioning and isolation circuits between data acquisition cards, sensors and the actuator are designed, installed and tested. Such circuits aim to reduce noise problems, solve the vibration problem encountered when dealing with incremental encoders, and protect the equipment, specially the DAQ cards and the servo driver, from high voltage levels, high current loadings and misconnections. The necessary protection is implemented using two types of isolation circuits:

1- Special analog isolation circuit used to connect the DAQ analog output port with the servo driver torque command terminals.
2- High frequency digital isolation circuits used to interface encoders' outputs with the DAQ inputs.

State feedback control theories are then applied to design robust tracking and disturbance rejection controllers for the cart, the single and the double inverted pendulum systems. These controllers are based on the linearized mathematical model of the system, and then they are applied to the real system which is highly nonlinear due to the dry friction forces, centrifugal forces and other nonlinearities. It is found that such linear controllers work well with the nonlinear system, and satisfying responses are obtained. Further improvements on system performance may be achieved using nonlinear control theories.

An extended observer for nonlinearities and disturbances estimation is then designed, where those disturbances related to the cart are statically compensated. Using such an approach, the disturbance rejection ability of the system is much improved compared to that obtained with the robust controller alone. Furthermore, with this feature it is possible to obtain a high disturbance rejection performance independent to the controlled system poles location.

xPC target technique, provided by MATLAB, is used for real-time controllers implementation, using a standard PC hardware with DAQ cards. In addition to the high real-time abilities obtained with such a technique, changes and modifications are introduced with high flexibility; which in turn encourages students and researchers to explore different ideas easily and quickly.

Moreover, network and internet host-to-target communications provided by the xPC target technique are successfully achieved. By means of such connections, it is possible to download the controller to the target PC, apply it to the developed inverted pendulum system and monitor the running application using a host PC located anywhere in the

world, without any need for traveling to the lab where the structure is installed, in other words, a global laboratory can be established with the help of such a technique.

7.2 Problems encountered and recommendations

Several problems and difficulties were encountered during working with this project. One of the main difficulties was to import the PCI-Quad04 DAQ which is used for encoders. This DAQ was available neither in the local market nor in the region. Thus, such a card was ordered form the primary company's center in the United States, and it took about three months till it reached. Finding a suitable way for isolating analog signals without being distorted or delayed formed another challenge. Even after finding the suitable capacitive isolation amplifier, it was extremely difficult to obtain such parts.

Since it is mounted on a rotating part, it is a real problem to find a suitable solution for connecting the encoder responsible for measuring the second link angle through a cable, without disturbing links motion. A recommended solution for such a problem is to use a wireless encoder instead of that currently used.

Further improvements on system performance can be achieved using an accurate solution for speed estimation, so as to get rid of quantization-related problems discussed in Chapter Six. Several ideas are being studied to tackle this problem including continuous observers, discrete observers, and extended ones, in addition to the filtered backward differentiation previously discussed.

Based on the results obtained in this project, two papers are submitted for publication. The first is accepted for presentation at ASME 2007 International Design Engineering Technical Conferences & Computers and Information in Engineering Conference, Las Vegas, USA, titled as "Development of a Flexible Educational Mechatronic System Based on xPC Target". The second is about "Control of a Double Inverted Pendulum on a Cart: theory and experimental results" submitted to the 6th Jordanian International

Mechanical Engineering Conference (JIMEC'6), Amman – Jordan. A copy of each paper is available at Appendix C.

The system in its current state can be used as an excellent test-bed for various control techniques. Although controllers based on linear control theories achieved a satisfying performance, it will be interesting to apply the principles of non-linear control and achieve further improvements in system performance. Furthermore, fuzzy logic, neural networks, digital control and optimal control methods can be applied, tested and compared by means of this apparatus.

Finally the developed DIPC system will be a valuable addition to control laboratories in this university. With such a system, experiments range from simple and basic ones, related to the cart, to highly complicated control problems, performed with single and double inverted pendulum systems, can be performed. Controller design, sampling frequency and computational and transport time delays effects on stability and response are relevant issues that can be demonstrated and tested.

Appendices

Appendix A

Mechanical and Electrical components

In this appendix, the main mechanical components of the DIPC system, shown in Fig. A.1, are demonstrated and briefly discussed. These components include:

Figure A.1 The developed DIPC system.

1- Base plate

Which is the base where the servomotor, ball bearings, linear guide, limit switches cams, and the dampers are assembled.

2- Ball bearing:

The function of ball bearing is to fix the pulley with the base, permitting them to rotate with minimal possible friction. In order to reduce the friction at those bearings, the lubricant and its keepers are removed as shown in Figure A.2.

Figure A.2 Ball bearing before and after removing the lubricant and its keeper.

It should be noted that the ball bearings used in this project are of flexible type, i.e. they can rotate freely within their housing. In order to prevent such motions, two sets of bearings are to be used, where problems of misalignment and high friction arise. To overcome this problem, an adhesive material called "Poxy-Ball" is used to fix the bearings in their housing preventing in turn those rotations.

3- Damper

Two dampers are installed at the linear guide ends, so as to protect the components against damages if a collision happens. Figure A.3 shows one of those dampers and how it is installed.

Figure A.3 The damper.

4- Electrical cable guide

Using the electrical-cables guide, shown in Fig. A.1, aims to keep the wires within a fixed path while the cart moves. So as to protect them against damages.

5- Encoder coupler

The encoder corresponds to the second link, is fixed with the first link by two screws, the second link is jointed with the shaft of the encoder which permits the links to move freely relative to each other.

Figure A.4 The encoder coupler

6- limit switches cams

Which are used to activate the electrical limit switches mounted on the cart, so as to prevent motion beyond these limits.

7- Interfacing circuit

The interfacing circuits used in this project are implemented on a single board as shown in Fig. A.5, the board is sprayed with an electrostatic material in order to reduce noise problems.

This interfacing circuit includes:

1- Digital isolation circuits used to interface the incremental encoders with the PCI_QUAD04 counter.

2- Analog isolation circuits used to isolate the NI DAQ analog output ports from the servo driver torque command terminals.

3- Torque control mode circuit, including:

   a. Servo on switch.

   b. Alarm clear switch.

4- +12 and +18 volt regulators.

5- Encoders' connection terminals.

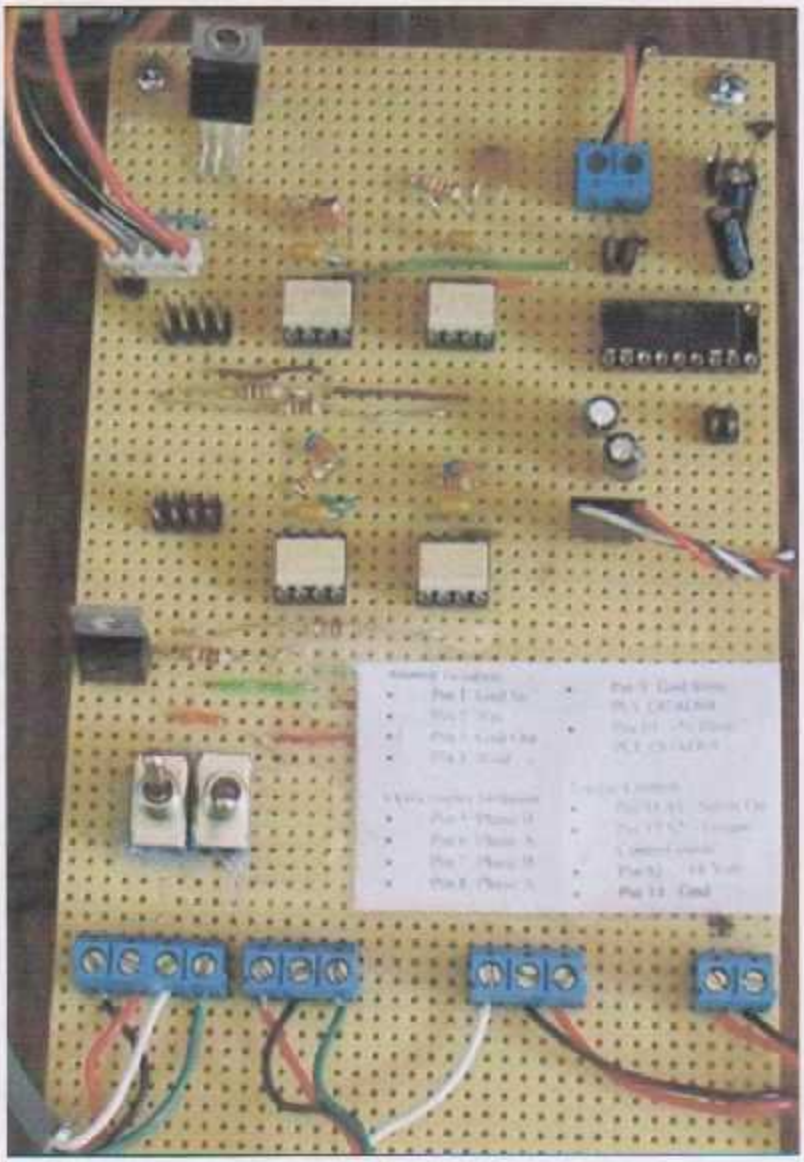

Figure A.5 Interfacing circuit.

Appendix B

Controllers design and implementation. m-files and Simulink models

B.1 Cart position tracking

```
%=======================================================================%
%==========              Cart position Tracking                 ======%
%=======================================================================%
% Defining the basic parameters for the system
% units are Kg.M.s

clear all

m=1.45;             %Cart mass in kg
r=0.020173;         %Pulley's radius in m
j=0.000153;         %Mass moment of inertia of the motor and pulley in
Kg.m2
d=0.00058;          %Motor viscous damping coefficient N.m.s/rad
mu=0.27;            %Friction Coefficient between the carriage and rail

%State space model-Linear
% System states are : [x ; x_dot ]
A=[0 , 1; 0 -d/(j+m*r^2)];
B=[0; 1/(j/r +m*r)];
C=eye(2);
D=0;
sys=ss(A,B,C,D)

%Robust tracking (Augmented system)
Ctrack=[1 0];
Aa=[A zeros(2,1) ;  -Ctrack 0 ];
Ba=[B;0];
Ca=[eye(2), zeros(2,1)];
Da=0;
poles=[-7.03 -7.05 -25];
k1=place(Aa,Ba,poles);
k=k1(1:2)
kc=k1(3)

% Extended observer
% The new state represents (Fdist-Ffric)
Ae=[0 1 0; 0 -d/(j+m*r^2) 1/(m+j*r^-2); 0 0 0];
Be=[0 ;1/(j/r +m*r); 0]
C= [1 0 0 ; 0 1 0];
De=0;
polese=6*[poles];
Le=place(Ae',C',polese)'
```

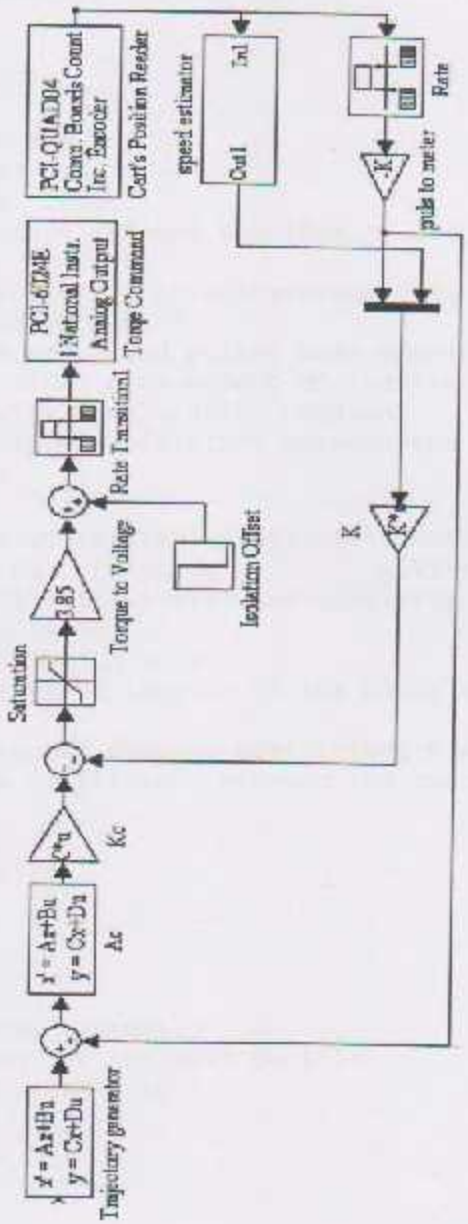

Figure B.1 Cart controller Simulink model

B.2 Single inverted pendulum self erection and stabilization controller

```
%=========================================================================%
%==========   Self Erecting and Stabilization controller    =============%
%=========================================================================%
% Defining the basic parameters for the system
% units are Kg.M.s

clear all

M = 1.40;            %Cart mass
m1 = .165;           %link1 mass
L1 = .335;           %link1 length
l1 = 0.162;          %distance between the link1's center of gravity and
                      its
                     %center of rotation(revolute joint)
r = .02;             % pulleys radius
J = 1.55e-4;         % the motor and pulley mass moment of inertia
J1 = 0.0013;         %the link1 mass moment of inertia
g = 9.81;            %gravity acceleration constant
fc=0.15;             %friction coefficient between the cart and the
                      rail

%%%%%%%%%%%%%%%%%%%%%%%%%%%%%%%%%%%%%%%%%%%%%%%%%%%%%%%%%%%%%%%%%%%%%%%
%%%%%%%%%%                  Self Erecting            %%%%%%%%%%
%%%%%%%%%%%%%%%%%%%%%%%%%%%%%%%%%%%%%%%%%%%%%%%%%%%%%%%%%%%%%%%%%%%%%%%
m=1.55;          %Cart mass in kg
r=0.020173;      %Pulley's radius in m
j=0.000153;      %Mass moment of inertia of the motor and pulley in
Kg.m2
d=0.00058;       %Motor viscous damping coefficient N.m.s/rad
mu=0.15;         %Friction Coefficient between the carriage and rail

%State space model-Linear
 As=[0 , 1; 0 -d/(j+m*r^2)];
Bs=[0; 1/(j/r +m*r)];
Cs=eye(2);
Ds=0;

%Robust tracking (Augmented system)
Ctracks=[1 0];    %Tracking for the cart position
Aas=[As zeros(2,1) ;  -Ctracks 0 ];
Bas=[Bs;0];
Cas=[eye(2), zeros(2,1)];
Das=0;
%poles=[-15.5 -16 -25];
poles=[-14.5 ,-15.5,-24];

kls=place(Aas,Bas,poles);
kself=kls(1:2)
kaself=kls(3)
```

```
%%%%%%%%%%%%%%%%%%%%%%%%%%%%%%%%%%%%%%%%%%%%%%%%%%%%%%%%%%%%%%%%%%%%
%%%%%%%%%%                   Stabilization               %%%%%%%%%%
%%%%%%%%%%%%%%%%%%%%%%%%%%%%%%%%%%%%%%%%%%%%%%%%%%%%%%%%%%%%%%%%%%%%
%The Mass matrix
m=[ M+m1+J/(r^2) , m1*l1
    m1*l1,  m1*(l1)^2+J1 ];
%The Quasi Stiffness matrix
km=[0   0
    0  m1*l1*g];
%Input matrix
b1=[1/r ; 0];
%Nonlinearities matrix
N=[1 0; 0 1];
%states are : [x ; theta1 ; x_dot ; theta1_dot ]
A=[zeros(2) eye(2); inv(m)*km zeros(2)]
B=[0;0; inv(m)*b1]
C=[eye(4)];
D=0;
eig(A)
%Controller with state feed back for the cart position
%1)Augmented System
Ctrack=[1 0 0 0];
Aa=[A zeros(4,1);-Ctrack 0];
Ba=[B ;0];
Ca=[C zeros(4,1)];
Da=0;
sipa=ss(Aa,Ba,Ca,Da)
%2) Controller design
poles=[-0.45 -0.5 -6 -6.1 -80]
k1=place(Aa,Ba,poles);
k=k1(1:4)
ka=k1(5)
```

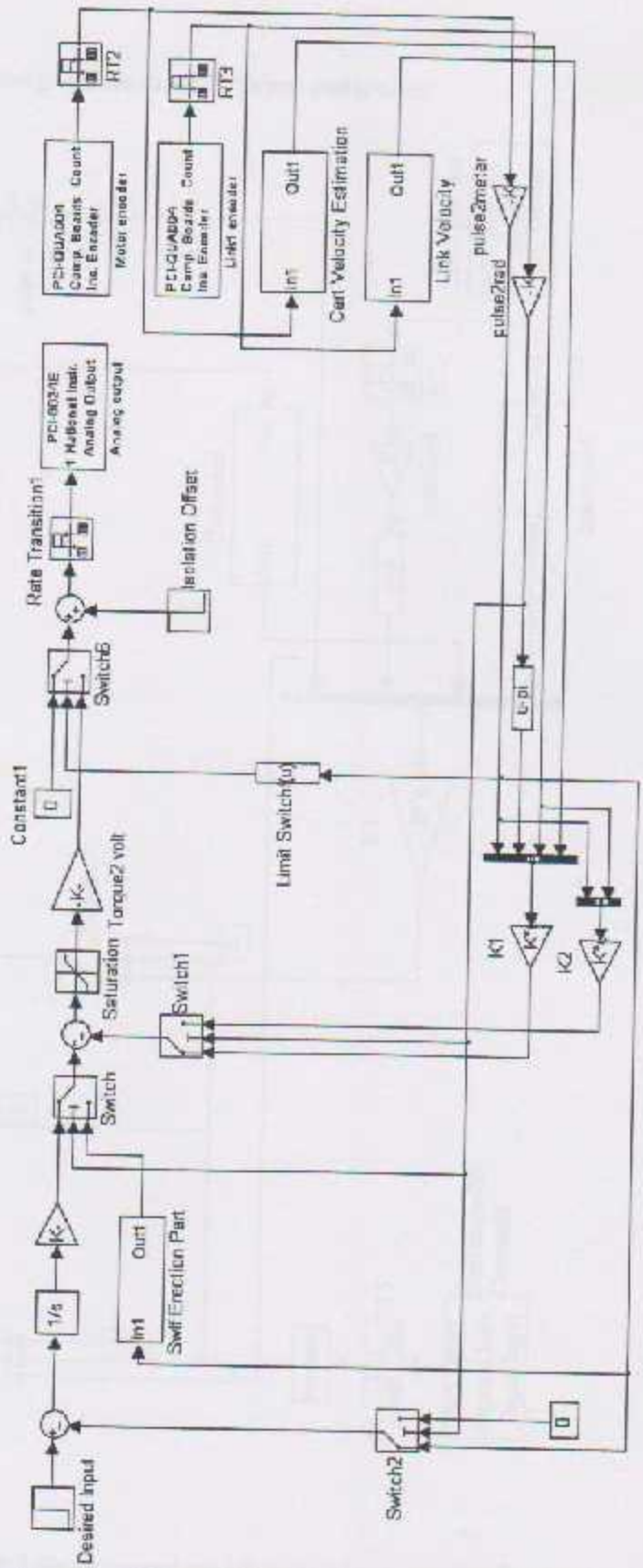

Figure B.2 Single inverted pendulum stabilization and self erection controller Simulink model

B.3 Single inverted pendulum multi layer controller

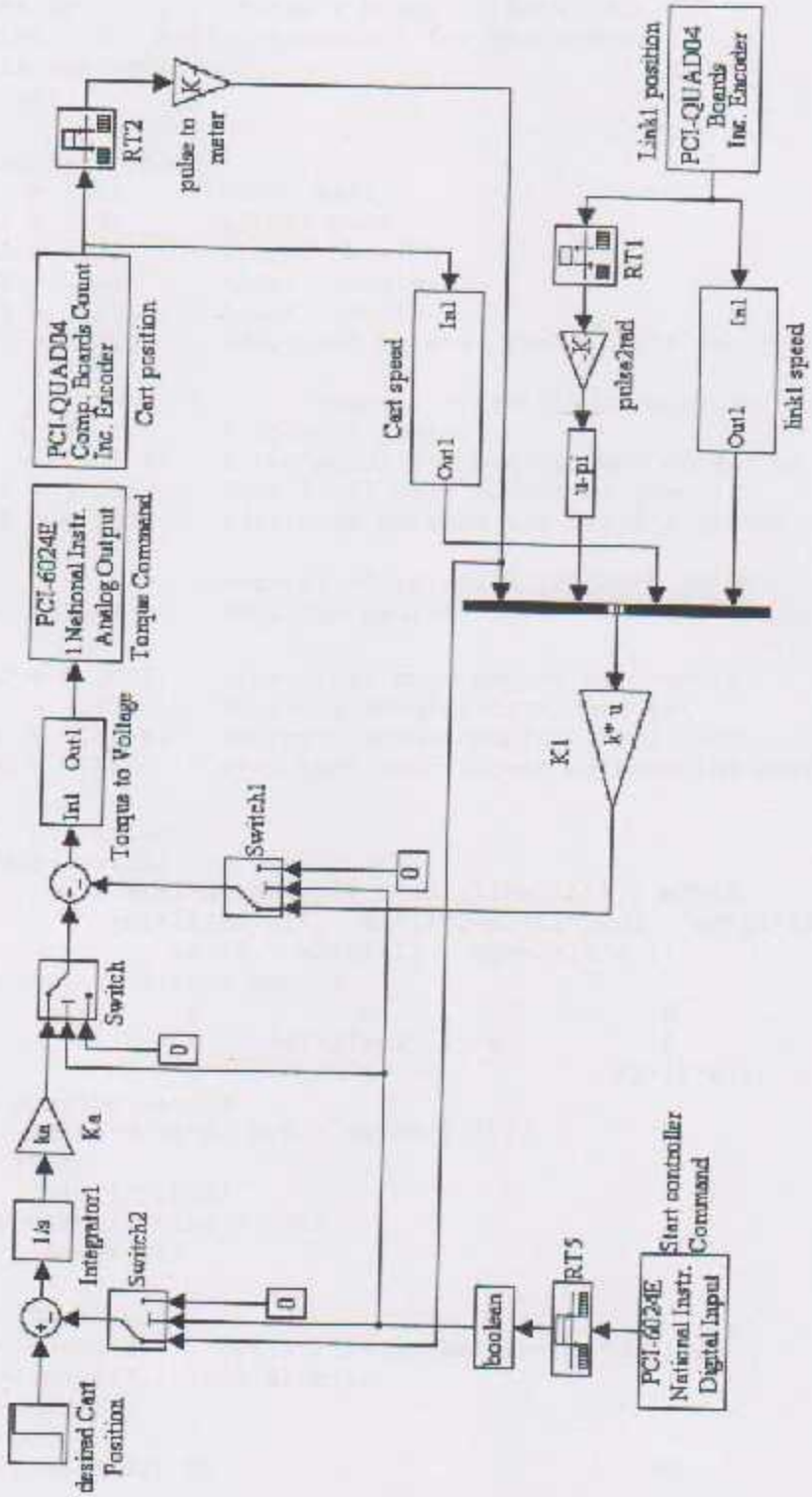

Figure B.3 Single inverted pendulum multi layer controller Simulink model

B.4 Double inverted pendulum stabilization controller

```
%==========================================================================
%========                  Double Inverted Pendulum              ==========
%==========================================================================
%Double Inverted Pendulum Stabilizing controller
%states are : [x ; theta1 ; x_dot ; theta1_dot ]
% Defining the basic parameters for the system
% units are Kg.M.s
clear all

%System parameters
    M  = 1.6;       %Cart mass
    m1 = .49;       %link1 mass
    m2 = .132;      %link2 mass
    L1 = .335;      %link1 length
    L2 = .285;      %link2 length
    l1 = 0.2;       %distance between the link1's center of gravity and
its
                    %center of rotation(revolute joint)
    r  = .02;       % pulleys radius
    J  = 1.55e-4;   % the motor and pulley mass moment of inertia
    J1 = 0.05;      %the link1 mass moment of inertia
    l2 = 0.125;     %distance between the link2's center of gravity and
its
                    %center of rotation(revolute joint)
    r  = .02;       %pulleys radius

    J2 = 0.0007;    %the link2 mass moment of inertia
    g  = 9.81;      %gravity acceleration constant
    d  = 5.8e-4;    %motor viscous damping coefficient
    fc = 0.2;       %friction coefficient between the cart and the rail

%Model Derivation
    %Mass matrix
        m= [ M+m1+m2+J/(r^2) , (m1*l1+m2*L1) , m2*l2
             (m1*l1+m2*L1),  m1*l1^2+m2*L1^2+J1 , m2*L1*l2
                m2*l2,  m2*L1*l2 , J2+m2*l2^2 ];
    %Quazi stiffness matrix
        km=[     0          0                  0
                 0    (m1*l1+m2*L1)*g          0
                 0          0              m2*l2*g];
    % Damping matrix
        dm=[-d/(r^2) 0 0 ; zeros(2,3)];
    % Input
        b1=[1/r;0;0]
    %Nonlinearities matrix
        N=eye(3);

%State Space model
    A=[zeros(3,3), eye(3);inv(m)*km, inv(m)*dm];
    B=[zeros(3,1);inv(m)*b1];
    C= eye(6);
    D=0;
    dip=ss(A,B,C,D)
```

```
%g=zpk(dlp)

%Controller Design
    %1)Augmented System
        Aa=[A zeros(6,1);-1 zeros(1,6)];
        Ba=[B;0];
        Ca=[C zeros(5,1)];
        Da=0;
        dipa=ss(Aa,Ba,Ca,Da)

    %2) Controller design
        poles=[-1.1 -1.3 -1.5 -5  -5.2 -5.5 -15]
        k1=place(Aa,Ba,poles)
        k=k1(1:6)
        ka=k1(7)
```

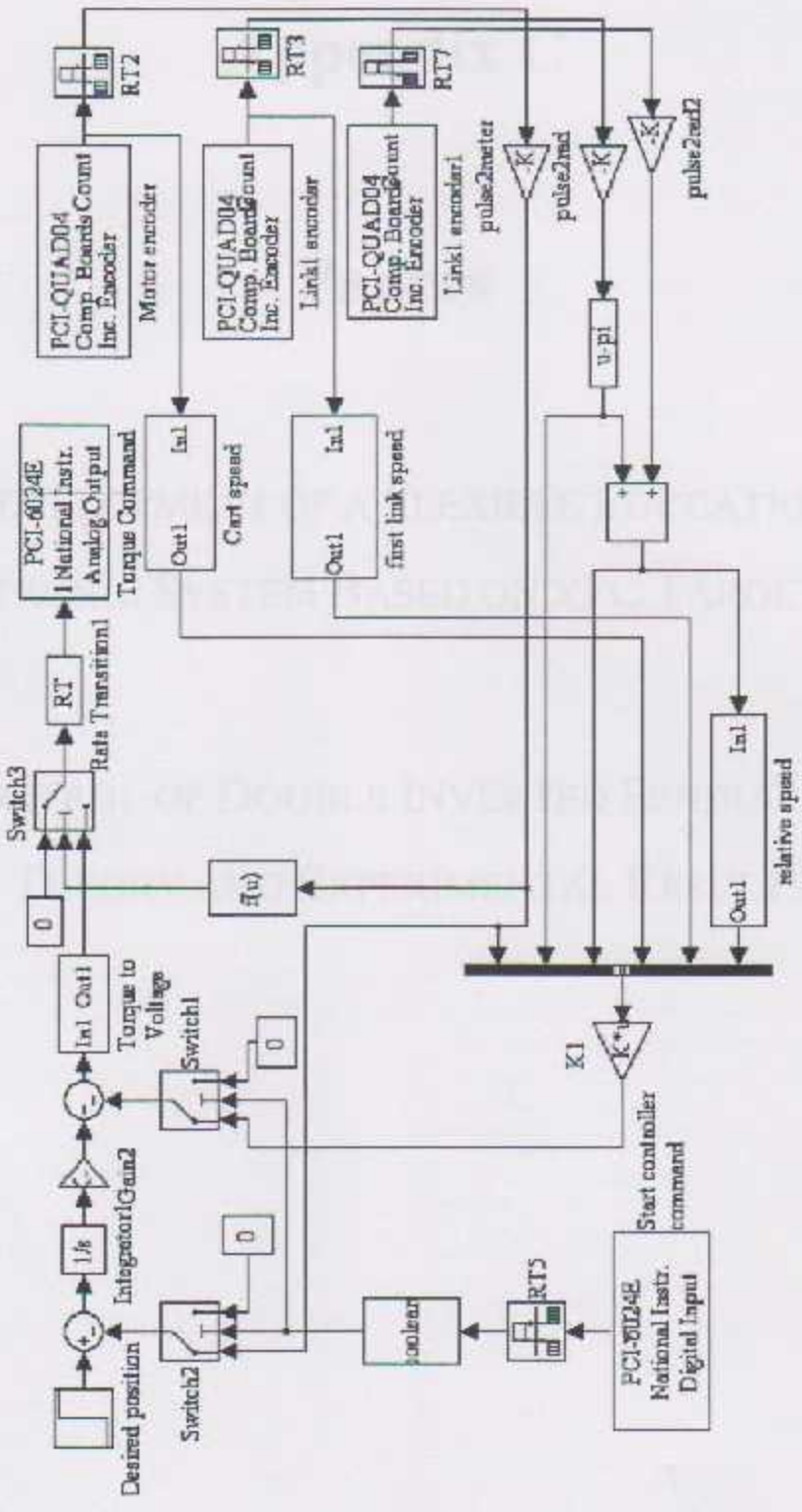

Figure B.4 DIPC stabilization controller Simulink model.

Appendix C

Papers

C.1 " DEVELOPMENT OF A FLEXIBLE EDUCATIONAL MECHATRONIC SYSTEM BASED ON XPC TARGET"

C.2 "CONTROL OF DOUBLE INVERTED PENDULUM ON A CART: THEORY AND EXPERIMENTAL RESULTS"

Proceedings of the ASME 2007 International Design Engineering Technical Conferences & Computers and Information in Engineering Conference
IDETC/CIE 2007
September 4-7, 2007, Las Vegas, Nevada, USA

DETC2007-34576

DEVELOPMENT OF A FLEXIBLE EDUCATIONAL MECHATRONIC SYSTEM BASED ON xPC TARGET

Karim A. Tahboub
tahboub@ppu.edu

Mohammad I. Albakri
mohammad_ppu@hotmail.com

Aziz M. Arafeh
azizcomB3@yahoo.com

Mechanical Engineering Department
Palestine Polytechnic University
Hebron – Palestine

ABSTRACT

In this article an educational embedded mechatronic system based on the MATLAB xPC target is presented. xPC target, a tool provided by MATLAB and its Simulink toolbox, offers a practical means for developing a hardware-in-the-loop (HIL) simulation environment. Since ordinary personal computers (PCs) can be used for modeling, analysis, design, monitoring, and control of the process, the setup becomes suitable for rapid-prototyping, research, and educational use. An application example of a double inverted pendulum on a cart that is digitally controlled is presented and discussed. The system is fully implemented by means of two PCs, MATLAB, Simulink, xPC target, a data acquisition card, an AC servomotor, and three optical encoders. It is shown that, through this technology, high sampling frequencies can be obtained by even using a Pentium III PC. Tele monitoring and control through a network are demonstrated.

1 INTRODUCTION

In mechatronic systems, digital computers and microcontrollers are indispensable for implementing control functions. Generally, any desktop PC with a Data Acquisition Card (DAQ) and appropriate software can be used as a controller. Using PCs as controllers seems to be very fascinating especially for educational and rapid prototyping purposes due to the ease with which changes and modifications in control logic are introduced. Unfortunately, that use is significantly limited when hard real-time requirements are present, since the existence of the operating system, such as Windows, Linux, ..., and other application software that runs side to side with the control software consumes a great deal of CPU and memory resources of the controlling PC. Thus, high sampling frequencies required to deal with fast dynamic systems can not be achieved. This major limitation in addition to other physical and financial limitations make most of the designers prefer the use of embedded controllers for implementing control functions.

Embedded controllers, usually in the form of microcontrollers, are special purpose systems in which the controller is fully dedicated for the control functions it performs, which means that hard real time requirement can be satisfied. Furthermore, microcontrollers are physically very small compared to any PC, and can operate in extreme conditions of vibration, temperature and humidity, so as to meet physical and environmental limitations of the controlled process [1]. Despite of all those advantages, the use of microcontrollers is limited if frequent changes in control algorithm are required, as in the case of educational applications, since the embedded controller needs to be reprogrammed each time a change is introduced.

One solution that combines the major advantages of the previous systems is the xPC target technique. This technique uses a standard PC hardware to implement control functions, providing in turn high flexibility in introducing changes and modifications in control algorithm. Furthermore, high sampling frequencies, necessary for dealing with rapid systems, can be obtained since this technique dedicates the controlling PC for running the controlling software.

An example in which the previously mentioned limitations of embedded and non-embedded systems clearly appear is inverted pendulum systems. These systems are usually used for educational and research purposes as test-beds for controllers and control techniques. Such systems have fast dynamic behavior, which implies that high real time control abilities are required; limiting in turn the possibility of using ordinary PCs for implementing control functions. On the other hand, the use of microcontrollers will not be suitable, since the ease with which changes in control logic are applied is an important performance criterion in inverted pendulum

systems. One solution for such a case is the xPC target technique.

The article is organized as follows. Section 2 presents the xPC target technique, discusses the software and hardware requirements, and illustrates the modes of operation. Section 3 reviews the problem of controlling a double inverted pendulum on a cart, while Section 4 presents the implementation of the HIL simulation environment using xPC target technique and shows some results. Finally, some concluding remarks and recommendations are given in Section 5.

2 OVERVIEW OF xPC TARGET

The xPC target technique is a solution for prototyping, testing and deploying real time systems, using standard PC hardware and its peripherals such as DAQ cards. This technique comes as a part of MATLAB software provided by MathWorks Company [2]. In particulate xPC target is a toolbox within MATLAB's Simulink.

MATLAB is a high performing language for technical computing. It integrates computation, visualization and programming in an easy-to-use environment, while Simulink is a software package for modeling, simulating and analyzing dynamic systems. It supports linear and nonlinear systems, modeled in continuous time, discrete time or hybrid of both.

In xPC target technique two PCs are used, host and target. With the host PC, one can design the controller, simulate it, and download it to the target PC. The target PC, which is connected to the controlled plant, is just used to run control functions in real time and monitor the controlled application.

xPC target technique is considered as an excellent solution for educational and rapid prototyping purposes due to the following facts:

- Changes and modifications in controller design are easily introduced to the host PC, and the modified controller is downloaded to the target PC almost with no effort. Furthermore, online tuning of some parameters is also possible.
- Hard real time requirements can be satisfied since the target PC processor is fully dedicated for running the controller.
- Host and target PCs can be connected serially, through network or even through the internet. In addition, the target PC can operate alone without any connection with the host.
- xPC target technique supports a wide range of DAQ cards and IO boards, which gives the designer a high level of flexibility to choose the suitable hardware.

All of that make xPC target technique an attractive solution for implementing control functions in educational applications, rapid prototyping processes and hardware-in-the-loop simulation.

2.1 Rapid Prototyping using xPC Target Technique

xPC target technique is a powerful tool for rapid prototyping processes. With the help of MATLAB, Simulink and xPC target technique, one can design, simulate and easily modify the controller for target application, and run that controller in real time. The rapid prototyping process using xPC target technique can be divided into the following sequence of steps:

1- Design the control system: MATLAB and Simulink provide a wide variety of functions and toolboxes that greatly help the designer throughout the design phases.
2- Simulate the model: after the controller has been designed, or even during the design process, it is possible to simulate that controller and check its response; thus any necessary improvements can be introduced before applying that controller to the real application.
3- Create the target application: by combining the real time workshop, xPC target and a C- compiler, an executable target application (control algorithm) is built, without any need for writing low level language programs for realizing the real-time controller.
4- Execute the target application in real time: the target PC is fully dedicated for running control algorithm for the controlled plant, resulting with high real time abilities.
5- Monitor the target application: using xPC target scopes, it is possible to monitor the running application either on host or target PCs. Saving the signal data to a file for later use is also possible.
6- Tune parameters: after the controller has been built and downloaded to the target PC, xPC target technique permits an online modification of some controller's parameters, such as gain values, and sampling time, with no need for rebuilding that controller.

2.2 Hardware and Software Requirements

As stated earlier, xPC target technique involves the use of two PCs, host and target. These ones should have the following features in terms of hardware and software, so as to be compatible with the xPC target technique.

Hardware requirements:

- Host PC:
  Any standard PC hardware that is able to operate the software requirements, provided that it has a 3.5 inch floppy drive, and a free serial and/or network port.
- Target PC:
  Any desktop or industrial PC, with:
  - 3.5 inch floppy drive.
  - Free serial port or a special Ethernet card.
  - The necessary I/O boards to communicate with the controlled application.

Software requirements:

- Host PC:
  - Microsoft windows platform.
  - MATLAB version 7.0.1 or higher.
  - Simulink version 6.1 or higher.
  - Real time workshop version 6.1.
  - xPC target toolbox version 2.6.1.
  - Visual C/C++ Professional Edition Version 5.0, 6.0, or 7.0. Or Watcom C/C++ Version 11 or 13.

- Target PC:
  No operating system is required. All operations are performed using the xPC target kernel, which can be thought of as a real-time operating system, booted from the target boot disk. The xPC Target kernel has no effect on any operating system installed on the target PC, which means that the target PC can be reused directly as a normal PC after the control process ends.

Figure 1 summarizes the main hardware and software features of the host and target PCs. Also it shows the way with which host PC, target PC and the controlled plant are connected.

2.3 xPC Target Operating Modes

xPC target technique provides three basic modes of operation: boot disk, DOS loader and stand alone options.

1. Boot Disk Mode

In this mode the target PC is booted from a floppy disk that contains the xPC target kernel, while the target application, which is built in Simulink, is downloaded, controlled and monitored directly by the host PC. One major specification determined within the xPC target kernel is the communication type between the host and target PCs. xPC target technique provides two ways of host-to-target communication, which are serial and network communication.

- Serial Communication
  In this case the host and target PCs are connected with a serial cable using RS232 ports. The serial communication allows a distance between host and target PCs up to 5 meters long, with a data transfer rate from 1200 to 115200 baud. With the serial communication one needs to specify the RS 232 host port (COM1, COM2 ...) to which the target PC is connected.

- Network (TCP/IP) communication
  With the network communication, the host and target PCs can be connected through a local area network (LAN), or even through internet. In this case both PCs need to have network cards. Host PC has no limitations on the card type to be used, while the target PC network card should be xPC target compatible. Table 1 lists the network cards that can be used with the target PC for network communication. In Network communication, it is necessary to specify the following parameters:
  - The type of the network card installed to the target PC, and its xPC target driver, as specified in Table 1.
  - The target PC IP address.
  - LAN subnet mask address, provided by the administrator.
  - TCP/IP target port: This property is set by default to 22222.

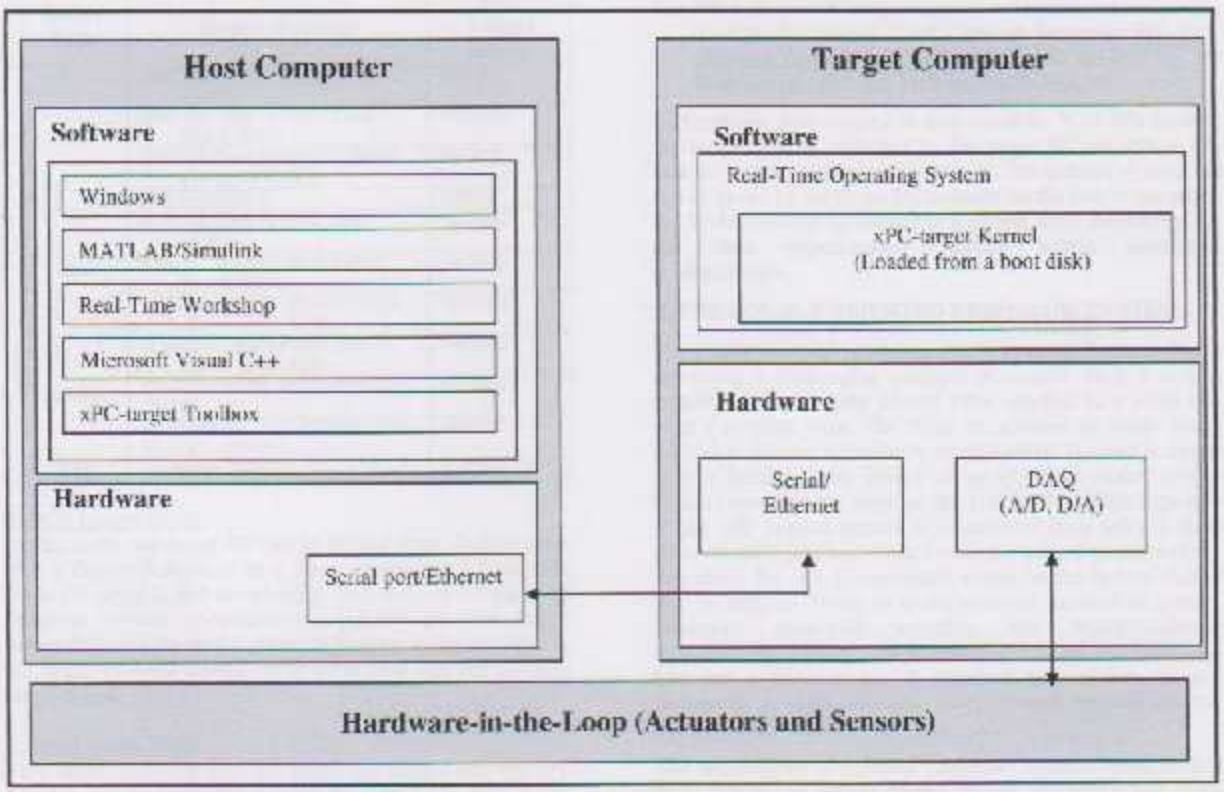

Figure1 Basic hardware and software requirements of host and target PCs used with xPC target technique.

- TCP/IP gateway address: This is by default set to 255.255.255.255, meaning that no gateway is used, which is the case when the host and target PCs are connected through a LAN. If the communication is performed from a host PC located in a LAN different from the target's one, it is necessary to define a gateway and its IP address. This is especially true when the connection is over the Internet. The IP address of the appropriate gateway should be provided by system administrator.

A host-to-target connection using network TCP/IP communication has the following advantages over serial RS-232 communication:

- Higher data throughput: Network communication using Ethernet card can transfer data up to 100 Mbit/second instead of the maximum data transfer rate of 115 kBaud available with serial communication.
- Longer distances between host and target computers: By using repeaters and gateways the distance between the host and target computers will not be restricted to the length of a serial cable. Communication over the Internet is also possible.

Table 1: Network cards compatible with xPC target technique

Board Type	Board Number	xPC Target Driver
PCI	SMC EZ Card10 SMC1208T (RJ45)	NE2000
	SMC EZ Card 10 SMC1208BT (RJ45, BNC)	NE2000
	SMC EZ Card 10 SMC1208BTA (RJ45, BNC, AUI)	NE2000
	Intel PRO/100 S	82559
ISA	SMC EZ Card 10 SMC1660T (RJ45)	NE2000
	SMC EZ Card 10 SMC1660BT (RJ45, BNC)	NE2000
	SMC EZ Card 10 SMC1660BTA (RJ45, BNC, AUI)	NE2000
PC/104	RealTime Devices USA CM202 (RJ45, BNC, AUI)	NE2000
	WinSystems Inc. PCM-NE2000-16 (RJ45)	NE2000
	WinSystems Inc. PCM-NE2000-16-BNC (BNC)	NE2000
SBC	Versalogic VSBC-8	SMC91C9X

2. DOS Loader Mode

In this mode the target PC can be booted from devices other than a floppy disk, such as a flash memory or a hard disk, while the target is still downloaded from the host PC either by serial or network communication. Unlike the boot floppy mode, DOS loader mode needs DOS copy to be installed to the target PC boot device; in order to load and run the xPC target kernel.

3. Stand Alone Mode

This mode combines both the target application and the xPC target kernel on the target boot device, which can be a floppy disk, flash memory or a hard disk. Thus both the application and kernel files are booted together on the target PC, eliminating any need for the connection between the host and target PCs. The target boot device in this mode will contain the following files:

- DOS files.
- *.rtb: This file contains the xPC Target kernel.
- xpcboot.com: This file executes the Target application in addition to the *.rtb file, which represents the real-time operating system.
- autoexec.bat: calls the xpcboot.com to boot the xPC Target kernel.

2.4 Monitoring the target application

xPC target technique permits the user to monitor the running application and acquire data signals from it, by means of xPC scopes. There are three main types of scopes that can be used with xPC target technique:

1- Target scope: data collected from the target application is displayed immediately on the target screen in either numerical or graphical form. Such scopes are created automatically by the xPC kernel at the moment the target application is downloaded to the target PC.

2- Host scope: this type of scopes collects signals data from the target application, and then sends it to the host PC, on which these signals are graphically displayed.

3- File scope: with such scopes, data is collected and stored on a predetermined file located at the target PC. This collected data can be then transferred to the host PC for examination, analysis, plotting or later use.

Furthermore, data logging is also possible. With this feature, the arrays of data collected by the target PC are sent to the host for saving, plotting, and analysis. The amount of data that can be saved by the target PC depends on the size of the target PC RAM, and can be limited to a certain value determined by the 'data import/export' feature within simulation configurations.

3 THE DOUBLE INVERTED PENDULUM SYSTEM

The double inverted pendulum (DIP) system, shown in Fig. 2 represents a challenging problem in control. Such a system consists of two serially jointed links attached to a small cart with a revolute joint. The links are allowed to rotate freely relative to the cart and relative to each other. The cart is driven over a linear rail by means of an electrical motor, whose torque represents the input of the system. The main objective of the DIP control system is to stabilize both links in their upper vertical position, while tracking a desired position of the cart along the rail. Disturbances acting on the system should also be rejected. Being an under-actuated mechanical system, inherently open-loop unstable, with highly-nonlinear dynamics, the DIP system is considered as an excellent test-bed for a wide range of classical and modern control techniques as state feedback, fuzzy control, optimal control, and nonlinear control.

The applications of inverted pendulum systems range widely from robotics to human beings motion simulation and space

rocket guidance systems. Originally inverted pendulum systems were used to illustrate the ideas of linear control theories, but the inherent nonlinear nature of such systems helped them to maintain their usefulness along the years, and they are now used to illustrate several ideas emerging in the field of modern nonlinear control.

Figure 2 DIPC system composed of two aluminum rods and a cart and actuated by an AC servomotor through a specially-designed rope-and-pulley mechanism

As an educational tool, inverted pendulum systems are used for testing various controllers and control implementation techniques including digital control. Sampling frequency and computational and transport time delays effects on stability and response are relevant issues that can be demonstrated and tested. Different controllers are tested and compared by a set of performance specifications including:

- Stabilization control.
- Position tracking.
- Disturbance rejection.
- Robustness.

The rapid dynamic behavior of inverted pendulum systems calls for a controller realization with high real-time abilities. At the same time, the use of these systems for educational purposes implies that frequent switching among control configurations and algorithms should be facilitated by a flexible platform. These two requirements qualify xPC target technique to be a perfect solution for implementing DIP control systems.

Nearly all works on inverted pendulum control address two problems, pendulums swing-up control and stabilization control [3]. Here, the design of a stabilization controller based on state feedback and disturbance compensation is discussed. Such a controller aims at stabilizing both links in their upper vertical position, and track a desired position of the cart along the rail.

The state-feedback controller design is based on the linearized state space model of the DIP system. Figure 3 illustrates the idea of state feedback control where the states vector $\mathbf{x}$ is fed back through the gain vector $\mathbf{k}$. The values of the gain vector is calculated to place the eigenvalues of the system in desired locations, so as to obtain the desired performance specifications. As three measurements corresponding to the position of the cart and the relative angular displacement of the rods are available, the other three states are estimated by differentiating the measurements or by means of an observer [4, 5].

To improve the overall performance of the system, the effects of the nonlinearities acting within the system, such as friction and centrifugal forces, as well as external disturbances are taken into account. Since these terms are not directly measurable, an extended observer (instead of a classical observer) is employed not only to estimate the states but also to estimate the other effects (nonlinearities and external disturbances). Having the estimate of these terms makes it possible to compensate for their effects. An extended observer is basically a classical observer where the external disturbances and nonlinearities are assumed to be regular states. Since these states are originally extraneous to the system, one cannot write down their corresponding differential equations governing their behavior in the time domain, which is necessary for completing the state-space model. A practical solution would be to assume that they are step-wise constant, thus their derivatives are set to zero [5].

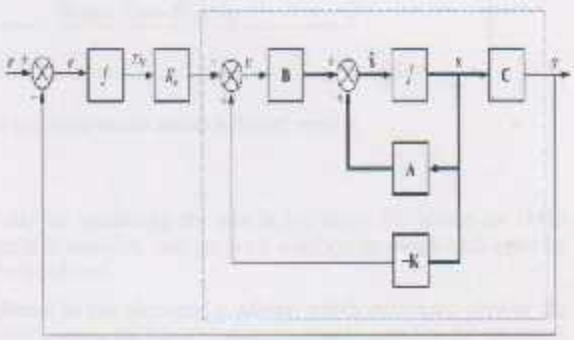

Figure 3 State feedback control architecture

Once the extended system is modeled, the measured outputs of the system are compared to those obtained by the means of the extended system model, and the error is fed back to the observer. In order to increase the convergence speed of that error signal, in other words to make the observer output matches that measured faster, the dynamics of the observer must be made much faster than that of the real system.

Theoretically, the desired speed of the observer is obtained by choosing an appropriate gain vector ($\mathbf{L}$), so as the poles of the error characteristic equation can be placed 5 to10 times faster than those of the real system. Thus the controller will receive the true estimated states instantaneously. However, in practice it is shown that the existence of measurement noise limits this freedom of having arbitrarily fast observers.

Figure 4 shows the complete state-feedback controller architecture where an extended observer is employed to

estimate the unmeasured states as well as the external disturbances and system nonlinearities. The latter are used in a disturbance compensation module that superimposes the tracking controller. Here, the high real-time computational requirements are evident.

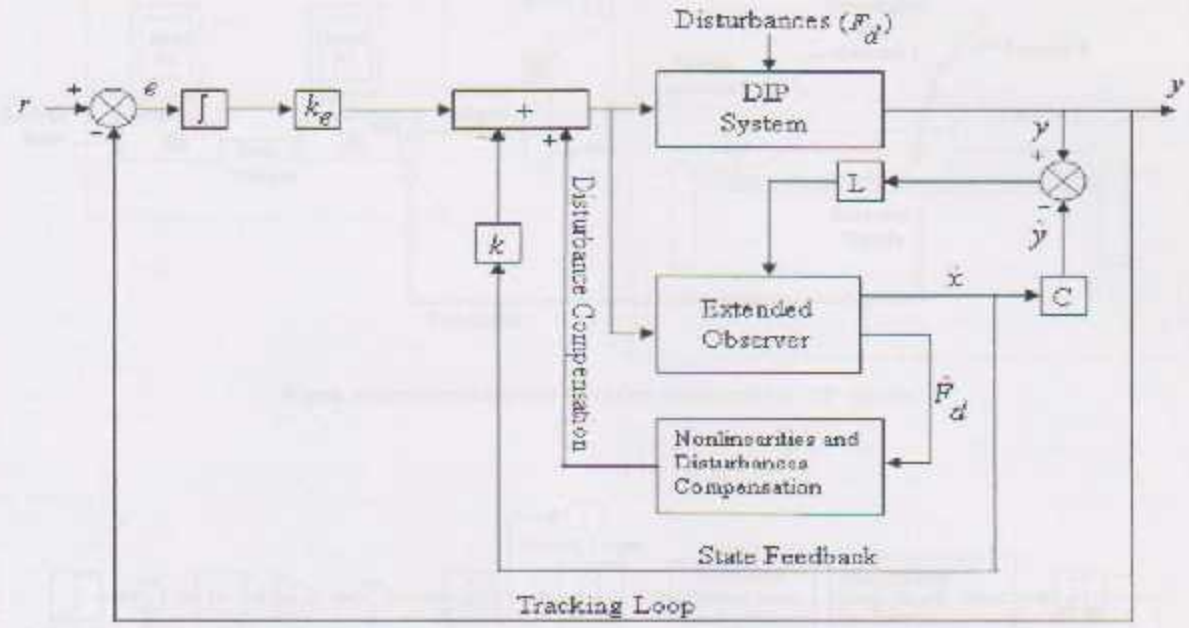

Figure 4 Using the extended observer outputs to compensate for the nonlinearities and disturbances effects in the DIP system.

4 IMPLEMENTATION OF DIP CONTROL SYSTEM USING xPC TARGET TECHNIQUE

Figure 5 demonstrates the hardware-in-the loop (HIL) simulation environment of the developed double inverted pendulum system [6, 7]. This environment consists of the actual DIP structure including the mechanical parts, sensors and actuators, in addition to the virtual control part that is implemented using xPC target technique.

The mechanical structure of the DIP system is equipped with three incremental optical encoders, two of them are used to measure the angular displacement of the two links, and the third for the linear displacement of the cart along the track. These measurements are fed back to the target PC, which represents the controller, so as to close the loop around the plant. The target PC is equipped with a special DAQ card for dealing with incremental encoders. This DAQ has built-in digital filtering circuits that significantly help to get rid of noise and vibration problems usually encountered when using incremental encoders. Fortunately, xPC target toolbox provides a wide variety of built-in functions that enable the user to directly obtain the measurements from the DAQ card, only by specifying the slot in the target PC where the DAQ card is installed, and the ports numbers to which each encoder is interfaced.

Based on the encoders' readings, which reflect the state of the DIP system, the torque value required to stabilize the system is determined by the controller. That torque is represented by an analog voltage signal generated by the target PC. This analog signal is then sent through the DAQ to the AC servomotor driver, which in turn orders the motor to generate the specified torque value.

Figure 6 shows the Simulink model used for controlling the DIPC system. It is worth noting that the maximum sampling frequency that can be achieved with xPC target technique depends not only on the target processor, but also on the controller complexity. With an 800 MHz target processor, and with a state feedback controller shown in Fig.6, a 0.25 ms sample time was achieved. This frequency exceeds the required frequency to deal with a rapid dynamic system as the DIP.

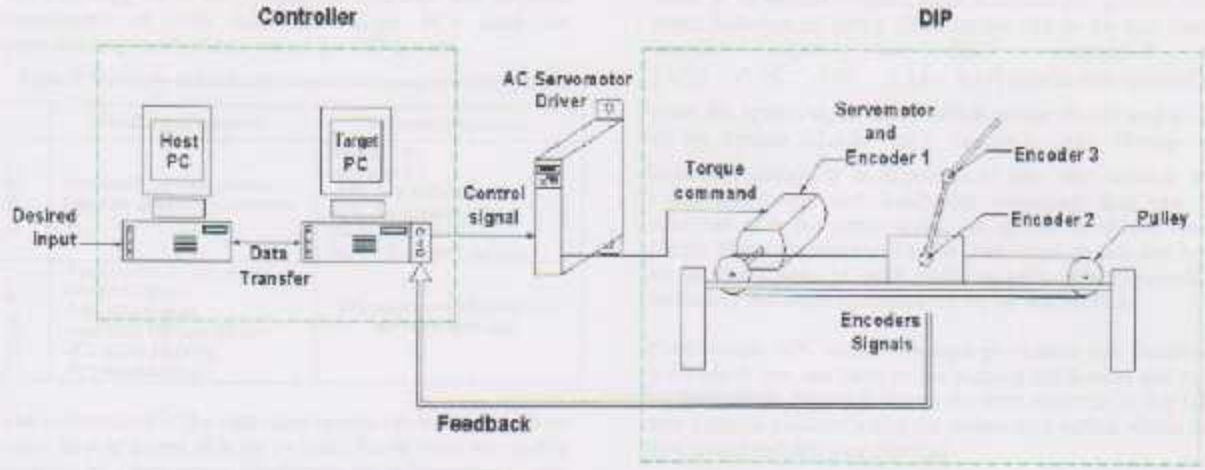

Figure 5 Hardware-in-the-loop simulation environment for DIP system.

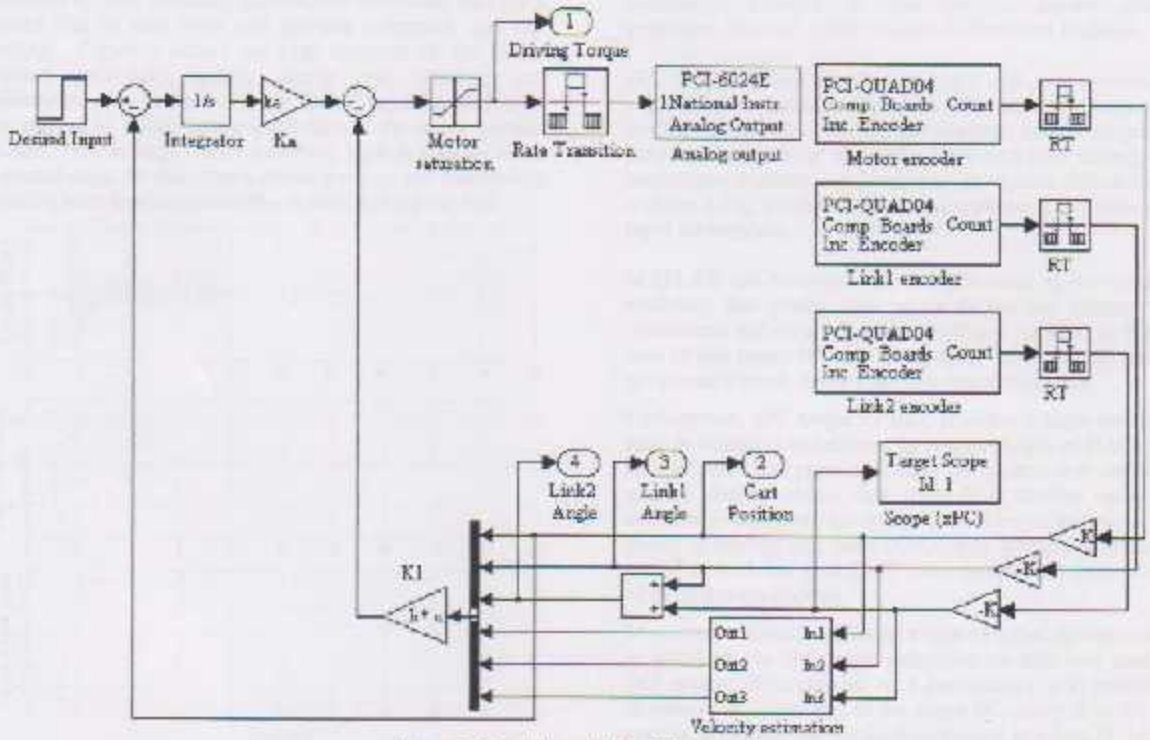

Figure 6 Simulink model for DIP controller

The following Table summarizes the hardware and software components of both host and target PCs used for implementing control functions of the DIP system.

Table 2: Hardware and software components used with DIP system.

	Hardware Components	Software Components
Host PC	Pentium IV 2.8 GHz processor, and other standard PC hardware.	-Matlab 7.0.1 Simulink 6.1 -Real time workshop 6.1 -xPC Target toolbox 2.6.1 Visual C++ version 6 -Active X controls package.
Target PC	-Pentium III 0.8 GHz processor. -64 MB SDRAM -3.5" floppy drive. -Intel PRO/100 network card. -PCI 6024E NI DAQ. -PCI Quad04 DAQ	xPC target kernel booted from the target boot disk.

The performance of the controlled system can be monitored on either host or target PCs, or on both. These plots are readily obtained by a host scope. Monitoring the performance by this technique does not slow down the controller as it is achieved by the "idle" host PC.

Many experiments were performed on the single inverted pendulum system, including stabilization controller, tracking a desired step or sine wave cart position command, and self erecting. Figure 7 shows the time response of the single inverted pendulum system during self erecting and stabilization process. In this experiment bang-bang controller was applied to swing up the pendulum to the upper vertical position, then an angle-based switching logic is used to move to second stage. In this stage a robust tracking and disturbance rejection state feedback controller is used to keep the link

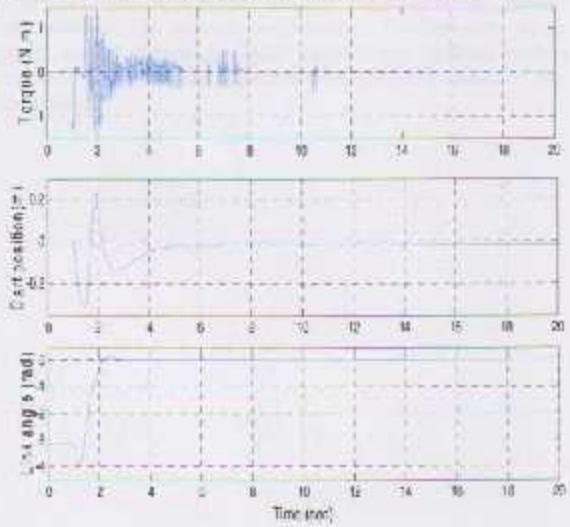

Figure 7 Single-inverted-pendulum-on-a-cart response during self erecting and stabilization process obtained using xPC target host scope. The first part of the figure shows the input torque (N-m) required to derive the system, and the other two parts represent the cart position and link's angle respectively.

stable at its vertical position, track a desired cart position, and reject disturbances acting either on the cart or the link itself. Results shown in Fig.7 correspond to $[-1.95 \quad -7.78 \quad -2.54 \quad -1.16 \quad 0.43]$ gain values required to place the system eigenvalues, which are the closed loop poles of the system at $[-0.45 \quad -0.5 \quad -6 \quad -6.1 \quad -70]$. During the controller design, it is important to take into account the maximum torque and bandwidth frequency that can be achieved with the servo motor, so as not to exceed these limits. Many experiments can be performed on this test-bed, so as the effects of pole location, gain values, sampling frequency and input saturation are tested and studied.

Furthermore, xPC target technique provides a web interface, with which one can monitor the running application and tune its parameters. Figure 8 shows the time response of the DIP cart position obtained using the screen shot option within the xPC target web browser interface.

5 CONCLUSIONS

In this article an educational embedded mechatronic system based on the MATLAB xPC target is presented. An application example of controlling a double inverted pendulum on a cart (DIPC) system is discussed in details.

xPC target is a tool provided by MATLAB and its interactive simulation environment Simulink. This has the advantage of having one friendly platform for analysis, design, simulation, hardware-in-the loop simulation, and real-time testing. This encourages students and researchers to explore different ideas without a big overhear. Thus, this combination facilitate for rapid prototyping.

MATLAB and Simulink provide a number of functions and toolboxes that greatly help in the design and simulation of controllers, not only using state feedback method, as it is the case in this paper, but also using many other techniques such as optimal control, fuzzy logic and neural networks.

Furthermore, xPC target toolbox provides a large number of built in functions and drivers for a wide variety of DAQ cards, parallel and serial ports, and other peripherals that enable the user to directly obtain data from these devices easily and efficiently. One more advantage of xPC target technique is its ability of dealing with multi DAQ cards, permitting in turn the use of several low-cost DAQ cards to meet the requirements of the target application.

Moreover, network and internet host-to-target communication provided by the xPC target technique are also very useful in DIP system. By means of such connections, it is possible to download the controller to the target PC, apply it to the DIP system and obtain the results immediately to a host PC located anywhere in the world, without any need for traveling to the Lab where the structure is installed, in other words, a global laboratory can be established with the help of such a technique.

Figure 8 DIP cart position response, obtained using xPC target web browser interface.

Inverted pendulum systems, including both single and double types, are used to experiment with various control problems, such as stabilization, position tracking, disturbance rejection, robustness and self erecting. Hybrid controllers with a switching logic are also applied.

Once the system is built and tested, it can be used as an excellent test bed for various control techniques. Although controllers based on linear control theories achieved a satisfying performance, it will be interesting to apply the principles of non-linear control and achieve further improvements in system performance. Furthermore, fuzzy logic, neural networks, digital control and optimal control methods can be applied, tested and compared by means of this apparatus.

6 ACKNOWLEDGMENTS

This project has been financially supported by a grant from TEMPUS project No. JEP_30078_2002 titled "Training of industrial systems integrators: FINSI".

7 REFERENCES

[1] Cetinkunt.N.S,2007,*MECHATRONICS*,John Wiley & Sons, Inc., River Street, Hoboken, New Jersey. pp 123-125, Chap Four.

[2] MathWorks.Co, MATLAB Help http://www.mathworks.com/support/product/XP/productnews/xpc_targetbox_ug.pdf.

[3] Bogdanov.A, 2004,"OPTIMAL CONTROL of a DOUBLE INVERTED PENDULUM on a CART",Technical Report CSE-04-006, Department of Computer Science & Electrical Engineering, OGI School of Science & Engineering, OHSU.

[4] Nise.N.S, 2004, *Control System Engineering*, Fourth edition, John Wiley and Sons, California State University, Pomona. pp 764.Chap Eight.

[5] Franklin.G.F, Powell J.D, Workman, M.L, 1997, *Digital Control of Dynamic Systems*. 3rd edition, Prentic Hall. Chapter eight.

[6] Wahyudi and Jamaludin , 2005,"*HARDWARE in the LOOP SIMULATION (HILS) BASED DESIGN and DESIGN AND ROBUSTNESS EVALUATION of an INTELEGENET GANTRY CRANE SYSTEM* ",KINTEX, Gyeonggi-Do, Korea.

[7] Hoyer.H, Gerke.M, Masar.I ,Ivanov.I, Rohrig.C, Bischoff.A, 2003,"Virtual LABORATORY FOR REAL-TIME CONTROL OF INVERTED PENDULUM /GANTRY CRANE", Prozeßsteuerung und Regelungstechnik Fern Universität , Hagen,Germany.

CONTROL OF A DOUBLE INVERTED PENDULUM ON A CART: THEORY AND EXPERIMENTAL RESULTS

Mohammad AlBakri, mohammad_ppu@hotmail.com Mechanical Engineering Department, Palestine Polytechnic University, Hebron, Palestine

Aziz Arafeh, azizcom83@yahoo.com Mechanical Engineering Department, Palestine Polytechnic University, Hebron, Palestine

Karim A. Tahboub, tahboub@ppu.edu Mechanical Engineering Department, Palestine Polytechnic University, Hebron, Palestine

ABSTRACT

In the article the double-inverted-pendulum-on-a-cart control problem is discussed. Through the graduation project of the first two authors, a corresponding system is designed and constructed at the Palestine Polytechnic University. Based on MATLAB and xPC, a flexible educational control setup is attained. A robust-tracking and disturbance-rejection state-feedback-based control configuration improved by an extended observer and explicit disturbance compensation is experimentally implemented and tested. Experimental results demonstrate the merits of the proposed control system.

Keywords: Double inverted pendulum, state feedback, robust tracking and disturbance rejection, extended observer.

1. INTRODUCTION

The double inverted pendulum on a cart (DIPC) represents a challenging control problem. This system consists of two jointed links attached to a small motorized cart with a revolute joint. The links are allowed to move freely relative to the cart and relative to each other. The cart is driven over a linear rail by means of an electrical motor, whose torque represents the only input of the system. The main objective of DIPC system is to stabilize both links in the upright vertical position, while tracking a desired position of the cart along the rail. Furthermore disturbance rejection is to be achieved. Being an under-actuated mechanical system, inherently open loop unstable, with high nonlinear dynamics, and with some of its states that are not directly measurable, DIPC is considered as an excellent test-bed for a wide range of classical and modern control techniques. Originally inverted pendulum systems were used to illustrate the ideas of linear control theories, but the inherent nonlinear nature of

such systems helped them to maintain their usefulness along the years, and they are now used to illustrate several ideas emerging in the field of modern nonlinear control [Bogdanov.A, 2004]. As an educational tool, inverted pendulum systems are used for testing various controllers and control techniques including state feedback methods, optimal control, nonlinear control, intelligent control techniques (such as neural networks and fuzzy logic) and digital control. Different controllers are tested and compared by a set of performance specifications including:

- Stabilization control.
- Position tracking.
- Disturbance rejection.
- Robustness.

Effects of sampling frequency and computational and transport time delays on stability and response are relevant issues that can be demonstrated and tested. The rest of the article is organized as follows. System nonlinear and lincarized mathematical models are derived in Section 2, these include effects as friction. In Section 3, a control method based on multivariable robust tracking and disturbance rejection improved by disturbance estimation and compensation is presented where experimental results are presented in Section 4. Finally in Section 5 results are discussed and conclusions are given.

2. MATHEMATICAL MODLING

Mathematical modeling of DIPC aims at abstracting all the important features of the system that govern its behavior and expressing them in terms of differential equations. The needed model accuracy, i.e. closeness to the actual system, depends on the purpose. Generally a simplified model is needed to study the main characteristics of the system, while a detailed model is needed for precise simulation and prediction studies.

1. Mathematical Model Derivation: DIPC system is presented graphically in Fig.1. In this figure the friction force and the disturbances acting on the system are included, so as to be modeled and counted for during controller design and simulation. Based on Fig.1, the total kinetic and potential energies of the system, dented by (T) and (U) respectively, are:

$$T = \frac{1}{2}M\dot{x}^2 + \frac{1}{2}\frac{J}{r_p^2}\dot{x}^2 + \frac{1}{2}J_1\dot{\theta}_1^2 + \frac{1}{2}J_2\dot{\theta}_2^2 + \frac{1}{2}m_1\left[\left(\dot{x} + l_1\dot{\theta}_1\cos\theta_1\right)^2 + \left(l_1\dot{\theta}_1\sin\theta_1\right)^2\right] + \frac{1}{2}m_2\left[\left(\dot{x} + L_1\dot{\theta}_1\cos\theta_1 + l_2\dot{\theta}_2\cos\theta_2\right)^2 + \left(L_1\dot{\theta}_1\sin\theta_1 + l_2\dot{\theta}_2\sin\theta_2\right)^2\right] \quad (1)$$

$$U = m_1 g y_1 + m_2 g y_2 = m_1 g l_1\cos\theta_1 + m_2 g\left[L_1\cos\theta_1 + l_2\cos\theta_2\right] \quad (2)$$

Based on Lagrange's approach:

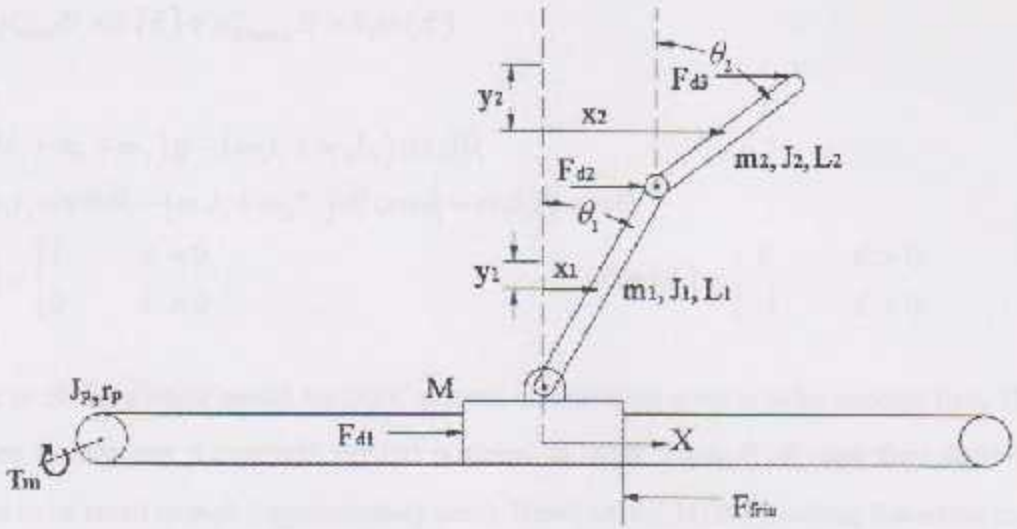

Figure 1 Double inverted pendulum system.

Where: M: Mass of the Cart.
m_1: Mass of the link1.
m_2: Mass of the link2.
J_1: Mass moment of inertia of the link1.
J_2: Mass moment of inertia of the link2.
l_1: Distance to center of mass of the link1.
l_2: Distance to center of mass of the link2.
J_p: Mass moment of inertia of the pulleys.
r_p: Radius of the pulley.
T_m: Input torque from the motor.
F_{fric}: Friction force.
d: the motor viscous damping coefficient.
F_{d1}: Disturbance force acting at the cart.
F_{d2}: Disturbance force acting at the first link.
F_{d3}: Disturbance force acting at the second link.

$$\frac{d}{dt}\left(\frac{\partial L}{\partial \dot{q}_n}\right)-\frac{\partial L}{\partial q_n}=Q_n \tag{3}$$

Where the Lagrangian term (L) is defined as the difference between the total kinetic energy (T), and the total potential energy (U). Applying Eq. (3) to each of the three generalized coordinates: x, θ_1 and θ_2, yields [AlBakri, Arafeh, 2007]:

$$\begin{bmatrix} M+m_1+m_2+J/r_p^2 & (m_1l_1+m_2L_1)\cos\theta_1 & m_2l_2\cos\theta_2 \\ (m_1l_1+m_2L_1)\cos\theta_1 & m_1l_1^2+m_2L_1^2+J_1 & m_2L_1l_2\cos(\theta_1-\theta_2) \\ m_2l_2\cos\theta_2 & m_2L_1l_2\cos(\theta_1-\theta_2) & m_2l_2^2+J_2 \end{bmatrix}\begin{bmatrix}\ddot{x}\\ \ddot{\theta}_1\\ \ddot{\theta}_2\end{bmatrix}+\begin{bmatrix} d/r_p^2 \\ 0 \\ 0\end{bmatrix}\dot{x}$$

$$\begin{bmatrix} 0 & -\dot{\theta}_1^2(m_1l_1+m_2L_1)\sin\theta_1 & -\dot{\theta}_2^2m_2l_2\sin\theta_2 \\ 0 & 0 & \dot{\theta}_2^2m_2L_1l_2\sin(\theta_1-\theta_2) \\ 0 & -\dot{\theta}_1^2m_2L_1l_2\sin(\theta_1-\theta_2) & 0 \end{bmatrix}+\begin{bmatrix} 0 \\ -(m_1l_1+m_2L_1)g\sin\theta_1 \\ -m_2l_2g\sin\theta_2\end{bmatrix}+ \tag{4}$$

$$\begin{bmatrix}1\\0\\0\end{bmatrix}F_{fric}=\begin{bmatrix}1/r_p\\0\\0\end{bmatrix}T_m+\begin{bmatrix}1 & 1 & 1\\ 0 & L_1\cos\theta_1 & L_1\cos\theta_1\\ 0 & 0 & L_2\cos\theta_2\end{bmatrix}\begin{bmatrix}f_{d1}\\f_{d2}\\f_{d3}\end{bmatrix}$$

The friction force (F_{fric}) acting on the cart is modeled as follows:

$$F_{fric} = \mu_{static} N \times \delta(\dot{x}) + \mu_{dynamic} N \times Sgn(\dot{x}) \tag{5}$$

Where:

$$N = (M + m_1 + m_2)g - (m_1 l_1 + m_2 L_1)\sin\theta_1 \ddot{\theta}_1 - m_2 l_2 \sin\theta_2 \ddot{\theta}_2 - (m_1 l_1 + m_2 L_1)\dot{\theta}_1^2 \cos\theta_1 - m_2 l_2 \dot{\theta}_2^2 \cos\theta_2$$

$$\delta(\dot{x}) = \begin{cases} 1 & \dot{x} = 0 \\ 0 & \dot{x} \neq 0 \end{cases} \qquad Sgn(\dot{x}) = \begin{cases} 1 & \dot{x} > 0 \\ -1 & \dot{x} < 0 \end{cases}$$

In order to obtain a linear model for DIPC system; an operating point is to be selected first. This point is chosen to represent the upright vertical position, in other words, θ_1, θ_2 and their derivatives are assumed to be small enough (approximately zero). Based on Eq. (4) the resulting linearized model that describes the system in the desired operating region is:

$$\underbrace{\begin{bmatrix} M + m_1 + m_2 + J/r_p^2 & (m_1 l_1 + m_2 L_1) & m_2 l_2 \\ (m_1 l_1 + m_2 L_1) & m_1 l_1^2 + m_2 L_1^2 + J_1 & m_2 L_1 l_2 \\ m_2 l_2 & m_2 L_1 l_2 & m_2 l_2^2 + J_2 \end{bmatrix}}_{M} \begin{bmatrix} \ddot{x} \\ \ddot{\theta}_1 \\ \ddot{\theta}_2 \end{bmatrix} + \underbrace{\begin{bmatrix} d/r_p^2 & 0 & 0 \\ 0 & 0 & 0 \\ 0 & 0 & 0 \end{bmatrix}}_{D_m} \begin{bmatrix} \dot{x} \\ \dot{\theta}_1 \\ \dot{\theta}_2 \end{bmatrix}$$

$$\underbrace{\begin{bmatrix} 0 & 0 & 0 \\ 0 & -(m_1 l_1 + m_2 L_1)g & 0 \\ 0 & 0 & -m_2 l_2 g \end{bmatrix}}_{K_m} \begin{bmatrix} x \\ \theta_1 \\ \theta_2 \end{bmatrix} = \underbrace{\begin{bmatrix} 1/r_p \\ 0 \\ 0 \end{bmatrix}}_{B} T_m + \underbrace{\begin{bmatrix} 1 & 1 & 1 \\ 0 & L_1 & L_1 \\ 0 & 0 & L_2 \end{bmatrix}}_{B_d} \begin{bmatrix} f_{d1} \\ f_{d2} \\ f_{d3} \end{bmatrix} \tag{6}$$

By inspecting Eq. (6), it could be noted that:

- The mass matrix (M) is symmetric, regular, and positive definite matrix.
- The quasi stiffness matrix (K_m) is a destabilizing matrix, since it tends to take the system away from its operating point.
- The system has dynamic coupling only in the mass matrix while there is no static coupling in the stiffness matrix.

2. DIPC State-Space Model: To obtain the state-space model for DIPC system, six states are needed. These are chosen to be $(x, \theta_1, \theta_2, \dot{x}, \dot{\theta}_1$, and $\dot{\theta}_2)$; the input to the system is the motor torque (T_m). Since the system is equipped with the necessary sensors, the first three states are the measurable

outputs of the system. Based on the previous discussion the state space model of the system is expressed as follows:

$$\begin{bmatrix}\dot{x}\\ \ddot{x}\end{bmatrix}=\begin{bmatrix}0 & I_2\\ -M^{-1}K_m & -M^{-1}D_m\end{bmatrix}\begin{bmatrix}x\\ \dot{x}\end{bmatrix}+\begin{bmatrix}0\\ M^{-1}B\end{bmatrix}T+\begin{bmatrix}0\\ M^{-1}B_d\end{bmatrix}F_d \qquad (7)$$

$$y=\begin{bmatrix}I_3 & \text{zeros}(3)\end{bmatrix}\begin{bmatrix}x\\ \dot{x}\end{bmatrix}$$

Where: $x=[x \quad \theta_1 \quad \theta_2]^T$

$$F_d=[f_{d1} \quad f_{d2} \quad f_{d3}]^T$$

3. CONTROL SYSTEM DESIGN

The control problem of DIPC can be divided into two major branches; stabilization and self erecting. The former, which is the subject of this paper, deals with the problem of making the cart tracks a desired position along the rail while keeping the two links stable at their vertical position. Furthermore such a controller should reject, within limits, disturbances acting on the cart or each of the two links. On the other hand, self erecting means to swing the links up from their stable lower position to the upright vertical point, which is beyond the scope of this paper. In this section a robust tracking and disturbance rejection controller is designed based on the derived linear state space model. The effects of disturbances and nonlinearities are then taken into consideration, firstly by estimating them with an extended observer, and then by compensating, partially, for their effects.

1. Robust Tracking and Disturbance Rejection: In order to have a robust controller that is able to track a desired cart position with zero steady state error, and reject disturbances acting on the system, the internal model control method is used to design the required controller, based on the Eq. (7). Let the disturbances acting on the system be modeled by the following state and output equations:

$$\dot{x}_d=A_d x_d \qquad (8)$$
$$F_d=C_d x_d$$

While the reference signal to be tracked is modeled as follows:

$$\dot{x}_r=A_r x_r \qquad (9)$$
$$r=C_r x_r$$

Given that the Eqs. (8) and (9) are the minimal realization of the proper rational functions that describes the disturbances and reference input respectively, in other words, the pairs (A_d, C_d) and (A_r, C_r) are observable. To design a controller that is able to track the desired input signal, and reject disturbances acting on the system, a "Θ" function is to be found, such that:

$$\Theta = s^q + \alpha_1 s^{q-1} + \cdots + \alpha_{q-1} s + \alpha_q \tag{10}$$

Which represents the least common multiple of the minimal polynomials of A_d and A_r. Based on the previous discussion, the controller is chosen as follows [Tahboub, 1993]:

$$\begin{aligned} \dot{x}_c &= A_c x_c + B_c e \\ y_c &= C_c x_c \end{aligned} \tag{11}$$

Where:

$$-A_c = \begin{bmatrix} 0 & 1 & 0 & \cdots & 0 \\ 0 & 0 & 1 & \cdots & 0 \\ \vdots & \vdots & \vdots & \ddots & \vdots \\ 0 & 0 & 0 & \cdots & 1 \\ -\alpha_q & -\alpha_{q-1} & -\alpha_{q-2} & \cdots & -\alpha_1 \end{bmatrix} \qquad -B_c = \begin{bmatrix} 0 \\ 0 \\ \vdots \\ 1 \end{bmatrix}$$

$$-C_c = I_q$$

- e : the error signal, which is the difference between the desired cart position and the actual one.

Figure 2 shows the control system configuration, where the models of the reference input, disturbances and controller are demonstrated with respect to the controlled plant.

The augmented system, according to [Tahboub, 1993], is given as follows:

$$\begin{bmatrix} \dot{x} \\ \dot{x}_c \end{bmatrix} = \underbrace{\begin{bmatrix} A & 0 \\ -B_c C_{track} & A_c \end{bmatrix}}_{A_a} \begin{bmatrix} x \\ x_c \end{bmatrix} + \underbrace{\begin{bmatrix} B \\ 0 \end{bmatrix}}_{B_a} u \tag{12}$$

Where $C_{track} = [1 \quad zeros]$, which represents the cart position.

Checking the controllability of the pair (A_a, B_a), the augmented system is found to be fully controllable, which means that it is possible to find a gain vector $[K \quad K_c]$, shown in Fig. 2, such that the eigenvalues of the system can be arbitrarily placed, to obtain the desired performance. One way for

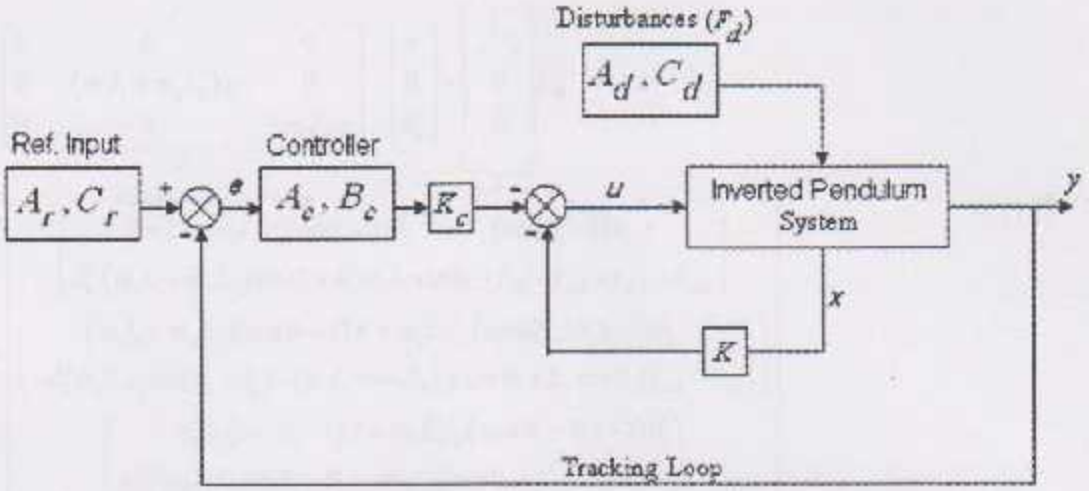

Figure 2 Robust tracking and disturbance rejection state-feedback controller configuration.

finding the feedback gains $[K \quad K_c]$ is solving a Riccati equation to minimize the quadratic performance index:

$$J = \int_0^\infty (x^T Q x + u^T R u) dt \tag{13}$$

Where:

Q : is a positive semidefinite symmetric matrix that represents the relative importance of the states.

R : is positive semidefinite matrix that represents the relative importance of control inputs.

2. Nonlinearities and Disturbance Estimation: As stated earlier, one of the challenges that face the control problem of DIPC is its nonlinear dynamics in addition to the immeasurable external disturbances acting on the system. These disturbances and nonlinearities were neglected when deriving the linearized model, which latter formed the base on which the robust state feedback controller was designed, as shown in the previous subsection. In order to improve the overall response of the system, and enhance its immunity against disturbances, an additional term denoted by (n) is added to the linearized model. This term includes all the nonlinearities and disturbances that were neglected during linearization. To be more precise, this term represents the difference between the nonlinear model of Eq. (4), and the linearized one of Eq. (6), as follows:

$$\underbrace{\begin{bmatrix} M + m_1 + m_2 + J/r_p^2 & (m_1 l_1 + m_2 L_1) & m_2 l_2 \\ (m_1 l_1 + m_2 L_1) & m_1 l_1^2 + m_2 L_1^2 + J_1 & m_2 L_1 l_2 \\ m_2 l_2 & m_2 L_1 l_2 & m_2 l_2^2 + J_2 \end{bmatrix}}_{\bar{M}} \begin{bmatrix} \ddot{x} \\ \ddot{\theta}_1 \\ \ddot{\theta}_2 \end{bmatrix} + \underbrace{\begin{bmatrix} d/r^2 & 0 & 0 \\ 0 & 0 & 0 \\ 0 & 0 & 0 \end{bmatrix}}_{\bar{D}} \begin{bmatrix} \dot{x} \\ \dot{\theta}_1 \\ \dot{\theta}_2 \end{bmatrix} +$$

$$\underbrace{\begin{bmatrix} 0 & 0 & 0 \\ 0 & -(m_1 l_1 + m_2 L_1)g & 0 \\ 0 & 0 & -m_2 l_2 g \end{bmatrix}}_{K} \begin{bmatrix} x \\ \theta_1 \\ \theta_2 \end{bmatrix} = \underbrace{\begin{bmatrix} 1/r_p \\ 0 \\ 0 \end{bmatrix}}_{B} T_m$$

$$+ \underbrace{\begin{bmatrix} \begin{pmatrix} (m_1 l_1 + m_2 L_1)(\cos\theta_1 - 1)\ddot{\theta}_1 + m_2 l_2(\cos\theta_2 - 1)\ddot{\theta}_2 + \\ \dot{\theta}_1^2(m_1 l_1 + m_2 L_1)\sin\theta_1 + \dot{\theta}_2^2 m_2 l_2 \sin\theta_2 + f_{d1} + f_{d2} + f_{d3} - F_{fric} \end{pmatrix} \\ \begin{pmatrix} (m_1 l_1 + m_2 L_1)(\cos\theta_1 - 1)\ddot{x} + m_2 L_1 l_2(\cos(\theta_1 - \theta_2) - 1)\ddot{\theta}_2 \\ -\dot{\theta}_2^2 m_2 L_1 l_2 \sin(\theta_1 - \theta_2) - (m_1 l_1 + m_2 L_1) g \sin\theta_1 + L_1 \cos\theta_1 (f_{d2} + f_{d3}) \end{pmatrix} \\ \begin{pmatrix} m_2 l_2(\cos\theta_2 - 1)\ddot{x} + m_2 L_1 l_2(\cos(\theta_1 - \theta_2) - 1)\ddot{\theta}_1 \\ +\dot{\theta}_1^2 m_2 L_1 l_2 \sin(\theta_1 - \theta_2) - m_2 l_2 g \sin\theta_2 + f_{d3} L_2 \cos\theta_2 \end{pmatrix} \end{bmatrix}}_{n} \tag{14}$$

Since these nonlinearities and disturbances (n) are not directly measurable; an extended observer is needed. Extended observers are basically classical observers where the nonlinearities and external disturbances (n), are assumed to be regular states. Since these states are originally extraneous to the system, one can not write down their corresponding differential equations describing their behavior in the time domain, which is necessary for completing the state-space model. A practical solution would be to assume that they are step-wise constant, thus their derivatives are set to zero.

Based on the previous discussion, and referring to Eq. (14), the extended state-space representation is:

$$\begin{bmatrix} \dot{x} \\ \ddot{x} \\ \dot{n} \end{bmatrix} = \underbrace{\begin{bmatrix} zeros(3) & I_3 & zeros(3) \\ -M^{-1}K & -M^{-1}D & M^{-1}N \\ & zeros(3,9) & \end{bmatrix}}_{Ae} \begin{bmatrix} x \\ \dot{x} \\ n \end{bmatrix} + \underbrace{\begin{bmatrix} zeros(3,1) \\ M^{-1}B \\ zeros(3,1) \end{bmatrix}}_{Be} T_m \tag{15}$$

$$y = \underbrace{I_9}_{Ce} \begin{bmatrix} x & \dot{x} & n \end{bmatrix}^T$$

Where: $N = I_3$.

To check the possibility for the disturbances and nonlinearities to be estimated by the extended observer with the available measurements, the condition:

$$rank \begin{bmatrix} sI - A & N \\ C & 0 \end{bmatrix} = \dim(\boldsymbol{x}) + \dim(\boldsymbol{n}) \tag{16}$$

should be satisfied for all complex numbers (s). This requires that the number of nonlinearities may not exceed the number of measurements, which is the case here. Finding that the system is fully observable, it is possible to estimate the nonlinearities and external disturbances. Within the extended

observer, and as the classical ones, the measured outputs of the system are compared to those estimated, and the error signal is fed back to the observer. In order to increase the convergence speed of the error signal, i.e. to make the observer outputs match those measured as fast as possible, the dynamics of the observer is made much faster than that of the controlled system. This is achieved by choosing an appropriate gain vector (L), so that the poles of the error characteristic equation can be placed far to the left from those of the controlled system. Based on the separation property [Chen, 1999], the controller and observer can be designed independently.

3. Compensating the Effects of Disturbances and Nonlinearities: The extended observer previously designed generates an estimate of the states in addition to the disturbances and nonlinearities. As these disturbances become known, it is possible to compensate for their effects using static compensation method, where a part of the control effort is dedicated to delete the effects of disturbances acting on the system. In fact, this method can be used only to compensate for the disturbances and nonlinearities acting on the cart, since, in contrast to those acting on the two links, there is a direct relation between cart nonlinearities and the input signal. Thus the control signal (u) becomes:

$$u = -kx - k_a x_c - r_p n_1 \tag{17}$$

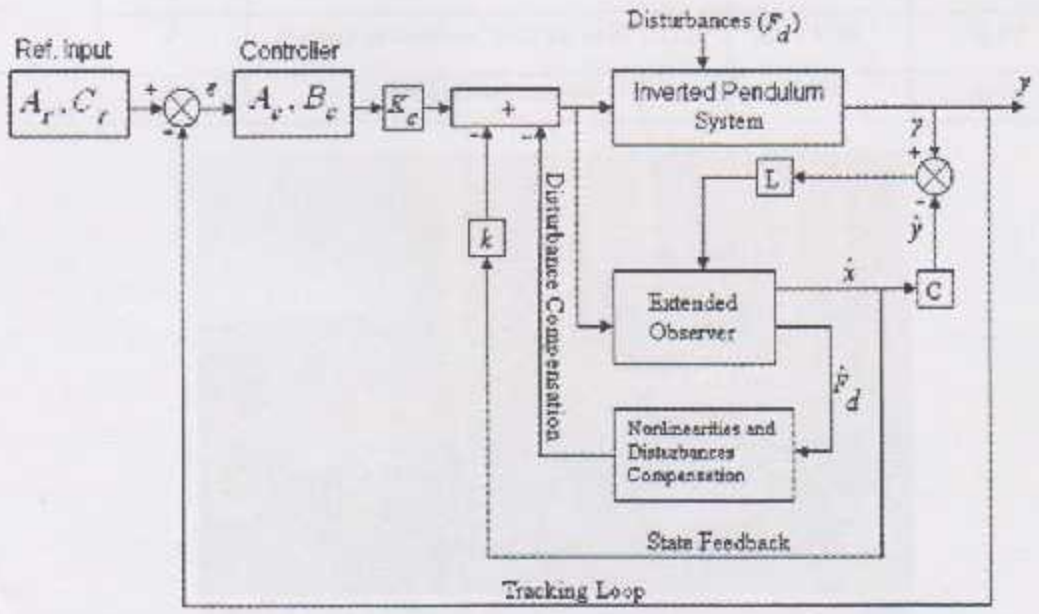

Figure 3 Using the extended observer outputs to compensate for the nonlinearities and disturbances effects in DIPC system.

Figure 3 shows the complete controller-observer configuration, with disturbance compensation used for controlling DIPC system.

4. EXPERIMENTAL RESULTS

In this section, the theoretical concepts previously discussed are applied practically to DIPC system. With such a system various control theories can be applied, compared and tested on the cart alone, the single and the double inverted pendulum systems. Table 1 shows system's parameters for which the controllers are designed, while Fig. 4 shows the developed DIPC system.

Table 1: DIPC parameters

Symbol	Description	Value	Units
M	Mass of the cart	1.45	Kg
m_1	Mass of rod1	0.33	Kg
m_2	Mass of rod2	0.132	Kg
L_1	Length of rod1	0.335	m
r_p	Radius of the pulley	0.02	m
l_1	Length of center of mass of rod1	0.2276	m
l_2	Length of center of mass of rod2	0.125	m
J_p	Moment of inertia of the 2 pulleys	1.55×10^{-4}	$Kg.m^2$
J_1	Moment of inertia of link1 about its C.O.G	0.0436	$Kg.m^2$
J_2	Moment of inertia of link2 about its C.O.G	6.98×10^{-4}	$Kg.m^2$
g	Gravitational constant	9.81	m/s^2

Figure 4 The experimental double-inverted-pendulum-on-a-cart setup

The developed DIPC system, shown in Fig. 4, consists of the two links, the cart, and the linear rail. The cart moves linearly over the rail by means of a special robe and pulley arrangement. The system is equipped with two incremental optical encoders, used for angles measurement. The input of the system is the torque generated by an AC servomotor coupled directly to the pulley's shaft, A real-time controller is implemented using a standard PC hardware equipped with two data acquisition cards. To achieve flexibility and hard real-time control requirements, xPC target technique is used. Further details about system implementation are available at [Tahboub, AlBakri, Arafeh, 2007]

The first experiment is performed on the cart alone, where a robust tracking and disturbance rejection state feedback controller is applied to track a desired step cart position command, while an extended observer is used to estimate the nonlinearities and disturbances acting on the system, which is then statically compensated. Figure 5 shows the actuating torque signal, cart position, and the estimated nonlinearities corresponding to the following poles locations and gain values:

- Controlled system poles $\begin{bmatrix}-7.03 & -7.05 & -25\end{bmatrix}$
- Feedback gains $\begin{bmatrix}k & k_e\end{bmatrix}=\begin{bmatrix}14.8 & 1.4 & -45.6\end{bmatrix}$
- Extended observer poles $6\times\begin{bmatrix}-7.03 & -7.05 & -25\end{bmatrix}$
- Observer gains $L_e=\begin{bmatrix}42 & -0.79 & -1\\ 1 & 192 & 11586\end{bmatrix}^T$

Based on Fig. 5, it could be noted that the extended observer estimates the friction force that acts on the cart, which is about 4 N, but with some overshoot. Furthermore, with the extended observer and static compensation, the disturbance rejection ability of the system is much enhanced compared to that obtained with the robust controller alone. Thus, with this feature, it is possible to obtain a high disturbance rejection performance independently of the controlled system poles location.

The second experiment is performed with the single inverted pendulum, where a self erecting and stabilization controller is applied. Such controller consists of two parts. The first is a bang-bang controller which tends to swing the links up to the inverted position, while the second part is a stabilization controller similar to that discussed at the previous sections. A switching logic is also used for transformation from one controller to another depending on the link's angle. Figure 6 shows the actuating torque signal, cart position, and link angle, for a self erecting and stabilization controller corresponding to the following poles locations and gain values:

- Controlled system poles $\begin{bmatrix}-0.45 & -0.5 & -6 & -6.1 & -70\end{bmatrix}$
- Controller gains $\begin{bmatrix}k & k_e\end{bmatrix}=\begin{bmatrix}-2.13 & -8.47 & -2.78 & -1.26 & 0.47\end{bmatrix}$

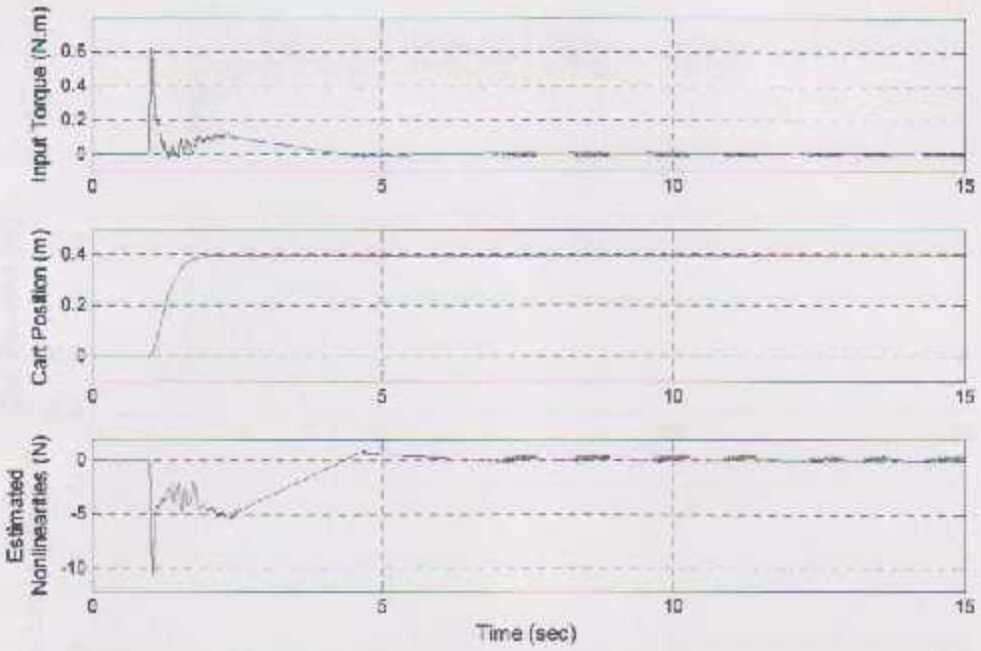

Figure 5 The response of a Cart position controller with an extended observer

The final experiment to be demonstrated here is performed on DIPC system, where a robust tracking and disturbance rejection controller is applied to track a desired step cart position command while keeping the two links stabilized at the upright vertical position. Figure 7 shows the actuating torque signal, cart position, and the angle of each link, corresponding to the following poles locations and gain values:

- Controlled system poles $\quad [-1 \quad -1.05 \quad -3 \quad -3.1 \quad -7 \quad -7.5 \quad -15]$
- Feedback gains $\quad [K] = [0.95 \quad 30.17 \quad -24.43 \quad 1.05 \quad 5.12 \quad -2.77]$

$$[K_c] = [-0.32]$$

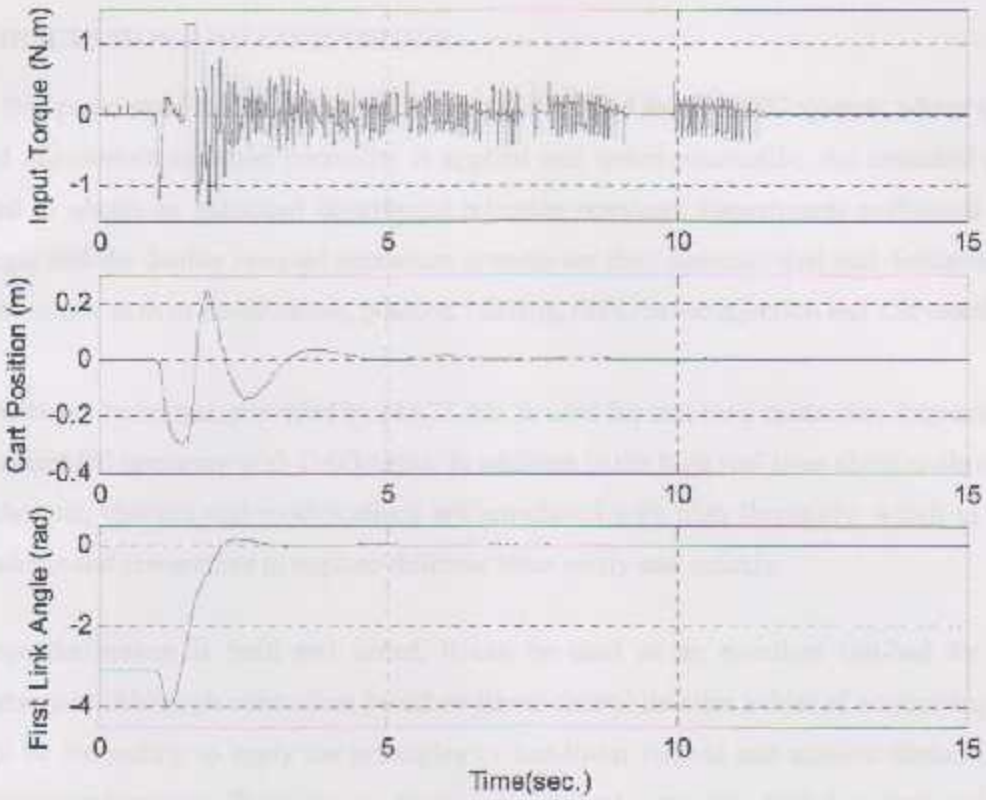

Figure 6 The response of the single inverted pendulum system due to a self erecting and stabilization controller.

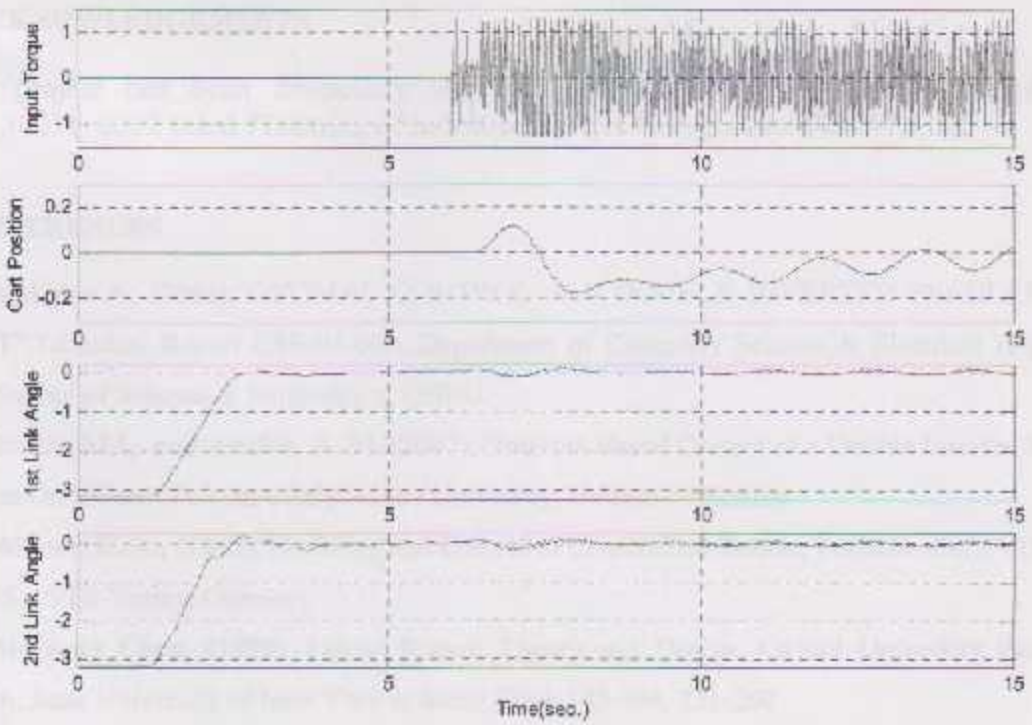

Figure 7 The response of the double inverted pendulum system due to a stabilization controller.

5. DISCUSSION AND CONLUSIONS

In this paper state feedback control theories are applied to the DIPC system, where a robust tracking and disturbance rejection controller is applied and tested practically. An extended observer is then used to obtain an enhanced disturbance rejection response. Experiments performed on the cart, the single and the double inverted pendulum systems are then demonstrated and discussed, where various controllers, such as stabilization, position tracking, disturbance rejection and self erecting, are applied.

xPC target technique, provided by MATLAB, is used for real-time controllers implementation, using a standard PC hardware with DAQ cards. In addition to the high real-time abilities obtained with such a technique, changes and modifications are introduced with high flexibility; which in turn encourages students and researchers to explore different ideas easily and quickly.

Once the system is built and tested, it can be used as an excellent test-bed for various control techniques. Although controllers based on linear control theories achieved a satisfying performance, it will be interesting to apply the principles of non-linear control and achieve further improvements in system performance. Furthermore, fuzzy logic, neural networks, digital control and optimal control methods can be applied, tested and compared by means of this apparatus.

6. ACKNOWLEDGEMENTS

This project has been financially supported by a grant from TEMPUS project No. JEP_30078_2002 titled "Training of industrial systems integrators: FINSI".

7. REFERENCES

1. **Bogdanov.A, (2004)**,"OPTIMAL CONTROL of a DOUBLE INVERTED PENDULUM on a CART",Technical Report CSE-04-006, Department of Computer Science & Electrical Engineering, OGI School of Science & Engineering, OHSU.

2. **AlBakri, M.I, and Arafeh, A. M, (2007)**, "Internet Based Control of a Double Inverted Pendulum System On a Cart", Palestine Polytechnic University, Hebron - Palestine.

3. **Tahhoub, K. A., (1993),** Modeling and Control of Constrained Robots, Fortschr.-Ber., VDI Reihe 8 Nr. 361, VDI-Verlag, Germany

4. **Chi-Tsong Chen, (1999).** Linear System Theory and Design, Oxford University Press, Third edition, State University of New York at Stony Book 143-164, 231-260

5. **Tahboub, K.A, AlBakri, M.I, Arafeh, A.M, (2007)**, "Development of a Flexible Educational Mechatronic System Based on xPC Target", accepted for presentation at ASME 2007 International

Design Engineering Technical Conferences & Computers and Information in Engineering Conference, Las Vegas, USA

References

[1] AC Servomotor Driver, Minas A-series Operating Manual, Matsushita Electric Industrial Co., LTD
http://industrial.panasonic.com/ww/i_e/25000/minas_a_e/minas_a_e.pdf

[2] Alkaraki A.S and others, Design of a Computer Controlled Double Inverted Pendulum Apparatus, 2006, Graduation project, Palestine Polytechnic University.

[3] Cetinkunt.S, Mechatronics, 2007, John Wiley & Sons,Inc.River Street, Hoboken, New Gersy.

[4] Chi-Tsong Chen, Linear System Theory and Design, Oxford University Press, Third edition, State University of New York at Stony Book.

[5] Fred A. Lewis & John A. Houdek ,7/31/02, Reactors Provide a Low Cost Solution to Inverter/Driver Power Quality, Reactors ,http://www.galco.com/circuit/reactors.htm

[6] Norman S. Nise, Control System Engineering, John Willey and Sons, Fourth edition, 2004, California State University, Pomona.

[7] Singiresus .RAO, Mechanical Vibration, Addison-Wesley publishing company, Purdue University, 1995.

[8] Tahboub, K. A., Modeling and Control of Constrained Robots, 1993, Fortschr.-Ber., VDI Reihe 8 Nr. 361, VDI-Verlag, Germany.

[9] PCI NI 6024E Card user manual,
http://cires.colorado.edu/jimenez-group/QAMSResources/Docs/PCI-6024E.pdf.

[10] PCI-QUAD04 User's Guide, 22/12/2006
www.measurementcomputing.com/PDFManuals/PCI-QUAD04.pdf.

[11]- Anonymous, 22/12/2006, http://zone.ni.com/devzone/cda/tut/p/id/4623#0.

[12]-Burr-Brown Corporation,1997,
http://www.alldatasheet.com/datasheet-pdf/pdf/56708/BURR-BROWN/ISO124P.html

[13]-MATLAB Help
http://www.mathworks.com/support/product/XP/productnews/xpc_targetbox_ug.pdf.

[14]-LSI Computer systems, Inc.
http://pdf1.alldatasheet.com/datasheetpdf/pdf/view-71316-LSI-7184.html.

[15]-Texas Instrument.
http://www.alldatasheet.com/datasheetpdf/pdf/26755/TI/AM26LS32ACD.html.

[16] Wikipedia, the free encyclopedia
http://www.wikipedia.com